



TECHNISCHE UNIVERSITÄT MÜNCHEN

Wissenschaftszentrum Weihenstephan Entwicklungsbiologie der Pflanzen

Endocytic trafficking of *Arabidopsis* receptor-like kinase STRUBBELIG

Jin Gao

Vollständiger Abdruck der von der Fakultät Wissenschaftszentrum Weihenstephan für Ernährung, Landnutzung und Umwelt der Technischen Universität München zur Erlangung des akademischen Grades eines

Doktors der Naturwissenschaften (Dr. rer. nat.)
genehmigten Dissertation.

Vorsitzender: Prof. Dr. Erwin Grill

Prüfer der Dissertation: 1. Prof. Dr. Kay H. Schneitz
2. Prof. Dr. Brigitte Poppenberger-Sieberer

Die Dissertation wurde am 22. 01. 2019 bei der Technischen Universität München eingereicht und durch die Fakultät Wissenschaftszentrum Weihenstephan für Ernährung, Landnutzung und Umwelt am 08. 04. 2019 angenommen.

I. Tables of contents

I. Tables of contents.....	1
II. Lists of figures	4
III. Lists of tables	5
IV. Abbreviations	7
V. Summary.....	10
VI. Zusammenfassung	12
1 Introduction	14
1.1 Intercellular signaling and trafficking	14
1.1.1 Plant meristems, organogenesis and cell-to-cell communication	14
1.1.2 Plasmodesmata provide cell-to-cell connectivity	16
1.2 Plant receptor-like kinases (RLKs) in communication	17
1.2.1 Classifications of plant RLKs.....	17
1.2.2 Functions of plant RLKs	20
1.3 The role of endocytosis in plants	21
1.3.1 Compartments of the plant endomembrane system.....	21
1.3.2 Multiple, complex endocytic pathways	22
1.3.3 CME, a central mechanism of PM-localized factors internalization.....	23
1.3.4 The best known PM factors for receptor mediated endocytosis in plants.....	26
1.4 The atypical leucine-rich repeat RLK, STRUBBELIG (SUB).....	30
1.4.1 SUB regulate tissue morphogenesis in Arabidopsis	30
1.4.2 SUB may represent an atypical RLK.....	33
1.4.3 <i>SUB</i> acts in a non-cell-autonomous fashion.....	34
1.4.4 Mechanistic basis of signaling through atypical RLKs	35
1.4.5 Novel components in SUB signaling pathway	37

Tables of contents

1.4.6 Intracellular localization of SUB	38
1.5 Objectives	38
2 Materials and Methods	39
2.1 Plant work, plant genetics and plant transformation.....	39
2.2 Recombinant DNA work.....	40
2.3 Arabidopsis genomic DNA extraction and genotyping PCR.....	43
2.4 RNA extraction from plant material and cDNA synthesis.....	44
2.5 Generation of various reporter constructs	45
2.5.1 Generation of pSUB/pUBQ10::SUB:EGFP constructs.....	45
2.5.2 Construction of Y2H vectors	45
2.5.3 Generation of root hair patterning construct pGL2::GUS:EGFP pGGZ001	45
2.6 Yeast-two-hybrid (Y2H) assay.....	46
2.7 Scanning electron microscopy (SEM)	46
2.8 Confocal laser scanning microscopy (CLSM)	47
2.9 Three dimensional ovule imaging using CLSM and MorphoGraphX...	48
2.10 Phenotyping flower organ	49
2.11 Drug treatments.....	49
2.12 Immunoprecipitation and western blot analysis	50
2.13 Growth media, growth conditions and frequently used buffers	50
2.14 Bioinformatics	52
3 Results.....	53
3.1 The endocytic route of SUB:EGFP	53
3.2 SUB:EGFP is ubiquitinated <i>in vivo</i>	58
3.3 SUB:EGFP internalization involves clathrin-mediated endocytosis.....	59
3.3.1 SUB interacts with Clathrin <i>in vivo</i>	59
3.3.2 CME is required for SUB internalization	60
3.4 SUB genetically interacts with CLATHRIN HEAVY CHAIN	62

Tables of contents

3.5 Characterization of the Arabidopsis CHC1 and CHC2	68
3.6 Mapping the interaction domain of CHC2 in a Y2H	69
3.7 SUB intracellular domain does not interact with the μ -adaptin of AP2 complex in a Y2H	71
3.8 <i>ap2</i> mutants do not rescue <i>sub-9</i> phenotype	72
4 Discussion	76
4.1 The endocytic route of SUB	76
4.2 SUB receptor is ubiquitinated <i>in vivo</i>	78
4.3 Signaling mediated by SUB involves CME	78
4.4 <i>SUB</i> genetically interacts with clathrin-mediated pathways in a tissue- specific manner	79
4.5 How does <i>AP2</i> relate to CME with respect to <i>SUB</i> signaling?.....	81
5 Conclusion.....	83
6 Supplement	85
7 References	90
8 Acknowledgements.....	113
9 Curriculum Vitae	115

II. Lists of figures

Figure 1 Schematic architecture of the shoot apical meristem of Arabidopsis.....	15
Figure 2 Representative RLKs and their classifications.	19
Figure 3 Endomembrane trafficking pathways in plant cells.....	22
Figure 4 proposed model of CME in plants.	24
Figure 5 The clathrin envelope of an endocytosed vesicle consists of several clathrin triskelia.	25
Figure 6 Schematic overview of the endocytic pathways of BRI1.	28
Figure 7 Schematic overview of the endocytic pathways of FLS2.	29
Figure 8 Phenotype comparison of the overall above-ground morphology of <i>Ler</i> and <i>sub-1</i>	31
Figure 9 Analysis of cellular defects in 4-day old main roots and stage 3 floral meristems of <i>sub-1</i> , <i>doq-1</i> , <i>qky-8</i> and <i>zet-2</i> mutants.	32
Figure 10 Overview of the domain architecture of SUB.	33
Figure 11 Subcellular localization of QKY and SUB.	36
Figure 12 Subcellular localization of SUB:EGFP.....	54
Figure 13 Subcellular localization of SUB:EGFP upon drug treatments. ...	56
Figure 14 <i>In vivo</i> ubiquitination of SUB.....	58
Figure 15 Co-immunoprecipitation of CHC with SUB:EGFP.....	59
Figure 16 Requirement of clathrin function for SUB endocytosis.....	61
Figure 17 Characterization of <i>chc</i> mutant alleles.	62
Figure 18 Expression pattern of the pGL2:: <i>GUS</i> :EGFP reporter in <i>chc2-2</i> and <i>chc2-2 sub-9</i> mutants.....	64
Figure 19 Phenotype comparison between Col-0, <i>sub-9</i> , <i>chc2-2</i> and <i>chc2-2</i> <i>sub-9</i>	64

Lists of figures and tables

Figure 20 Expression pattern of pGL2::GUS:EGFP in wild-type, <i>chc2-1</i> , <i>chc2-1 sub-9</i> , <i>chc1-2</i> , and <i>chc1-2 sub-9</i> mutants.	66
Figure 21 Comparison of the floral phenotypes between Col-0, <i>sub-9</i> , and various <i>chc</i> mutants.	67
Figure 22 Structure properties of CHC2 and conservation between the Arabidopsis CHC1 and CHC2 proteins.	68
Figure 23 SUB-ICD interacts directly with CHC2.	70
Figure 24 SUB-JM interact with CHC2-2.	70
Figure 25 Y2H analysis of SUB-ICD deletion variants with AP2 μ subunit.	71
Figure 26 Phenotypical characterization of <i>ap2a1</i> and <i>ap2a1 sub-9</i>	72
Figure 27 Phenotypical analysis of <i>ap1/2b2</i> and <i>ap1/2b2 sub-9</i>	73
Figure 28 The <i>ap2m</i> and <i>ap2m sub-9</i> mutants show multiple morphological abnormalities.	74
Figure 29 Phenotypical analysis of <i>ap2s</i> and <i>ap2s sub-9</i>	75
Figure 30 Schematic model of the SUB trafficking to and from the cell surface.	77
Figure 31 Hypothetical scheme of the molecular mechanisms underlying the <i>SUB</i> signaling pathway with respect to root hair patterning.	80
Figure 32 SUB-JM and KD domain sequence with putative protein endocytic motifs.	82

III. Lists of tables

Table 1 PCR reaction mix and cycler program.	41
Table 2 Backbone vectors used in this work.	42
Table 3 Reaction mix and steps involved in cDNA synthesis.	44

Lists of figures and tables

Table 4 Number of periclinal cell divisions in the L2 layer of stage 3 floral meristems.....	65
Table 5 Comparison of integument defects between <i>sub-9</i> , <i>chc</i> and <i>chc sub-9</i> mutants.	66
Table 6 Comparison of integument defects between <i>sub-9</i> , <i>ap2</i> and <i>ap2 sub-9</i> mutants.	74

IV. Abbreviations

3-AT	3-amino-1,2,4-triazole
AA	Amino acid
AD	Activation domain of GAL4 TF
ANT	AINTEGUMENTA
AP2	Adaptor protein complex 2
AP2M	μ -adaptin of AP2
BAK1	BRI1 associated kinase 1
BD	DNA-binding domain of GAL4 TF
BFA	Brefeldin A
BKI1	BRI1 KINASE INHIBITOR 1
BR	Brassinosteroid
BRI1	BRASSINOSTEROID INSENSITIVE 1
CCPs	Clathrin-coated pits
CCVs	Clathrin-coated vesicles
CHC1, CHC2	CLATHRIN HEAVY CHAIN1, and 2
CHX	Cycloheximide
CIE	Clathrin-independent endocytosis
CLC	CLATHRIN LIGHT CHAIN
CLV1, CLV3	CLAVATA1, and 3
CLSM	Confocal laser scanning microscopy
CME	Clathrin-mediated endocytosis
Col-0	Columbia-0
ConcA	Concanamycin A
Co-IP	Co-immunoprecipitation
CR4	CRINKLY4
CRR2	CRINKLY4-RELATED 2
DMSO	Dimethyl sulfoxide
DNA, cDNA, gDNA, T-DNA	Deoxyribonucleic acid, complementary DNA, genomic DNA, transfer DNA
DRP	Dynamin-related protein
DUM	Domain of unknown function
EGF	Epidermal growth factor
EGFP	Enhanced green fluorescent protein
ER	Endoplasmic reticulum

Abbreviation

FER	FERONIA
FLS2	FLAGRLLIN SENSING2
FM	Floral meristem
FM4-64	N-(3-triethylammoniumpropyl)-4-(4-diethylaminophenylhexatrienyl) pyridinium dibromide
GCN	General control non-derepressible
GL2	GLABRA2
GUS	β -glucuronidase
HAP13	HAPLESS13
IKA	Ikarugamycin
ILV	Intra-luminal vesicle
LB	Lysogeny broth
LE	Late endosome
<i>Ler</i>	Landsberg <i>erecta</i>
LRR	Leucine-rich repeat
LysM	Lysin motif
MAPK	Mitogen-activated protein kinase
mKO	Monomeric Kushiba Orange
ML1	MERISTEM LAYER 1
mPS-PI	Modified pseudo-schiff propidium iodide
MS	Murashige and Skoog
MVB/PVC	Multivesicular body/prevacuolar compartment
OC	Organizing center
PBS	Phosphate buffered saline
p35S	Cauliflower mosaic virus 35S promoter
PCR	Polymerase chain reaction
PD	Plasmodesmata
PEPR	Peptides peps receptor
PFA	Paraformaldehyde
PIN1, PIN2	PINFORMED 1, and 2
PIP2	Phosphatidylinositol 4,5-bisphosphate
PM	Plasma membrane
PMSF	Phenylmethylsulfonyl fluoride
PR5	Pathogenesis related protein 5
PR5K	PR5-like receptor kinase
PZ	Peripheral zone
QKY	QUIRKY
RAM	Root apical meristem

Abbreviation

RLK	Receptor-like kinase
RME	Receptor-mediated endocytosis
RNA	Ribonucleic acid
ROI	Region of interest
RT	Room temperature
RZ	Rib zone
SAM	Shoot apical meristem
SCM	SCRAMBLED
SC	Stem cell
SDS-PAGE	Sodium dodecyl sulfate polyacrylamide gel electrophoresis
SEL	Size exclusion limit
SEM	Confocal laser scanning microscopy
SERK1	SOMATIC EMBRYOGENESIS RECEPTOR-LIKE KINASE 1
SLG	Self-incompatibility-locus glycoproteins
SR2200	SCRI Renaissance 2200
SUB	STRUBBELIG
TF	Transcription factor
TGN/EE	Trans-Golgi network/early endosome
TM	Transmembrane region
TNFR	Tumor necrosis factor receptor
TPC	TPLATE complex
TUM	Technische Universität München
TyrA23	Tyrphostin A23
UBQ	UBIQUITIN 10
UTR	Untranslated region
WAK	Wall-associated receptor kinase
WM	Wortmannin
WT	Wild type
WUS	WUSCHEL
Y2H	Yeast-two-hybrid
YPD	Yeast extract peptone dextrose
ZET	ZERZAUST

V. Summary

Signaling mediated by cell surface receptor-like kinases is central to the coordination of growth patterns during organogenesis. Receptor-like kinase signaling is in part controlled through endocytosis and subcellular distribution of the respective receptor kinase. For the majority of plant cell surface receptors the underlying trafficking mechanisms are not characterized.

In *Arabidopsis*, tissue morphogenesis relies on the atypical receptor-like kinase STRUBBELIG (SUB) and was shown to be involved in intercellular communication. In the current work, the endocytic mechanism of SUB is investigated. Biochemical analysis revealed that functional SUB:EGFP fusion protein is ubiquitinated *in vivo*. Microscopic analysis showed that plasma membrane-bound SUB:EGFP becomes internalized in a clathrin-dependent fashion. SUB:EGFP was also found to associate with the trans-Golgi network and to accumulate in multivesicular bodies and the vacuole. Co-immunoprecipitation (Co-IP) experiments revealed that SUB:EGFP and clathrin are present within the same protein complex. Moreover, SUB and CLATHRIN HEAVY CHAIN 2 (CHC2) physically interact in yeast. Genetic analysis showed that *SUB* and *CHC2* promote root hair patterning. By contrast, *SUB* behaves as a negative regulator of a clathrin-dependent process during floral development. An important component of clathrin-mediated signaling, a medium subunit of adaptor protein complex 2 (AP2M) did not show any interaction with SUB in yeast-two-hybrid assay. The *ap2* single mutants also failed to rescue *sub-9* phenotype suggesting higher order mutants are required for further analysis. In conclusion, the data indicate that SUB undergoes clathrin-mediated endocytosis, that this process does not depend on stimulation of SUB signaling by an exogenous agent, and that

Summary

SUB genetically interacts with clathrin-dependent pathways in a tissue-specific manner.

VI. Zusammenfassung

Die durch Zelloberflächenrezeptorkinasen vermittelte Signalübertragung ist von zentraler Bedeutung für die Koordination von Wachstumsmustern während der Organogenese. Die entsprechende Signalvermittlung wird zum Teil durch Endozytose und die subzelluläre Verteilung der jeweiligen Rezeptorkinase gesteuert. Für die meisten pflanzlichen Zelloberflächen-Rezeptoren sind die Transportmechanismen nicht charakterisiert.

In Arabidopsis hängt die Gewebemorphogenese von der atypischen, Rezeptorkinase STRUBBELIG (SUB) ab. In der vorliegenden Arbeit wurde der endozytische Mechanismus von SUB untersucht. Die biochemische Analyse zeigte, dass ein funktionales SUB:EGFP-Fusionsprotein *in vivo* ubiquitiniert wird. Mikroskopische Analysen zeigten weiter, dass das plasmamembrangebundene SUB:EGFP Clathrin-abhängig internalisiert wird, mit dem trans-Golgi-Netzwerk assoziiert, und sich in multivesikulären Körpern und der Vakuole anreichert. Koimmunopräzipitations-Experimente deuten darauf hin, dass SUB:EGFP und Clathrin im gleichen Proteinkomplex lokalisiert sind. Darüber hinaus interagieren SUB und CLATHRIN HEAVY CHAIN 2 (CHC2) in Hefe physisch miteinander. Die genetische Analyse zeigte, dass SUB und CHC2 die Wurzelhaarmusterung beeinflussen. Im Gegensatz dazu verhält sich SUB als negativer Regulator eines Clathrin-abhängigen Prozesses während der Blütenentwicklung. Eine wichtige Komponente der Clathrin-vermittelten Endozytose, eine mittlere Untereinheit des Adapterproteinkomplexes 2 (AP2M) zeigte keine Interaktion mit SUB im Yeast-Two-Hybrid-Assay. Die *ap2*-Einzelmutanten konnten den *sub-9*-Phänotyp ebenfalls nicht retten, was darauf schließen lässt, dass Mutanten höherer Ordnung für die weitere Analyse erforderlich sind. Zusammenfassend deuten die Daten darauf hin, dass SUB eine Clathrin-vermittelte Endozytose durchläuft, dass dieser

Zusammenfassung

Prozess nicht von der Stimulation des SUB-Signals durch einen exogenen Wirkstoff abhängt, und dass SUB gewebeabhängig differentiell mit einem Clathrin-abhängigen Prozess genetisch interagiert.

1 Introduction

The control of cell division patterns plays a central role in understanding the mechanisms of plant and animal development. To generate a functional adult body, multicellular eukaryotes need well organized cell divisions and cell specification (Meyerowitz, 1997). Intercellular communication is essential for this process.

1.1 Intercellular signaling and trafficking

1.1.1 Plant meristems, organogenesis and cell-to-cell communication

The activity of forming new organs is established post-embryonically in plants while the process of an animal occurs early on in embryogenesis. The above-ground organs of higher plants ultimately originate from the shoot apical meristem (SAM), which gives rise to leaves and flowers. Thus, comprehensive coordinated regulation of cell division and expansion in meristems plays crucial roles in tissue morphogenesis.

Plant meristems containing undifferentiated cells produce diverse organs are responsible for growth. Generally, meristems can be divided into three types according their location: apical meristems (at the tips), intercalary meristems (in the middle) and lateral meristems (at the sides). The embryonic SAM develops tissues via proliferation and differentiation of cells in peripheral areas and the root apical meristem (RAM) properly arises various types of root tissues in proximal and distal orientations, respectively. The cell fate in the shoot meristem is dependent on its position. The shoot meristem contains 3 distinct layers (Satina *et al.*, 1940). The outermost L1 layer (1 cell thick) and L2 layer (1 cell thick) which lies below the L1 layer, comprise the tunica and cells within the L1 and L2 layers divide strictly perpendicular to the surface of the meristem (anticlinal cell division). Cells of the innermost L3 layer divide randomly and make up the corpus.

L1 will form the epidermis while L2 and L3 produce cortex and vascular tissue. Moreover, three additional functional zones are recognized in SAM. The central zone (CZ) contains infrequently dividing stem cells, the multipotent peripheral zone (PZ) is the place where lateral organs are initiated, and the underlying rib zone (RZ) creates the pith tissue (Lyndon, 1998) (Figure 1).

Recent studies have shown the maintenance of the stem cell population is intimately balanced with cell recruitment into differentiating tissues through intercellular communication involving a complex signaling network. WUSCHEL (WUS), a homeobox transcription factor (TF), is expressed in the organizing center (OC) which is a group of roughly 25-30 cells in the L3 (Yadav *et al.*, 2011). WUS protein migrates into the CZ and activates a negative regulator CLAVATA3 (CLV3). Besides, WUS suppresses the leucine-rich repeat receptor kinase CLAVATA1 (CLV1) directly (Busch *et al.*, 2010; Yadav *et al.*, 2011). The central CLV-WUS feedback loop is required for shoot meristem function (Dodsworth, 2009). The formation and maintenance of the specialized tissues depend on the spatiotemporal coordination of cell number, morphology, location and expression of differentiated functions.

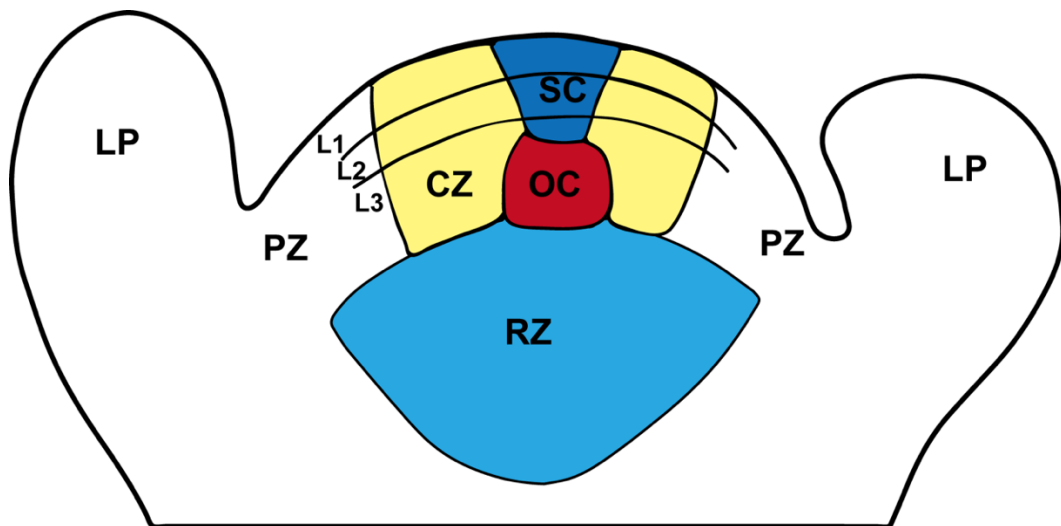


Figure 1 Schematic architecture of the shoot apical meristem of Arabidopsis.

Picture shows the stem cells (SC), the central zone (CZ), the organizing center (OC), the peripheral zone (PZ), the three layers L1 to L3, and the rib zone (RZ).

1.1.2 Plasmodesmata provide cell-to-cell connectivity

A main goal in understanding the mechanism of the intercellular communication is determining how proteins move between cells and what molecules mediate movement. Comprehensive studies in plants have established that cell-to-cell communication involves the intercellular trafficking of regulatory proteins, RNAs and protein-RNA complexes through the plasmodesmata (PD) and allows non-cell autonomous regulation of plant physiology and development (Lucas *et al.*, 1995; Oparka, 2004; Lucas and Lee, 2004; Gallagher and Benfey, 2005; Kim and Zambryski, 2005; Sager and Lee, 2018). Plant cells connect to their adjacent cells via PD which are one of the key cellular structures that distinguish plants from the animal system. Structurally, an individual channel consists of the cytoplasmic sleeve that is formed between the endoplasmic reticulum and the plasma membrane leaflets. PD vary in number and structure, and undergo constant adjustments to their permeability in response to many internal and external cues (Sager and Lee, 2018). Non-selective cell-to-cell movement of materials through the PD can be achieved by simple diffusion (Crawford and Zambryski, 2000; Wu, 2003). Targeted trafficking of macromolecules requires the interaction of proteins with PD or associated proteins to increase the size exclusion limit (SEL) of PD for their movement (Lucas *et al.*, 1995; Kim *et al.*, 2002). The maximum capability of molecules of PD transport defines PD aperture, known as the PD SEL. Receptor-like protein kinases that are important for controlling growth and developmental processes are partially associated with PD. For example, the receptor-like kinase STRUBBELIG (SUB) and C2-domain-containing receptor-like protein QUIRKY (QKY) interact at PD, which is thought to promote movement of unidentified intercellular factors needed for tissue morphogenesis (Vaddepalli *et al.*, 2014).

1.2 Plant receptor-like kinases (RLKs) in communication

All in all, protein kinases are known as molecular switches that regulate a protein by their phosphotransfer capability and play crucial roles in intercellular communication. Numerous studies over the years have shown protein kinases play prominent roles in cell differentiation, growth, development and physiology facets of high plants, which include organogenesis, hormone signaling, stress responses and disease resistance (Torii *et al.*, 1996; Clark, 1997; Torii and Clark, 2000; Tang *et al.*, 2005; Gish and Clark, 2011; Jagodzick *et al.*, 2018).

1.2.1 Classifications of plant RLKs

RLKs in plants belong to the same group of protein kinases as the Pelle family kinases in animals. The Arabidopsis genome sequence revealed more than 610 RLKs that represent 2.5% of the protein coding genes (Shiu and Bleecker, 2003; Morris and Walker, 2003; Liang and Zhou, 2018). Plant RLKs generally are predicted proteins with a signal peptide, an extracellular domain, a single transmembrane region, and cytoplasmic kinase domain. The very large family of Arabidopsis RLKs has been classified into several groups based on their domain organization (Torii and Clark, 2000; Shiu and Bleecker, 2001a, 2001b) (Figure 2).

S-domain class: S-RLKs possess an extracellular S-domain homologous to the self-incompatibility-locus glycoproteins (SLG) of *Brassica oleracea* (Nasrallah *et al.*, 1988). The S-domain consists of 12 conserved cysteine residues (10 of which are absolutely conserved) in a consensus CX5CX5CX7CXCX_nCX7CX_nCX3CX3CXCX_nC. The broad expression of many S-domain RLKs in many tissues and their induction linked to pathogenesis suggest possible roles in both developmental control and disease responses (Dwyer *et al.*, 1994; Pastuglia *et al.*, 1997; Pastuglia *et al.*, 2002).

LRR class: To date the largest class, are the leucine-rich repeat (LRR)-RLKs, with over 200 members in Arabidopsis. LRRs are 24 residue motifs that have a high portion of leucine and other hydrophobic residues. The number of LRRs in each LRR-RLK varies from just one or two to more than twenty-five. Ligands for some of these receptors have been identified, and they include endogenous proteins, sulfonated peptides, steroids and pathogen-derived peptide elicitors (Matsubayashi *et al.*, 2002; Gómez-Gómez and Boller, 2002; Butenko *et al.*, 2009).

TNFR class: CRINKLY4 (CR4) possesses tumor necrosis factor receptor (TNFR)-like repeats. The TNFR -like repeat motif has a conserved arrangement of six cysteines. ACR4, encoded by the Arabidopsis ortholog of CR4, is an epidermal-specific proteins that mediates several aspects of epidermal patterning, in addition to integument development in ovules (Gifford *et al.*, 2003; Gifford *et al.*, 2005).

EGF class: The cell wall-associated receptor kinases (WAKs) represent the epidermal growth factor (EGF) class. WAKs are encoded by five highly similar genes clustered in a 30-kb locus in Arabidopsis (He *et al.*, 1999; Kohorn and Kohorn, 2012). All WAKs contain the same conserved spacing of cysteine residues in the extracellular domain, the characteristic of the EGF repeat of metazoans (Sampoli Benitez and Komives, 2000).

PR class: A relatively smaller class of RLK members contain thaumatin-like domains. The Arabidopsis PR5K (PR5-like receptor kinase) is the known example of this class. The extracellular domain of PR5K exhibits sequence similarity to PR5 (pathogenesis related protein 5), whose expression is induced upon pathogen attack (Wang *et al.*, 1996). Thaumatin domains possess antifungal activity and *in vitro* chitinase activity (Fritig *et al.*, 1998).

Lectin class: All the LecRLKs possess three domains: an N-terminal lectin domain, an intermediate transmembrane domain, and a C-terminal kinase domain.

On the basis of lectin domain variability, LecRLKs have been subgrouped into three subclasses: L-, G-, and C-type LecRLKs. LecRLKs play important roles in development, stress conditions and hormonal response (Vaid *et al.*, 2013).

LysM class: Lysin motif receptor-like kinases contain three lysin motifs (LysMs) in their extracellular region. A LysM is a protein domain of about 40 AA found in most living organisms except in Archaea (Buist *et al.*, 2008; Buendia *et al.*, 2018). The LysM domain is conserved among prokaryotes and eukaryotes. Legume isoforms of RLKs with LysM-containing extracellular domains recognize symbiotic bacterial signals that trigger plant responses to facilitate the formation of nodules for nitrogen fixation (Arrighi *et al.*, 2006; Mulder *et al.*, 2006).

CrRLK1L class: Named after *Catharanthus roseus*, the species in which its first member (CrRLK1) was identified (Schulze-Muth *et al.*, 1996). CrRLK1L protein kinase subfamily, which contains FERONIA (FER), THESEUS1, HERKULES1 and HERKULES2 plays a central role in regulating fertilization, in monitoring the integrity of the cell wall and in cell expansion mechanisms such as cell elongation and tip growth, as well as having indirect links to plant-pathogen interactions (Hématy and Höfte, 2008; Galindo-Trigo *et al.*, 2016).

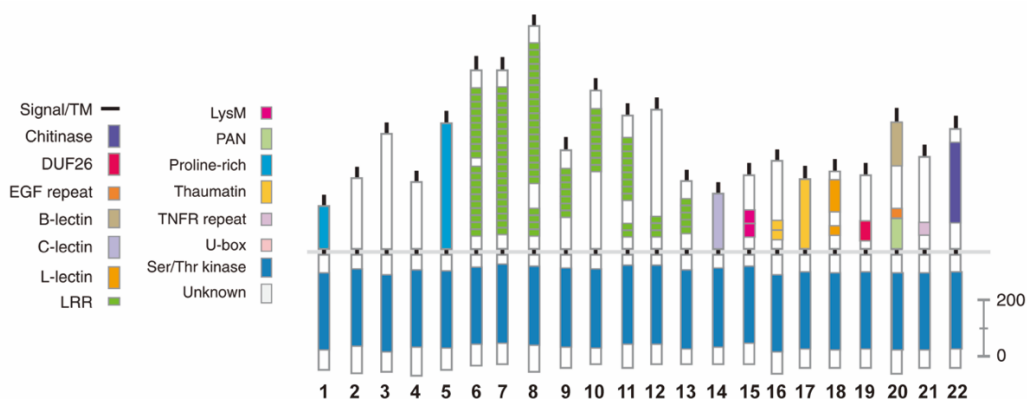


Figure 2 Representative RLKs and their classifications.

Introduction

The gray line represents the plasma membrane. The domains above the gray line are the putative extracellular domains with signal sequences. The area below the gray line represents the cytoplasmic side. PERK is the only representative with an extracellular domain but no signal sequence. The signal peptides are presumably absent in mature proteins and are displayed to demonstrate their presence in the RLKs. These representative RLKs are numbered as follows: 1, PERK; 2, RKF3; 3, CrRLK1; 4, LRK10; 5, At5g56890; 6, Xa21; 7, CLAVATA1; 8, BRI1; 9, TMKL1; 10, At1g53340; 11, TMK1; 12, LRRPK; 13, SERK; 14, At1g52310; 15, At3g26700; 16, WAK1; 17, PR5K; 18, LecRK1; 19, RKF2; 20, SRK; 21, CRINKLY4 and 22, CHRK1. TM, transmembrane region; DUF, domain of unknown function; EGF, epidermal growth factor; B-lectin, agglutinin; C-lectin, C-type lectin; L-lectin, legume lectin; LRR, leucine-rich repeat; LysM, lysin motif; PAN, plasminogen/apple/nematode protein domain; TNFR, tumor necrosis factor receptor. (Modified from Shiu S-H and Bleecker 2001b).

1.2.2 Functions of plant RLKs

Plant RLKs are involved in various biological processes by responding to a broad spectrum of external signals. On the one hand, RLKs involved in plant-microbe interactions and stress responses (Tang *et al.*, 2017). For instance, the Arabidopsis LRR-RLKs FLAGELLIN SENSING2 (FLS2) and EFR recognize a conserved 22-amino acid epitope (flg22) of the N terminus of the bacterial flagellin and a conserved N-terminal epitope (elf18) of the bacterial elongation factor Tu (EF-Tu), respectively (Gómez-Gómez and Boller, 2000; Bauer *et al.*, 2001; Kunze *et al.*, 2004; Zipfel *et al.*, 2006). On the other hand, RLKs are involved in the control of plant growth and development in normal conditions. One of the first receptor kinases shown to regulate plant development was CLV1, regulating stem cell maintenance and differentiation (Clark, 1997). The Brassinosteroids (BRs) are steroid hormones regulating a wide range of physiological processes during the plant life cycle from seed development to the modulation of flowering and senescence (Gruszka, 2013). ERECTA plays a crucial role in cell proliferation during organogenesis (Torii *et al.*, 1996). And ACR4 is required for normal L1 cell layer organization (Gifford *et al.*, 2005).

1.3 The role of endocytosis in plants

Endocytosis can be defined as a dynamic process by which cells take up extracellular material and cell surface proteins via vesicle compartments and that is controlled by a network of regulatory proteins (Fan *et al.*, 2015; Paez Valencia *et al.*, 2016). Endocytosis has been more extensively studied in animals than in plants. In the last decade, however, endocytosis in plant cells has received considerable attention, demonstrating its pivotal role in a plethora of cellular, development, and physiological processes, including cellular polarization, nutrient uptake, hormone transport, metal ion homeostasis, cytokinesis, signaling transduction, pathogen defense, and development (Robatzek *et al.*, 2006; Irani *et al.*, 2012; Du *et al.*, 2013; Barberon *et al.*, 2014; Luschnig and Vert, 2014; Wang *et al.*, 2015b; Mbengue *et al.*, 2016; Ortiz-Morea *et al.*, 2016; Yu *et al.*, 2016; Li and Pan, 2017).

1.3.1 Compartments of the plant endomembrane system

Plant cells exhibit a sophisticated endomembrane system that physically and functionally interconnects membranous compartments, allowing exchange of materials, such as proteins, polysaccharides, and lipids to their suitable cell locations (Morita and Shimada, 2014). These compartments are the plasma membrane, trans-Golgi network/early endosome (TGN/EE), multivesicular body/prevacuolar compartment (MVB/PVC), vacuole, Golgi apparatus and endoplasmic reticulum (Pizarro and Norambuena, 2014; Heucken and Ivanov, 2018) (Figure 3). The maintenance of the PM composition is in part achieved through exocytosis/secretion and endocytosis (Paez Valencia *et al.*, 2016; Reynolds *et al.*, 2018). In general, plant cells internalize PM-bound material or cargo via membrane transport into the trans-Golgi network (TGN), an organelle that also functions as an early endosome (EE) and that serves as a sorting hub for

subsequent trafficking pathways. The cargo may get recycled back to the PM via secretory vesicles. Cargo may also be destined to degradation via endosomal transport to multivesicular bodies (MVBs), also known as late endosomes (LEs), containing intra-luminal vesicles (ILVs). MVBs eventually fuse with the tonoplast discharging their content into the vacuolar lumen where it becomes degraded.

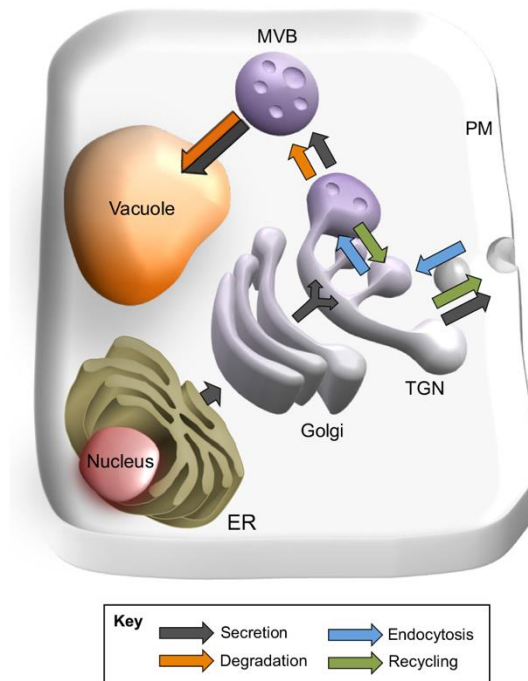


Figure 3 Endomembrane trafficking pathways in plant cells.

Proteins leaving the ER pass the Golgi and localize to the TGN, where the pathways towards the cell surface and the vacuole split (dark grey arrows). Proteins destined for the vacuole are transported into the MVB. PM material is endocytosed towards the TGN (blue arrow) and sent for vacuolar degradation via the MVB (orange arrows). During the early stages of MVB maturation, certain proteins can be retrieved from the vacuolar pathway and be recycled (green arrows). (Modified from Heucken and Ivanov, 2018).

1.3.2 Multiple, complex endocytic pathways

Endocytosis involves the internalization or uptake of PM proteins or extracellular materials into the cell via a series of vesicle compartments and thus plays a crucial role in cell-to-cell communication and cellular responses to environmental stimuli (Murphy *et al.*, 2005). Internalization of PM proteins is

mediated by clathrin-dependent and clathrin-independent endocytosis (Geldner and Robatzek, 2008; Robinson *et al.*, 2008; Irani and Russinova, 2009; Fan *et al.*, 2015; Paez Valencia *et al.*, 2016; Reynolds *et al.*, 2018). Similar to animal cells, clathrin-mediated endocytosis (CME) is the main mechanism for the entry extracellular material into plant cells. Several PM-resident receptors and transporters have been identified as endocytic cargoes, including leucine-rich repeat receptor-like kinases (RLKs) such as brassinosteroid (BR) insensitive 1 (BRI1) and flagellin sensing 2 (FLS2) and PEP RECEPTOR1 (PEPR1) in *Arabidopsis thaliana* (Robatzek, 2006; Di Rubbo *et al.*, 2013; Ortiz-Morea *et al.*, 2016). There also has been increasing recognition of the importance of a non clathrin-dependent mechanism(s) in plants. For example, in *Arabidopsis* the membrane micro-domain associated flotillin (Flot1) participates in clathrin-independent endocytosis (CIE) (Li *et al.*, 2012). Moreover, environmental conditions such as salt stress appear to influence cargo distribution between CME and CIE pathways (Baral *et al.*, 2015). Studies of fluid-phase endocytosis in plants have primarily relied on the use of ikarugamycin (IKA), which is a natural product that has been utilized as a CME inhibitor in plants and animals (Elkin *et al.*, 2016), to distinguish between CME and CIE uptake of extracellular markers.

1.3.3 CME, a central mechanism of PM-localized factors internalization

CME is regulated by multiple factors at multiple stages. CME is a central mechanism for the internalization of PM-localized material or cargo (Dhonukshe *et al.*, 2007; Paez Valencia *et al.*, 2016; Reynolds *et al.*, 2018). CME involves the budding of cargo-containing clathrin-coated vesicles (CCVs) from the PM. The CCVs are uncoated in seconds to form uncoated vesicles that fuse with the early endosome (EE) where the cargo is further sorted, either for recycling back to the PM, or to the vacuole for degradation (Figure 4).

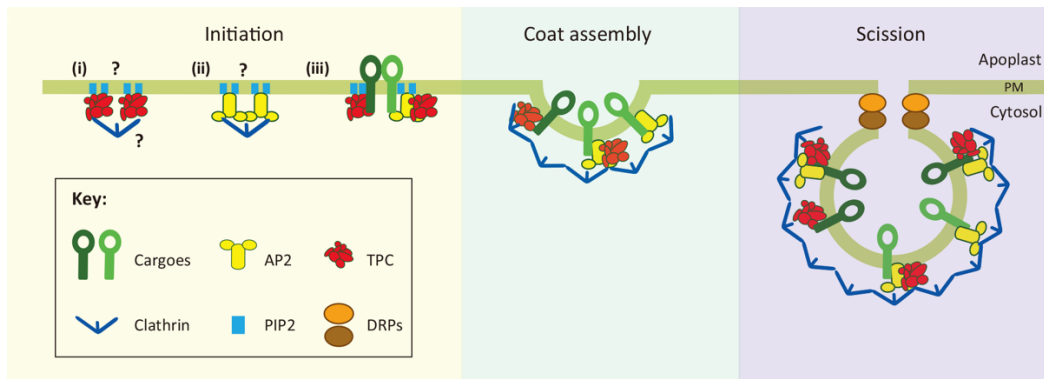


Figure 4 proposed model of CME in plants.

CME might start through stochastic association of the adaptors **(i)** TPLATE complex (TPC) and/or **(ii)** adaptor protein 2 complexes (AP2) with phosphatidylinositol 4,5-bisphosphate (PIP2) at the plasma membrane (PM); if the association with the cargo is stable enough, CME will proceed; or **(iii)** assembly of CME components induced by cargo sequestration. The initial adaptor proteins recruit additional clathrin triskelia, which polymerize and lead to coat assembly. After vesicle maturation, dynamin-related proteins (DRPs) are recruited to the neck site of the forming bud, where they polymerize and induce the scission of vesicle. Question marks indicate speculative events of plant CME: adaptor recruitment independently of cargo; TPC association with PIP2; and clathrin association with TPC independently of AP2. (Modified from Zhang *et al.*, 2015).

CME components in Arabidopsis. CCVs consist of vesicles surrounded by a polyhedral lattice of clathrin triskelia being made of three clathrin heavy chains (CHCs), each bound by a clathrin light chain (CLC) (Fotin *et al.*, 2004) (Figure 5). In Arabidopsis, three genes encode CLC chains while the likely redundant acting CHC1 and CHC2 encode clathrin heavy chains (Scheele and Holstein, 2002). Clathrin is also present at the TGN/EE, at a subpopulation of MVB/LEs, and at the cell plate indicating that it functions in multiple vesicular trafficking steps, and cytokinesis in the plant cell (Samuels *et al.*, 1995; Staehelin and Moore, 1995; Konopka *et al.*, 2008; Fujimoto *et al.*, 2010; Stierhof and El Kasmi, 2010; Van Damme *et al.*, 2011; Kang *et al.*, 2011; Ito *et al.*, 2012).

Besides clathrin, other components of the CME machinery have been reported. For example, the adaptor protein complex 2 (AP2) of Arabidopsis has been shown to be similar to its mammalian counterpart consists of four subunits (Di Rubbo *et al.*, 2013). The heterotetrameric AP2 comprising of two large (α , β 2) subunits, a medium (μ 2) and a small (σ 2) subunit, serves as a central player in the

initiation of clathrin-coated pit (CCP) nucleation (Bashline *et al.*, 2013; Fan *et al.*, 2013; Kelly *et al.*, 2014). The *ap2* mutants of *Arabidopsis* have been found to be defective in BR responses and reproductive organ development (Di Rubbo *et al.*, 2013; Yamaoka *et al.*, 2013). Recently, the activation of self-incompatibility signaling in transgenic *Arabidopsis* is considered to be independent of AP2-based CME (Yamamoto *et al.*, 2018). TPLATE, one of the adaptin-like proteins, was identified as a plant-specific adaptor complex for endocytosis and is involved in cell plate formation (Van Damme *et al.*, 2011; Gadeyne *et al.*, 2014; Zhang *et al.*, 2015). In addition, TPLATE plays critical role in the regulation of cellulose synthesis in *Arabidopsis* seedlings (Sánchez-Rodríguez *et al.*, 2018).

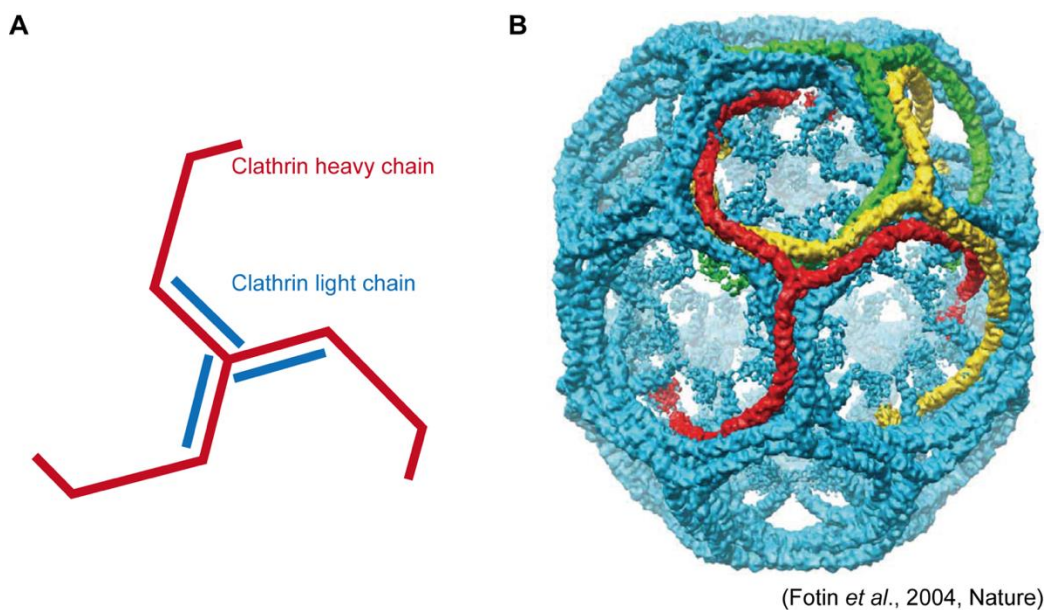


Figure 5 The clathrin envelope of an endocytosed vesicle consists of several clathrin triskelia.

(A) Schematic representation of a clathrin triskelion. A clathrin triskelion is formed by three clathrin heavy chains and three clathrin light chains, which join together at the center to form hexagonal barrel. (B) Structural representation of a complete clathrin envelope (Modified from Fotin *et al.*, 2004).

Following CCP initiation and cargo selection, maturation of CCPs involves further clathrin coat assembly and the recruitment of additional accessory proteins. For example, *Arabidopsis* AP180 can bind clathrin and promote clathrin assembly *in vitro* (Barth and Holstein *et al.*, 2004). TASH3 contains a Src homology 3 (SH3)

domain reported to recruit dynamin-related proteins (DRPs) (Gonzalez-Gutierrez *et al.*, 2007; Gadeyne *et al.*, 2014). DRPs, a large family of GTPase proteins, mediate membrane tubulation and scission. DRP2A and DRP2B were described as players during the scission of CCPs in Arabidopsis (Fujimoto *et al.*, 2010; Taylor, 2011).

1.3.4 The best known PM factors for receptor mediated endocytosis in plants

Fine-tuning the spatio-temporal dynamics of receptor-mediated endocytosis and endosomal trafficking is a central element in the regulation of RLK-dependent signal transduction. Such a mechanism can for example maintain the steady-state level of RLKs at the PM through recycling internalized RLKs back to the PM, promote signaling by activated RLK complexes localized on endosomes, or attenuate RLK signaling by controlled removal of activated receptors from the PM followed by sorting into MVBs and finally degradation in the vacuole (Geldner and Robatzek, 2008; Irani and Russinova, 2009; Di Rubbo and Russinova, 2012; Bakker *et al.*, 2017; Critchley *et al.*, 2018).

Following their internalization and subsequent trafficking upon RLK stimulation by exogenous application of ligand has been instrumental in analyzing the endocytic pathways of several plant RLKs, including BRASSINOSTEROID INSENSITIVE 1 (BRI1) (Rusinova *et al.*, 2004; Geldner *et al.*, 2007; Irani *et al.*, 2012; Di Rubbo *et al.*, 2013), FLAGELLIN SENSING 2 (FLS2) (Robatzek *et al.*, 2006; Beck *et al.*, 2012; Du *et al.*, 2013; Mbengue *et al.*, 2016), or PEP1 RECEPTOR 1 (PEPR1) (Ortiz-Morea *et al.*, 2016).

Brassinosteroid insensitive1 (BRI1), a constitutive endocytosis RLK

The LRR RLK BRI1, which is responsible for the perception of brassinosteroid (BR) in Arabidopsis (Kinoshita *et al.*, 2005), is one of the prime examples for the known ligand-receptor pairs. BRI1 plays fundamental roles in

BR signaling and plant development (Wang *et al.*, 2001; Wang and He, 2004). Knock-out mutants of *BRI1* are extremely dwarfed and completely BR insensitive (Clouse *et al.*, 1996; Li and Chory, 1997; Kinoshita *et al.*, 2005). It was shown that BRI1 is present at the PM as well as in intracellular mobile vesicle in root meristem cells (Rusinova *et al.*, 2004; Geldner *et al.*, 2007). BRI1-GFP colocalizes with the endocytic tracer FM4-64 and the trans-Golgi network/early endosome marker VHAa1-RFP, and its localization is sensitive to brefeldin A (BFA), an inhibitor of endosomal trafficking (Rusinova *et al.*, 2004; Irani *et al.*, 2012; Wang *et al.*, 2015a). Exogenous application of BR, depletion of endogenous BR levels, and reapplication of BR to previously depleted plants did not cause any changes in the BRI-GFP endosomal pool (Geldner *et al.*, 2007). Thus, BRI1 endocytic trafficking appears to be constitutive (ligand-independent). Recently, a BR analog labeled with a small fluorophore, Alexa Fluor 647, allowed the specific tracking of the endocytosis of the BRI1-ligand complexes in Arabidopsis meristem root tip cells (Irani *et al.*, 2012). Taken together, upon perceiving BRs, plant cells activate BRI1 kinase to trigger the dissociation of the inhibitory BRI1 KINASE INHIBITOR 1 (BKI1), thus enabling sequential transphosphorylation of BRI1 and its co-receptor BRI1 associated kinase 1 (BAK1) to form an active receptor complex, thereby initiating BR signaling (Figure 6).

Ligand-regulated receptors

Another well-studied LRR-RLK is FLAGELLIN SENSING 2 (FLS2) recognizing bacterial flagellin (flg22). Flagellin perception is essential for efficient host defense, since *fls2* mutant plants exhibit an enhanced disease susceptibility to bacterial infections (Zipfel *et al.*, 2004). Transgenic lines that express a functional FLS2-GFP fusion driven by its native promoter revealed subcellular localization of the nonactivated receptor at the PM. Upon activation with flg22, FLS2-GFP was found to transfer into endocytic compartments, followed by degradation. This induced uptake of FLS2 was specific to its ligand and required for receptor

activation (Robatzek *et al.*, 2006). The internalization of FLS2 requires BAK1 and can be abolished by single amino acid substitutions in the FLS2 kinase domain that may be subject to posttranslational modifications, such as phosphorylation and ubiquitination (Robatzek *et al.*, 2006; Salomon and Robatzek, 2006; Chinchilla *et al.*, 2007). Interestingly, FLS2 localizes to bona fide endosomes through two different endocytic trafficking routes depending on its activation status (Beck *et al.*, 2012). FLS2 constitutively recycle in a BFA sensitive behavior while flg22-activated receptors traffic via ARA7/Rab F2b- and ARA6/Rab F1-positive endosomes insensitive to BFA (Figure 7). Lately, the treatment of Arabidopsis cotyledons with an N-terminally labeled fluorescent TAMRA-flg22 revealed the concomitant uptake of the ligand with the receptor (Mbengue *et al.*, 2016).

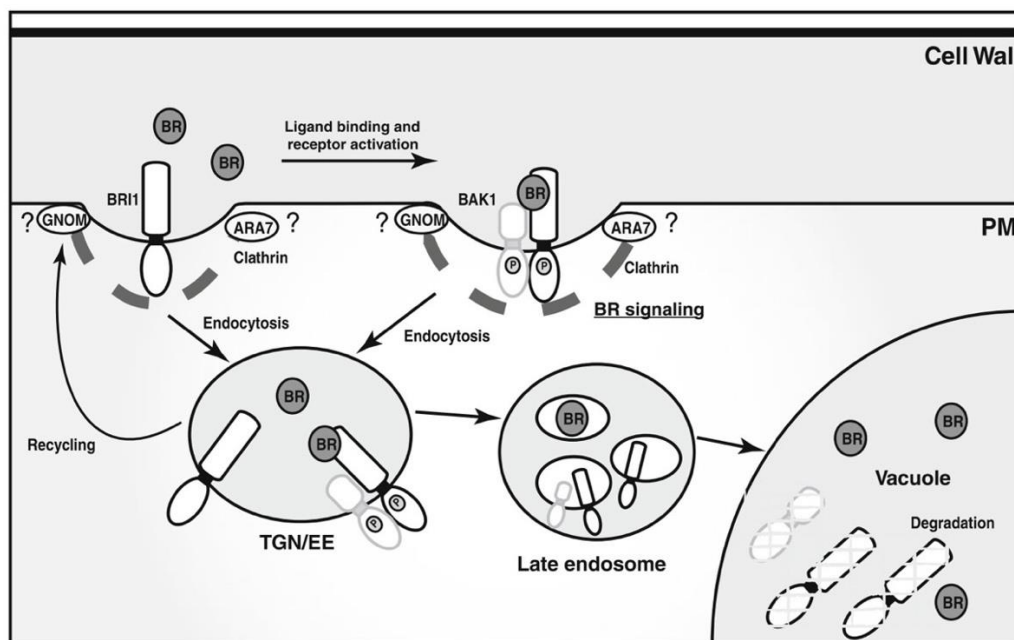


Figure 6 Schematic overview of the endocytic pathways of BRI1.

Independent of ligand BRI1 undergoes constitutive endocytosis. Upon BR binding, BRI1 form complex with BAK1, activated BRI1 undergoes clathrin-mediated endocytosis and is sorted to TGN/EE. Subsequently, BRI1 either recycled back to the PM or targeted to the vacuole. (Modified from Di Rubbo and Russinova, 2012)

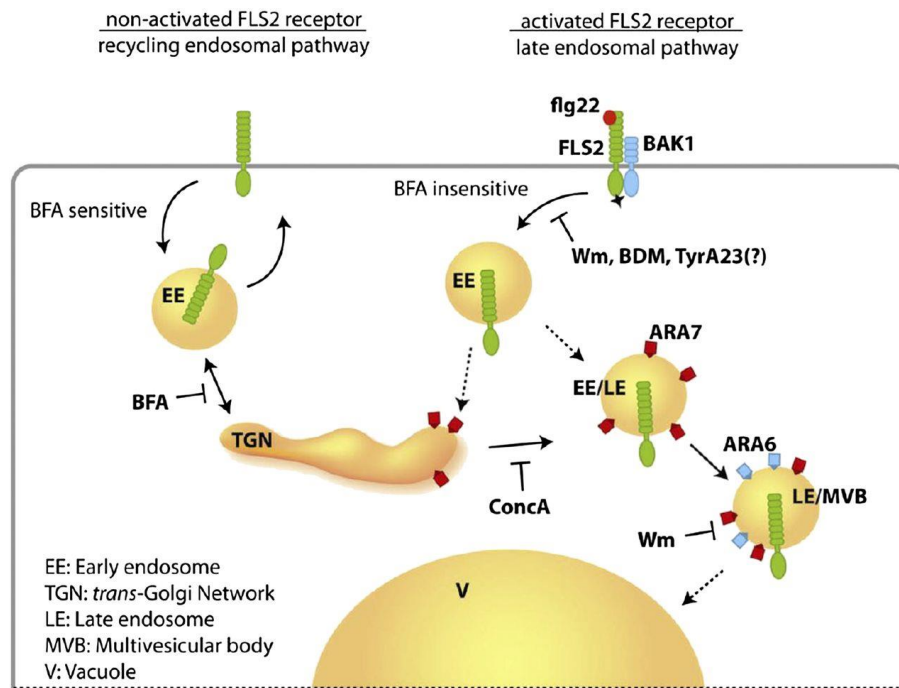


Figure 7 Schematic overview of the endocytic pathways of FLS2.

Depending on its activation status, FLS2 enters two distinct endosomal pathways. The nonactivated receptor follows a recycling and BFA-sensitive endosomal pathway. FLS2 receptors activated by its ligand flg22 traffic via a BFA-insensitive pathway and are sequentially transported via ARA7/Rab F2b- and ARA6/Rab F1-positive and ConcA- and Wm-sensitive endosomes to the vacuole. (Modified from Beck *et al.*, 2012)

In addition to FLS2, receptors for damage-associated endogenous peptides such as PEP RECEPTOR 1 (PEPR1) and PEPR2 perceive the *Arabidopsis thaliana* elicitor peptides (*AtPeps*) family (Tang *et al.*, 2015). The 10 C-terminal amino acids of *AtPep1* bind the PEPR1-LRR domain and trigger interaction between PEPR1 and its coreceptor (BAK1). The PEPR-mediated signaling components and responses have been studied extensively (Huffaker *et al.*, 2006; Krol *et al.*, 2010). Only recently, the *AtPep1* was shown to decorate the PM in a receptor-dependent manner and cointernalized with PEPRs (Ortiz-Morea *et al.*, 2016). Although some PEPR1-GFP labeled intracellular puncta were detected even without pep1 treatment, their presence was induced by pep1 in a time- and dose-dependent manner and was largely colocalized with the endocytic tracer FM4-64. The *AtPep1*-PEPR trafficking is largely independent of V-ATPase

activity at the TGN/EE and PEPR1 secretion depends on ARF-GEF. Inducible overexpression of the Arabidopsis clathrin coat disassembly factor, Auxilin2, which inhibits CME, impaired the *AtPep1*-PEPR1 internalization and compromised *AtPep1*-mediated responses (Ortiz-Morea *et al.*, 2016).

1.4 The atypical leucine-rich repeat RLK, STRUBBELIG (SUB)

1.4.1 SUB regulate tissue morphogenesis in Arabidopsis

Control of tissue morphogenesis in *Arabidopsis thaliana* involves the leucine-rich repeat (LRR) receptor-like kinase (RLK) STRUBBELIG (SUB) which was first identified based on an ovule phenotype (Schneitz *et al.*, 1997; Chevalier *et al.*, 2005). SUB, also known as SCRAMBLED (SCM), controls several developmental processes, including floral morphogenesis, integument outgrowth, leaf development and root hair patterning (Kwak *et al.*, 2005; Chevalier *et al.*, 2005; Fulton *et al.*, 2009; Lin *et al.*, 2012).

At the macroscopic level, aboveground of *sub* mutants show a pleiotropic phenotype. Inflorescences are characterized by reduced height, an irregularly twisted stem, and an aberrant phyllotaxis of flowers. Flowers open prematurely and show a large percentage of twisted and often notched petals. Furthermore, all flowers exhibit twisted carpels and about 70 percent of *sub-1* ovules showed aberrant initiation of the outer integument. This results in outer integuments with gaps that often resemble “multifingered clamps” or “scoops”. In particular the distal or micropylar cells of the outer integument can show aberrant size and shape. Moreover, 4-week old *sub-1* plants exhibit obviously reduced plant height compared to wild type (Figure 8).

In addition, *sub* mutants displayed temperature-sensitive leaf development defects (Lin *et al.*, 2012). The *sub-2* mutant in the Col-0 background was identified and displayed impaired blade development, asymmetric leaf shape and altered

venation patterning under high ambient temperature (30°C), but these defects were less pronounced at normal growth temperature (22°C).

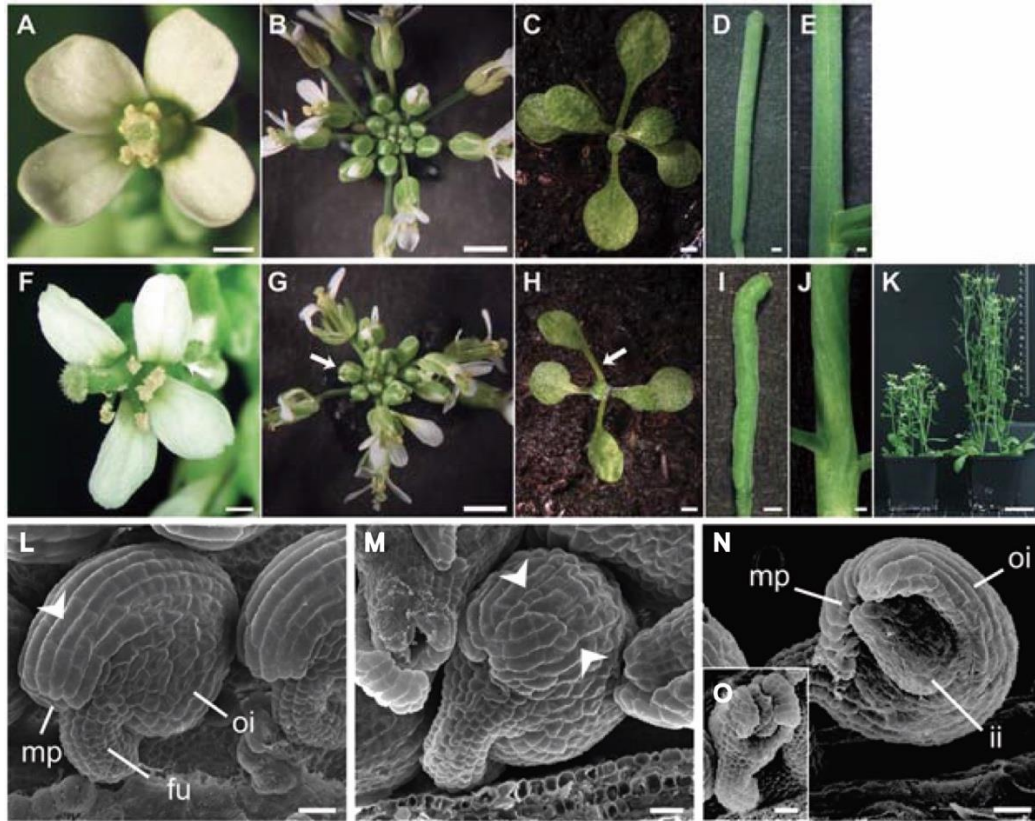


Figure 8 Phenotype comparison of the overall above-ground morphology of *Ler* and *sub-1*.

(A-E) Wild-type *Ler*. (F-K) *sub-1*. (A, F) An open stage 13 flower from a 30-day old plant. Note the misorientation of petals due to twisting in the basal end of the petal structure (arrows). (F) Petals can also show small notches. (B, G) Top view of a 30-day inflorescence. (G) Flower phyllotaxis is irregular. Arrows mark prematurely opened flower buds. (C, H) Top view of a 12-day rosette. (H) Leaf petioles can be twisted (arrow). (D, I) Morphology of mature siliques. (E, J) A lateral view of a section of stems from a 30-day plant. (K) Plant height *sub-1* (left) in comparison to *Ler* (right). (L-N) Scanning electron micrographs of stage 4 ovules. (L) Wild-type *Ler*. The arrow marks one of the elongated cells of the distal outer integument. (M) *sub-1*. A mild phenotype is shown. Note the irregular size and shape of cells at the distal outer integument (arrow heads, compare to (L)). (N, O) *sub-1*. Strong phenotypes are depicted. Note the half-formed outer integument. (O) shows an example where the outer integument shows several gaps. Scale bars: (A, D, E, F, I, J) 0.5 mm, (B, C, G, H) 2 mm, (K) 3 cm, (L, M, N, O) 20 μ m. (Modified from Fulton *et al.*, 2009).

At the cellular level, occasional periclinal divisions in the L2 layer of stage-3 floral meristem were observed, and the shape of the L2 layer cells seemed more

irregular in *sub-1* mutant (Figure 9). The horizontal stem sections of 30-day old *sub-1* stem revealed reduced number of epidermal, cortex, and pith cells. The pith cells in particular appeared smaller. Furthermore, SUB also helps unspecified root epidermal cells to interpret their position in relation to underlying cortical cells and establish root hair cell identities in an independent study (Kwak *et al.*, 2005; Chevalier *et al.*, 2005; Kwak and Schiefelbein, 2007; Fulton *et al.*, 2009).

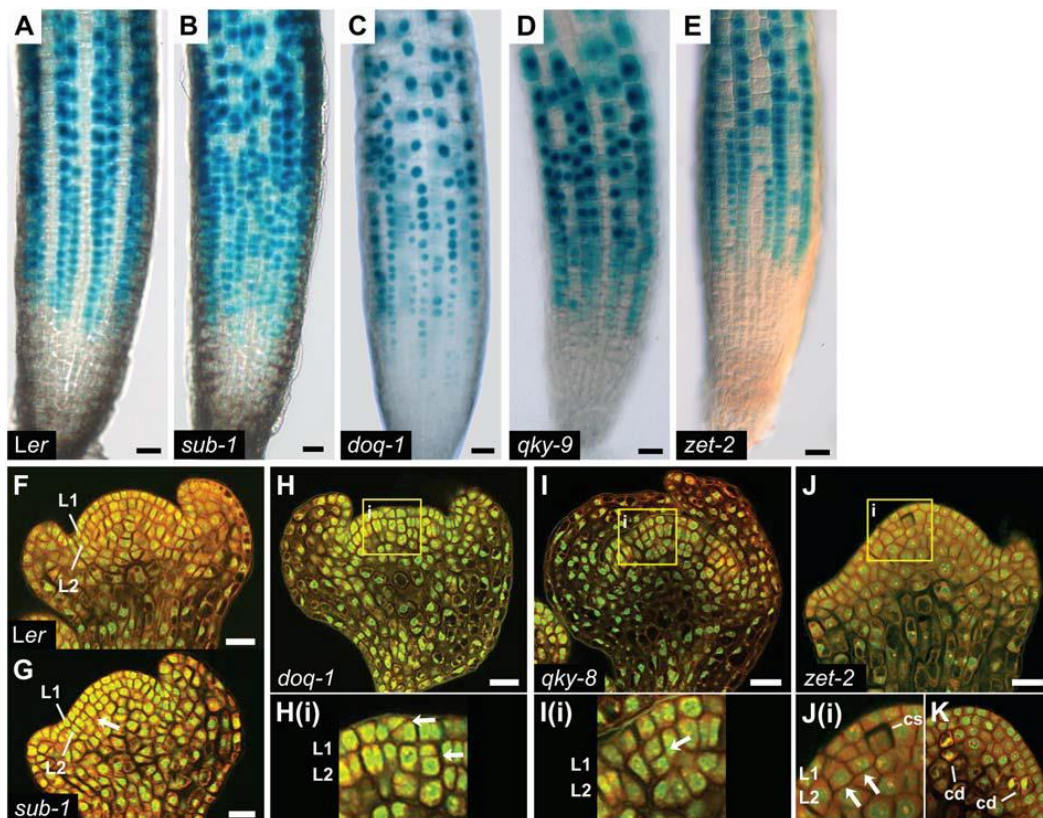


Figure 9 Analysis of cellular defects in 4-day old main roots and stage 3 floral meristems of *sub-1*, *doq-1*, *qky-8* and *zet-2* mutants.

(A-E) Expression of the GL2::GUS reporter in whole-mount main roots. (A) WT *Ler* root. The reporter is detected in regular files of non-hair cells. (B-E) GL2::GUS reporter expression is patchy. (F-K) Mid-optical sections through propidium-iodide-stained stage 3 floral meristems. (F) WT *Ler*. Note the regular arrangement of cells in the L1 and L2. (G) *sub-1*. The arrow marks a periclinal cell division event. (H) *doq-1*, (I) *qky-8*, (J-K) *zet-2*. The regions marked by the square (i) are shown at higher magnification in (Hi), (Ii), (Ji). (Hi) The arrows highlight aberrant oblique and periclinal cell divisions in the L1 and L2, respectively. (Ii) The arrow labels a periclinal cell division in the L2. (Ji) The arrows highlight periclinal cell divisions. A cell undergoing cell separation is indicated. (K) Disintegrating cells are marked. Abbreviations: cd, cell disintegration;

cs, cell separation; L1, L1 cell layer; L2, L2 cell layer. Scale bars: (A-E) 25 μ m, (F-K) 20 μ m. (Modified from Fulton *et al.*, 2009).

1.4.2 SUB may represent an atypical RLK

SUB is predicted to encode a LRR-RLK of 768 aa with a calculated molecular mass of 84.5 KDa. Sequence analysis predicts that *SUB* contains a signal peptide of 24 aa, a SUB domain shared between the LRR-V members, six LRRs, a proline-rich region, a transmembrane domain (TM), a juxta-membrane domain (JM), and a carboxyl-terminal kinase domain (KD) (Kwak *et al.*, 2005; Chevalier *et al.*, 2005; Fulton *et al.*, 2009; Vaddepalli *et al.*, 2011) (Figure 10).

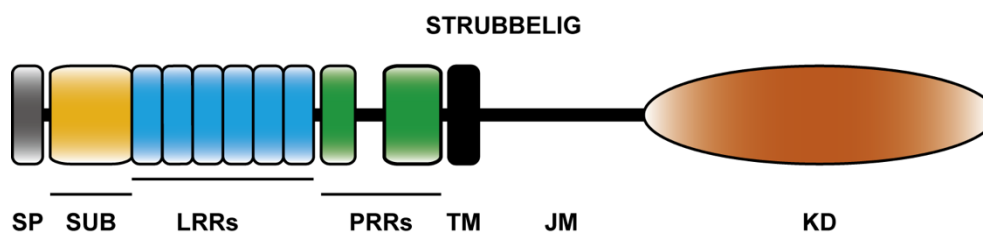


Figure 10 Overview of the domain architecture of SUB.

Abbreviations: JM, juxtamembrane domain; KD, kinase domain; LRR, leucine-rich repeat; PRR, proline-rich repeat; SP, signal peptide; SUB, SUB-domain; TM, transmembrane domain. Length of *SUB* protein: 768 amino acids. (Modified from Vaddepalli *et al.*, 2011).

SUB kinase domain has the characteristics of a typical protein kinase (Hanks and Quinn, 1991). However, there are two notable alterations within the catalytic loop of the WT *SUB* kinase domain. *SUB* carries an asparagine at a position (N-625) where functional protein kinases usually contain an aspartate. In addition, *SUB* features a lysine at position 630. In contrast, plant RLKs with experimentally detectable kinase activity feature an asparagine at this position. Both residues are important for the catalytic mechanism (Johnson *et al.*, 1996; Huse and Kuriyan, 2002). Biochemical assays using bacterially expressed fusion proteins indicate that the *SUB* kinase domain lacks enzymatic phosphotransfer activity. In a genetic

approach, three different mutant variants *SUB*_{G506A}, *SUB*_{K525E} and *SUB*_{E539A}, which are predicted to affect ATP binding to eliminate kinase activity, were introduced into *sub-1* mutant. Interestingly, they were able to rescue all above-ground aspects of the *sub-1* mutant phenotype. Moreover, several substitutions such as two semi-conserved threonines (T486A/E and T494A) in the juxtamembrane and kinase domains and the single serine in the activation loop (S656A) were tolerated which indicate that phosphorylation of these residues is not required for SUB function. Although the phenotypic *sub-4* and *sub-19* alleles hint the importance of the kinase domain for SUB function, SUB represents an atypical receptor kinase as enzymatic activity of its kinase domain is not required for its function *in vivo* (Chevalier *et al.*, 2005; Vaddepalli *et al.*, 2011).

1.4.3 SUB acts in a non-cell-autonomous fashion

Reporter assays using a functional translational fusion between SUB and EGFP indicate that SUB is expressed in a broad fashion in floral meristems and young ovules (Chevalier *et al.*, 2005). In particular, SUB:EGFP expression in the distal nucellus of ovule primordia can rescue to a large extent defects in the integuments, tissue that originates from the central chalaza. In floral meristems, the reporter was detected in the L3 layer is sufficient to rescue the L2 division plane defects (Yadav *et al.*, 2008). Further clonal analysis of SUB:EGFP fusion proteins driven by tissue-specific promoters shows that SUB affect development of neighboring cells in a non-cell-autonomous fashion. In ovules, the WUSCHEL (WUS) promoter governs expression specifically in the nucellus, a tissue distal to the integuments (Groß-Hardt *et al.*, 2002). MERISTEM LAYER 1 (ML1) promoter activity is exclusively detected in the epidermis throughout much of plant development (Lu *et al.*, 1996; Sessions *et al.*, 1999). While *AINTEGUMENTA* (*ANT*) and *SUB* expression patterns largely overlap there are some noteworthy distinctions. In the inflorescence meristem *ANT* is detected

throughout the flower primordia and developing floral organs, but is not observed in the central zone and interior L3 or deeper layers (rib zone) of the inflorescence meristem (Elliott *et al.*, 1996; Long and Barton, 2000). During ovule development *ANT* expression can be seen throughout stage 1 ovules but subsequently becomes restricted to the chalaza, developing integuments, and the distal part of the funiculus (Elliott *et al.*, 1996; Balasubramanian and Schneitz, 2000). *WUS::SUB:GFP* could rescue the *sub* ovule phenotype to a large extent, the *ML1::SUB:GFP* transgene could amend all scored aspects of the *sub* phenotype, although some cell division problems in the stem remained, and the *ANT::SUB:GFP* rescue *sub* phenotype precluding the small reduction in stamen number (Yadav *et al.*, 2008; Fulton *et al.*, 2010).

1.4.4 Mechanistic basis of signaling through atypical RLKs

In plants little is known about signaling by atypical kinase. In general, the corresponding mechanisms are believed to rely on regulated protein-protein interactions (Kroither *et al.*, 2001; Boudeau *et al.*, 2006; Castells and Casacuberta, 2007). Known mechanisms potentially depend on the phosphorylation of the atypical RLK by other kinases or on the stimulation of functional kinases by the atypical RLK. For example, the *Arabidopsis thaliana* protein CRINKLY4-RELATED 2 (AtCRR2) can be phosphorylated *in vitro* by its homologue ACR4, indicating that these two receptors may form a heterodimer involved in ACR4 signaling (Cao *et al.*, 2005). In contrast, a maize atypical receptor kinase, MARK was found to interact with the functional GCN (general control non-derepressible)-like MIK (MARK-interacting kinase) *in vitro* and in COS-7 cells (Llompart *et al.*, 2003), but apparently the MIK interaction did not result in the phosphorylation of MARK. Interestingly, it brought about a several fold stimulation of MIK kinase activity.

Introduction

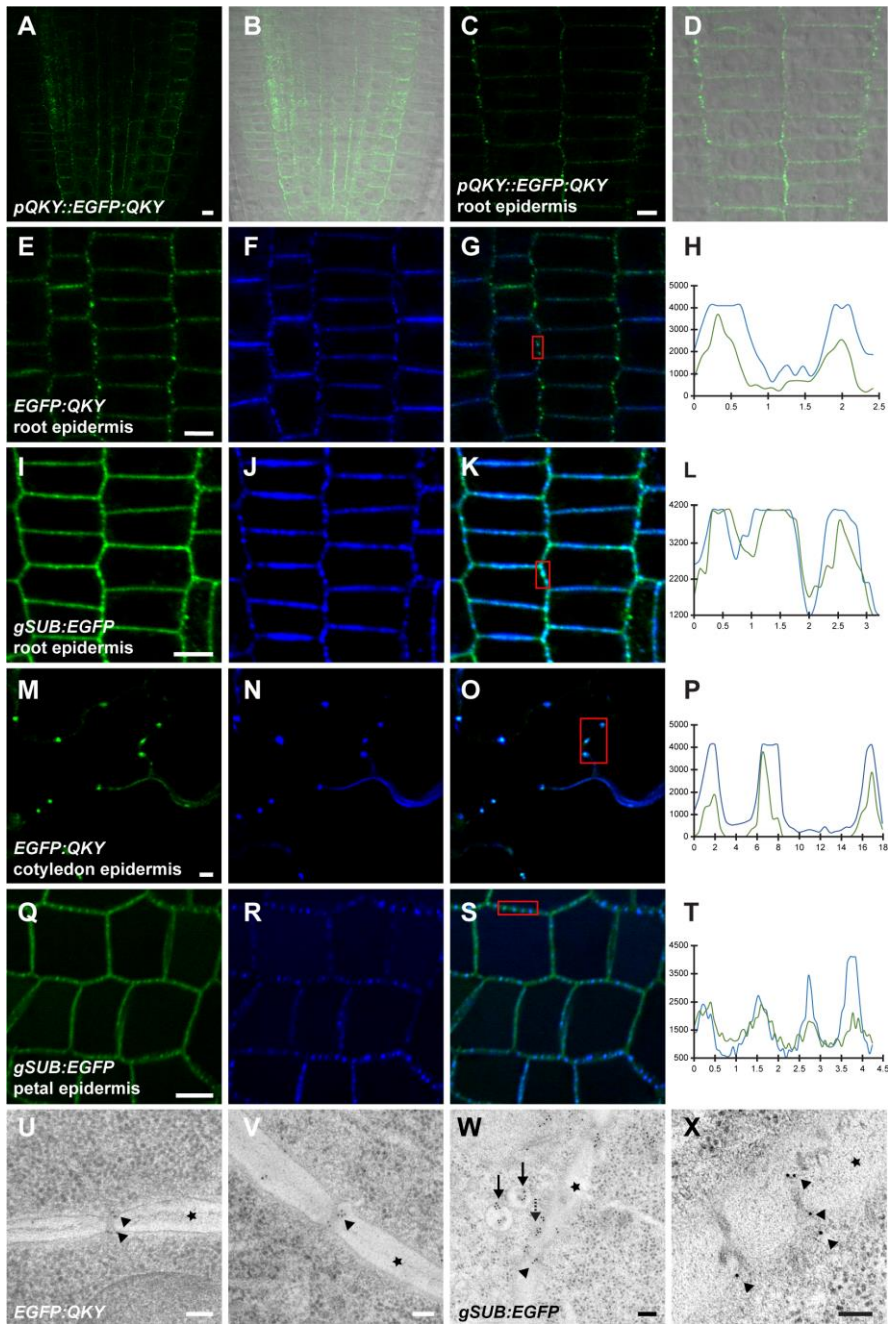


Figure 11 Subcellular localization of QKY and SUB.

(A-G, I-K, M-O, Q-S) Confocal micrographs of 6-day *qky-8* pQKY::EGFP:QKY roots. There is punctate signal distribution along the circumference of individual cells. (A) Overview of root tip. (B) Overlay with differential interference contrast (DIC) channel. (C,D) Similar to A,B but at higher magnification. (E-G, M-O) Confocal micrographs of *qky-8* EGFP:QKY stained with Aniline Blue. (I-K, Q-S) Confocal micrographs of *sub-1* gSUB:EGFP stained with Aniline Blue. (E,I,M,Q) GFP signal. (F,J,N,R) Aniline Blue signal. (G,K,O,S) Overlay of Aniline Blue and GFP channels. (H,L,P,T) Intensity profiles measured along a line connecting the dots highlighted by the red rectangle in G,K,O,S, respectively. The x-axis marks the distance in μm . The y-axis denotes arbitrary intensity units. (U-X) Immunogold electron micrographs. The reporters are

indicated. Subepidermal cortical cells in the flank of the root just behind the meristem of 7-day seedlings are depicted. Arrowheads indicate signals at plasmodesmata. The asterisk indicates the cell wall. (U) Signal is seen at the neck region of a plasmodesma. (V) Signal is detected in a more central region of a plasmodesma. (W) Signal can also be seen at multivesicular bodies (black arrows) and plasma membrane (blue arrow). (X) Signal is detected at plasmodesmata. Scale bars: 5 μm in A-G,I-K,M-O,Q-S; 0.1 μm in U-X. (Modified from Vaddepalli *et al.*, 2014)

1.4.5 Novel components in SUB signaling pathway

Using a forward genetic approach three additional genetic factors were identified, *QUIRKY* (*QKY*), *ZERZAUST* (*ZET*), and *DETORQUEO* (*DOQ*) (Fulton *et al.*, 2009). The *qky-8*, *zet-2* and *doq-1* mutants showed a *sub*-like phenotype and cellular defects, in outer integument development, floral organ shape, stem twisting, the floral meristem and root hair patterning (Figure 9). *QKY*, *ZET* and *DOQ* were proven to contribute to *SUB*-dependent organogenesis and shed light on the mechanisms, which are dependent on signaling through the atypical receptor-like kinase *SUB* (Fulton *et al.*, 2009).

SUB not only localizes to the plasma membrane (PM) but is also present at PD (Yadav *et al.*, 2008; Vaddepalli *et al.*, 2014), channels interconnecting most plant cells (Otero *et al.*, 2016; Sager and Lee, 2018), where it physically interacts with the PD-specific protein *QKY* (Vaddepalli *et al.*, 2014) (Figure 11). In line with a function in RLK-mediated control of PD-based intercellular communication *SUB* and *QKY* function in a non-cell-autonomous manner (Yadav *et al.*, 2008; Vaddepalli *et al.*, 2014) indicating that *SUB* signaling involves a yet unknown factor that moves between cells. More recently, a genetic link of *SUB* signaling to cell wall biology has also been put forward as the cell wall-localized β -1,3 glucanase *ZET* participates in *SUB* signal transduction and *sub*, *qky* and *zet* mutants share overlapping defects in cell wall biochemistry (Fulton *et al.*, 2009; Vaddepalli *et al.*, 2017) (Figures 9 and 11).

1.4.6 Intracellular localization of SUB

SUB can be found in internal compartments as well (Kwak and Schiefelbein, 2008; Yadav *et al.*, 2008; Vaddepalli *et al.*, 2011; Wang *et al.*, 2016a). SUB is glycosylated in the endoplasmic reticulum (ER) (Hüttner *et al.*, 2014), subject to ER-associated protein degradation (Vaddepalli *et al.*, 2011; Hüttner *et al.*, 2014). It was recently shown that ovules of plants homozygous for a hypomorphic allele of *HAPLESS13* (*HAP13*) preferentially accumulate signal from a functional SUB:EGFP reporter in the cytoplasm, rather than the PM (Wang *et al.*, 2016a). *HAP13/AP1M2* encodes the $\mu 1$ subunit of the adaptor protein (AP) complex AP1 that is present at the TGN/EE network and is involved in post-Golgi vesicular trafficking to the PM, vacuole and cell-division plane (Park *et al.*, 2013; Teh *et al.*, 2013; Wang *et al.*, 2013). Interestingly, ovules of plants with reduced *HAP13/AP1M2* activity show *sub*-like integuments (Wang *et al.*, 2016a). These results indicate that the AP1 complex is involved in subcellular distribution of SUB in a functionally relevant manner.

1.5 Objectives

Plant RLKs are involved in the coordination of growth pattern during organogenesis. The trafficking mechanisms for most plant cell surface receptors are unclear. The atypical receptor-like kinase SUB-mediated signaling pathway regulates cell proliferation, cell size and cell shape during plant development. To thoroughly characterize SUB function, it is crucial to determine the endosome trafficking of SUB within the cell. In this study, I wanted to further assess the internalization and subsequent endocytic trafficking behavior of SUB.

2 Materials and Methods

2.1 Plant work, plant genetics and plant transformation

Arabidopsis thaliana (L.) Heynh. var. Columbia (Col-0) and var. Landsberg (*erecta* mutant) (*Ler*) were used as wild-type strains. Plants were grown as described earlier (Fulton *et al.*, 2009). The *sub-1* (in *Ler*) was described previously (Chevalier *et al.*, 2005). The *sub-9* mutant (Col), carrying a T-DNA insertion (SAIL_1158_D09), was described in (Vaddepalli *et al.*, 2011). The *chc1-1* (SALK_112213), *chc1-2* (SALK_103252), *chc2-1* (SALK_028826) and *chc2-2* (SALK_042321) alleles (all Col) (Alonso *et al.*, 2003) were described in (Kitakura *et al.*, 2011). The T-DNA lines *ap2a1* (SALK-045252), *ap1/2b2* (SALK-150980), *ap2m* (SALK-083693) and *ap2s* (SAIL-240-C03) (all Col) were obtained from NASC and described in (Bashline *et al.*, 2013; Kim *et al.*, 2013; Yamaoka *et al.*, 2013). Wild-type and mutant plants were transformed with different constructs using *Agrobacterium* strain GV3101/pMP90 (Koncz and Schell, 1986; Sambrook *et al.*, 1989) and the floral dip method (Clough and Bent, 1998). Transgenic T1 plants were selected on Kanamycin (50 µg/ml), Hygromycin (20 µg/ml) or Glufosinate (Basta) (10 µg/ml) plates, and around 10 dag, viable seedlings were transferred to soil for further inspection. The hydroxytamoxifen-inducible line INTAM>>RFP-HUB/Col line (HUB) was described previously (Robert *et al.*, 2010; Kitakura *et al.*, 2011).

Seedlings were grown on half-strength Murashige and Skoog (1/2 MS) agar plates (Murashige and Skoog, 1962). Before sowing seeds on 1/2 MS, they were surface sterilized in 3.5% (V/V) sodium hypochlorite (NaOCl) plus 0.1% (V/V) Triton X-100 for 10min on a rotator to prevent bacterial and fungal growth on plates. Seeds were washed three times with ddH₂O and stratified for 4d at 4 °C prior to incubation. Dry seeds were sown on soil (Patzer Einheitserde, extra-

gesiebt, Typ T, Patzer GmbH & Co. KG, Sinnatal-Jossa, Germany) situated above a layer of perlite, stratified for 4 days at 4 °C and then placed in a long day cycle (16 hrs light) using Philips SON-T Plus 400 Watt fluorescent bulbs. The light intensity was 120-150 $\mu\text{mol}/\text{m}^2\text{sec}$. The plants were kept under a lid for 7-8 days to increase humidity (50-60%) and support equal germination.

2.2 Recombinant DNA work

For DNA and RNA work standard molecular biology techniques were used. DNA and RNA used for cloning were extracted from *Arabidopsis thaliana* using the NucleoSpin Plant II kit (Macherey-Nagel GmbH und Co. KG) and the NucleoSpin RNA plant kit (Macherey-Nagel GmbH und Co. KG). RNA was used as a template, mRNA was reverse transcribed into cDNA using the RevertAid 1st strand cDNA synthesis kit (Fermentas) and a poly-T primer according to the manufacturer's protocol. Cloning was performed using standard methods described in (Sambrook *et al.*, 1989). PCR-fragments used for cloning were obtained using Q5 high-fidelity DNA polymerase (New England Biolabs, Frankfurt, Germany). Restriction enzymes and T4 DNA Ligase used for cloning were also received from NEB GmbH and used according to the manufacturer's protocols. PCR products were purified using the NucleoSpin Gel and PCR clean-up kit (Macherey-Nagel GmbH und Co. KG) according to the manufacturer's protocol. Plasmids were isolated with the NucleoSpin Plasmid kit (Macherey-Nagel GmbH und Co. KG) according to the manufacturer's protocol. *Escherichia coli* strain DH10 β was used for amplification of the plasmids. Bacteria were grown on corresponding selection media (Lysogeny broth). Antibiotics for bacterial selection were used at final concentrations as follows:

Kanamycin 50 $\mu\text{g}/\text{mL}$; Ampicillin 100 $\mu\text{g}/\text{mL}$; Gentamycin 25 $\mu\text{g}/\text{mL}$; Spectinomycin 100 $\mu\text{g}/\text{mL}$; Tetracyclin 12.5 $\mu\text{g}/\text{mL}$; and Rifampicin 10 $\mu\text{g}/\text{mL}$.

All PCR-based constructs were sequenced by MWG-Biotech AG following the company's standards. Sequencing results were aligned with geneious software to reference sequences received from The Arabidopsis Information Resource (TAIR, www.arabidopsis.org). The plasmids pCAMBIA2300 (www.cambia.org) and pGGZ001 (Lampropoulos *et al.*, 2013) were used as binary vectors. Details of the PCR reaction mix and steps involved in PCR using both Q5 high-fidelity DNA polymerase and Taq polymerase have been summarized in Table 1. Vectors used in this work are listed in Table 2. Detailed information for all oligonucleotides used in this study are listed in supplementary material Table S1.

Table 1 PCR reaction mix and cyclor program.

Reaction mix for Q5[®] High-Fidelity DNA polymerase based PCR amplification

Components/reaction	Volume (µl)
5x Q5 Reaction buffer	10
2 mM dNTPs	5
10 µM Forward primer	2.5
10 µM Reverse primer	2.5
Q5 High-Fidelity DNA polymerase (2 U/µl)	0.5
Template DNA (100 ng made upto 2.5 µl)	2.5
Sterile double distilled water	to 50

PCR Cyclor program for Q5 polymerase

Temperature	Time	Cycles
98 °C	30 sec	1 cycle
98 °C	15 sec	25 - 35 cycles
X °C	10 sec	
72 °C	30 sec/kb	
72 °C	3 min	1 cycle

Reaction mix for Taq polymerase based PCR amplification

Components/reaction	Volume (µl)
10x Standard <i>Taq</i> Reaction buffer	2.5
2 mM dNTPs	2.5
10 µM Forward primer	0.5

Materials and Methods

10 μ M Reverse primer	0.5
Taq polymerase (5 U/ μ l)	0.125
Template DNA (100 ng made up to 1 μ l)	1
Sterile double distilled water	17.875

PCR Cycler program for Taq polymerase

Temperature	Time	Cycles
95 °C	2 min	1 cycle
95 °C	20 seconds	30 - 40 cycles
X °C	20 seconds	
72 °C	1 min/ kb	
72 °C	5 min	1 cycle

Table 2 Backbone vectors used in this work.

Name	Purpose	Description
pGADT7-GW	Yeast two-hybrid interaction test	Express a protein of interest fused to a GAL4 activation domain
pGBKT7-GW	Yeast two-hybrid interaction test	Express a protein fused to GAL4 DNA binding domain
pGGA000	GG entry vector	Entry vector for promoter region of interest
pGGB003	GG entry with N-decoy	Entry vector carrying N-decoy in case no N-tag is needed
pGGC000	GG entry vector	Entry vector for CDS of interest
pGGD001	GG entry vector with linker-GFP	Entry vector carrying GFP as C-tag
pGGE009	GG entry with tUBQ	Entry vector carrying terminator of <i>UBQ10</i>
pGGF005	GG entry with Hygromycin-R	Entry vector carrying Hygromycin resistance for plant selection
pGGZ001	GG destination vector	Destination vector, binary vector for plant transformation
pCambia2300		Binary vector for plant transformation

2.3 Arabidopsis genomic DNA extraction and genotyping PCR

DNA was extracted from a small piece of leaf tissue of diameter ~ less than 1 cm. Leaf disk was frozen in liquid nitrogen and grinded to a fine powder (Qiagen grinder or pestle). The powdered tissue was suspended in 500 µl gDNA extraction buffer and incubated for 15 min at 65 °C using a thermo mixer at 1000 rpm after brief vortexing. 300 µl chloroform was added and mixed thoroughly by inverting Eppendorf tubes. The mixture was centrifuged for 10 min at 13000 rpm. 400 µl of the supernatant was transferred into a new tube (make sure to avoid any interphase junk). 280 µl of isopropanol was added to the supernatant (70% vol of supernatant), mixed by inversion, incubated 5 min at room temperature and centrifuged for 15 min at 12000 rpm. The pellet was washed with 1 ml ice cold 70% ethanol, dried completely and resuspended in 50 µl 5 mM Tris-HCl PH 5.8 or ddH₂O. The entire preparation was stored at 4 °C until use.

PCR-based genotyping was performed with the following primer combinations: *sub-9*, SUB_LP158, SUB_RP158, and SAIL_LB2; *chc2 salk-042321*, CHC2-LP321, CHC2-RP321, and SALK_LBb1.3; *chc2 salk-028826*, CHC2_LP826, CHC2_RP826, and SALK_LBb1.3; *chc1 salk-112213*, CHC1_LP213, CHC1_RP213, and SALK_LBb1.3; *chc1 salk-103252*, CHC1_LP252, CHC1_RP252, and SALK_LBb1.3; *ap2a1 salk-045252*, AP2A1_LP252, AP2A1_RP252, and SALK_LBb1.3; *ap1/2b2 salk-150980*, AP1/2B2_LP980, AP1/2B2_RP980, and SALK_LBb1.3; *ap2m salk-083693*, AP2M_LP693, AP2M_LP693, and SALK_LBb1.3; *ap2s sail-240-C03*, AP2S_LPC03, AP2S_RPC03, and SAIL_LB2. Primers were designed on T-DNA Primer Design website (<http://signal.salk.edu/tdnaprimers.2.html>).

2.4 RNA extraction from plant material and cDNA synthesis

Total RNA was isolated from the 7 day old seedlings using the kit according to the instructions given in the manufacturer's manual. Purified total RNA in RNase- free water were quantified and analyzed for purity using the NanoPhotometer P330 (Implen GmbH). Isolated RNA was stored at -80 °C until use. First-strand cDNA synthesis was performed using the RevertAid 1st strand cDNA synthesis kit (#1622, Thermo Scientific) accordingly. Details of the reaction mix and steps involved in the cDNA synthesis have been summarized in Table3.

Table 3 Reaction mix and steps involved in cDNA synthesis.

<u>Reaction mix for the cDNA synthesis</u>		
Components per reaction	Volume (µl)	
5x Reaction Buffer	4	
RiboLock RNase Inhibitor (20 U/µl)	1	
10 mM dNTP Mix	2	
RevertAid M-MuLV RT (200 U/µl)	1	
Oligo (dT) ₁₈ primer	1	
Template RNA	1 µg	
Nuclease-free water	to 20µl	
<u>Steps for cDNA synthesis</u>		
Step	Temperature (°C)	Incubation time (min)
Step 1	42	60
Step 2	70	5
Step 3	4	forever

2.5 Generation of various reporter constructs

2.5.1 Generation of pSUB/pUBQ10::SUB:EGFP constructs

The pCAMBIA2300-based pSUB::SUB:EGFP construct was described previously (Vaddepalli *et al.*, 2011). To obtain UBQ10 promoter, a 2 kb promoter fragment of *UBQ10* (At4g05320) was amplified from *Ler* genomic DNA using primers pUBQ(KpnI)_F and pUBQ(AscI)_R. The resulting PCR product was digested using KpnI/AscI and used to replace the pSUB fragment in pSUB::SUB:EGFP pCambia2300.

2.5.2 Construction of Y2H vectors

The backbone vectors for the Yeast two-hybrid (Y2H) analysis were pGADT7 AD (AD) and pGBKT7 BD (BD). The Coding sequences of *CHC2* and *AP2M* was amplified from Col-0 cDNA. Amplicons were purified and digested with ClaI/Sall for cloning into AD. In order to map CHC2 interaction domains by yeast-two-hybrid assay, various truncated fragments of CHC2 were generated by PCR and ligated into pGADT7. *SUB* intracellular domain fused to the GAL4 DNA-binding domain (GBD) was described previously (Vaddepalli *et al.*, 2014). Coding sequences of *SUB* juxta, *SUB* juxta 1st and *SUB* juxta 2nd and *SUB* kinase domain were cloned into pGBDT7 by former lab members. All constructs were verified by sequencing.

2.5.3 Generation of root hair patterning construct pGL2::GUS:EGFP

pGGZ001

The pGL2::GUS:EGFP construct was assembled using the GreenGate system (Lampropoulos *et al.*, 2013). The promoter region of *GL2* (AT1G79840) was amplified with primer pGL2 _F1 and pGL2_R1 from genomic Col-0 DNA.

The internal BsaI site was removed during the procedure as described in (Lampropoulos *et al.*, 2013). The GUS coding sequence was amplified from plasmid pBI121 (Jefferson *et al.*, 1987) with primer GUS_F and GUS_R, digested with BsaI and used for further cloning. Vectors were further assembled with pGGA006, pGGB003, pGGD001, pGGE009, and pGGF005 (all kindly provided by Jan Lohmann) to pGGZ001::pGL2:GUS:EGFP:tUBQ.

2.6 Yeast-two-hybrid (Y2H) assay

For Y2H, the above-mentioned GAD- and GBD-fusion constructs were co-transformed into yeast strain AH109 (MATa, trp1-901, leu2-3, 112, ura3-52, his3-200, gal4 Δ , gal80 Δ , LYS2::GAL1UAS-GAL1TATA-HIS3, MEL1, GAL2UAS-GAL2TATA-ADE2, URA3::MEL1UAS-MEL1TATA-lacZ) (Clontech/TaKaRa, USA). Transformants were selected after 3 days growth on synthetic complete medium lacking leucine and tryptophan (-LW) at 30 °C. To test for interaction, transformants were streaked on yeast synthetic drop-out (SD) plates lacking leucine, tryptophan and histidine (-LWH) supplemented with 2.5 mM 3-amino-1,2,4-triazole for 2 days at 30 °C.

2.7 Scanning electron microscopy (SEM)

For scanning electron microscopy analysis, carpel were obtained from freshly open flower buds and dissected before suspending in fixative (2% glutaraldehyde (SIGMA G5882), 69% acetone, 29% H₂O) overnight. Fixed ovules were washed with 70% acetone (4×15 minute, followed by 6×30 minute). During fixation II, ovules were washed for 15 minute in 50% acetone in 50mM cacodylate buffer pH 7.0, followed by 10 minute in 25% acetone in 50mM cacodylate buffer, 10 minute in 10% acetone/cacodylate buffer, and finally, washed with 50mM cacodylate for 5 minute. Washed ovules were then treated with 2% osmium-tetroxide in 50mM cacodylate buffer for 2 hours. Osmium

tetroxide was removed by washing 2 times with 50mM cacodylate buffer, and then followed with a 10 minute wash with 10% acetone/cacodylate buffer. In the end the ovules were passed through an acetone series (10%, 20%, 40%, 60% and 70%) for 30 minute each and stored at 4 °C. Fixed ovules were passed through a minimum of three 100% acetone washes before critical point drying. Specimens were mounted on stubs and dissected using fine tip needle. The tissues were coated with gold particles and examined with the TM3000 tabletop scanning electron microscope (HITACHI). Scanning electron microscopy was performed essentially as reported previously (Schneitz *et al.*, 1997; Sieburth and Meyerowitz, 1997).

2.8 Confocal laser scanning microscopy (CLSM)

To assess the cellular structure of floral meristems samples were stained with modified pseudo-Schiff propidium iodide (mPS-PI) (Truernit *et al.*, 2008). Confocal laser scanning microscopy was performed with an Olympus FV1000 setup using an inverted IX81 stand and FluoView software (FV10-ASW version 01.04.00.09) (Olympus Europa GmbH, Hamburg, Germany) equipped with a water-corrected 40x objective (NA 0.9) at 3x digital zoom. For SUB:EGFP subcellular localization upon drug treatments or colocalization with endosomal markers confocal laser scanning microscopy was performed on epidermal cells of root meristems located about 8 to 12 cells above the quiescent center using a Leica TCS SP8 X microscope equipped with GaAsP (HyD) detectors. The following objectives were used: a water-corrected 63x objective (NA 1.2), a 40x objective (NA 1.1), and a 20x immersion objective (NA 0.75). Scan speed was set at 400 Hz, line average at between 2 and 4, and the digital zoom at 4.5 (colocalization with FM4-64), 3 (drug treatments) or 1 (root hair patterning). EGFP fluorescence excitation was done at 488 nm using a multi-line argon laser (3 percent intensity) and detected at 502 to 536 nm. FM4-64 fluorescence was excited using a 561 nm laser (1 percent intensity) and detected at 610 to 672 nm. For the direct

comparisons of fluorescence intensities, laser, pinhole, and gain settings of the confocal microscope were kept identical when capturing the images from the seedlings of different treatments. The intensities of fluorescence signals at the PM were quantified using Leica LAS X software (version 3.3.0.16799). For the measurement of the fluorescence levels at the PM optimal optical sections of root cells were used for measurements. On the captured images the fluorescent circumference of an individual cell (ROI, region of interest) was selected with the polygon tool. The mean pixel intensity readings for the selected ROIs were recorded and the average values were calculated. For determination of colocalization, the distance from the center of each EGFP spot to the center of the nearest FM4-64, mKO or mRFP signal was measured by hand on single optical sections using ImageJ/Fiji software (Schindelin *et al.*, 2012). If the distance between two puncta was below the resolution limit of the objectives lens (0.24 μm) the signals were considered to colocalize (Ito *et al.*, 2012). Arabidopsis seedlings were covered with a 22 \times 22 mm glass cover slip of 0.17 mm thickness (No. 1.5H, Paul Marienfeld GmbH & Co. KG, Lauda-Königshofen, Germany). Images were adjusted for color and contrast using ImageJ/Fiji software.

2.9 Three dimensional ovule imaging using CLSM and MorphoGraphX

Carpel were obtained from appropriate flower buds and dissected before suspending in fixative 4 % paraformaldehyde (PFA) in 1 \times PBS pH7.3 for one to two hours at room temperature with gentle agitation or overnight at 4 °C. The fixed tissues were washed twice for 1 min in 1 x PBS. Then the tissues were transferred to ClearSee solution at room temperature with gentle agitation for overnight or more. Cleared ovules were stained with (0.1 %) SCRI Renaissance 2200 (SR2200) stain (Musielak *et al.*, 2015) in 1x PBS for 30 min. Subsequently, the ovules were transferred to ClearSee solution for another 30 min before imaging (Ursache *et al.*, 2018). Ovules were mounted on slides and dissected from the carpel wall. For

imaging, a Leica TCS SP8 X microscope with 63 x glycerol objective was used. SR2200 was excited with a 405-nm laser line and emission recorded between 415 and 476 nm (405/415–476). The confocal images of the ovules were used to construct a 3D image with MorphoGraphX 2.0 (Barbier de Reuille *et al.*, 2015).

2.10 Phenotyping flower organ

Whole flowers and silique micrographs were obtained using an Olympus SZX12 stereomicroscope equipped with a XC CCD camera and Cell Sense Dimension software. Whole plant pictures were taken with a Nikon COOLPIX B500 digital camera (NIKON CORP.). Images were manipulations such as brightness and contrast, were carried out using ImageJ/Fiji and Adobe Photoshop CS6 software (Adobe System Inc.).

2.11 Drug treatments

The transgenic *sub-1/pSUB:SUB:EGFP* seeds were used. Brefeldin A (BFA), cycloheximide (CHX), tyrphostin A23 (TyrA23), Wortmannin (WM), Concanamycin A (ConcA) were obtained from Sigma-Aldrich and used from stock solutions in DMSO (50 mM BFA, cycloheximide, TyrA23; 30 mM Wortmannin, 2 mM ConcA). FM4-64 was purchased from Molecular Probes (2 mM stock solution in water). Five day-old seedlings were incubated for the indicated times in liquid 1/2 MS medium containing 50 μ M BFA, 50 μ M cycloheximide, 75 μ M TyrA23, 33 μ M Wortmannin, and 2 μ M ConcA. For FM4-64 staining seedlings were incubated in 4 μ M FM4-64 in liquid 1/2 MS medium for 5 minutes prior to imaging. 4-hydroxytamoxifen was obtained from Sigma-Aldrich (10 mM stock solution in ethanol). Seedlings were grown for 3 days on 1/2 MS plates, transferred onto 1/2 MS plates containing 2 μ M 4-hydroxytamoxifen (or ethanol as mock treatment) for four days and then imaged using confocal microscopy.

2.12 Immunoprecipitation and western blot analysis

500 mg of 7-day wild-type or transgenic seedlings were lysed using a TissueLyser II (Qiagen) and homogenized in 1 ml lysis buffer A (50mM Tris-HCl pH7.5, 100 mM NaCl, 0.1 mM PMSF, 0.5% Triton X-100, protease inhibitor mixture (Roche)). Cell lysate was mildly agitated for 15 min on ice and centrifuged for 15 minutes at 13000 g. For lines carrying GFP-tagged proteins supernatant was incubated with GFP-TRAP_MA magnetic agarose beads (ChromoTek) for 2 hours at 4 °C. Beads were concentrated using a magnetic separation rack. Samples were washed four times in buffer B (50mM Tris-HCl pH7.5, 100 mM NaCl, 0.1 mM PMSF, 0.2% Triton X-100, protease inhibitor mixture (Roche)). Bound proteins were eluted from beads by heating the samples in 30 µl 2x Laemmli buffer for 5 minutes. Samples were separated by SDS-PAGE and analyzed by immunoblotting according to standard protocols. Primary antibodies included mouse monoclonal anti-GFP antibody 3E6 (Invitrogen/Thermo Fisher Scientific), mouse monoclonal anti-ubiquitin antibody P4D1 (Santa Cruz Biotechnology), and polyclonal anti-CHC antibody AS10 690-ALP (Agrisera). Secondary antibodies were obtained from Pierce/ThermoFisher Scientific: goat anti-rabbit IgG antibody (1858415) and goat anti-mouse IgG antibody (1858413).

2.13 Growth media, growth conditions and frequently used buffers

Ingredients are dissolved in deionized H₂O, and all growth media need to be autoclaved.

For DNA gel electrophoresis

5x TBE running buffer (pH should be 8.3)

450 mM Tris Base

400 mM boric acid

10 mM EDTA pH 8

For DNA extraction

100 mM Tris/HCl pH 8

Materials and Methods

250 mM NaCl
25 mM EDTA pH 8
0.5% (v/v) SDS

For Glycine-SDS polyacrylamide gel electrophoresis according to Laemmli

Protein lysis buffer

50 mM Tris/HCl pH 7.5
150 mM NaCl
0.1 mM PMSF
protein inhibitor cocktail
0.5% (v/v) Triton-X 100

Coomassie R-250 staining solution

0.25% (w/v) Coomassie Brilliant Blue R-250
0.50% (v/v) Ethanol
10% (v/v) Glacial acetic acid

Coomassie R-250 destaining solution

0.50% (v/v) Ethanol
10% (v/v) Glacial acetic acid

10x SDS running buffer

0.25 M Tris
2 M Glycine
1% (w/v) SDS

For transfer and immunodetection of proteins

10x Transfer buffer

40 mM Tris base
40 mM Glycine

TBST buffer

0.1% (w/v) Tween 20 in TBS buffer

TBS buffer

10 mM Tris/HCl (pH 7.4)
150 mM Sodium chloride

Blocking buffer

5% (w/v) Skim milk powder in TBST buffer

For standard molecular biology/cloning

Lysogeny broth (LB) medium

1% tryptone, 0.5% yeast extract, 10% NaCl, (0.9% bacto agar)

For plant tissue culture

½ Murashige-Skoog medium

0.22% MS medium powder, (1% sucrose), 0.9% Agar (plant cell culture tested)

For yeast growth culture

YPD medium

2% tryptone, 1% yeast extract, (2.4% bacto agar), 2% glucose

SD-LW

0.67% yeast nitrogen base (double drop-out; SD lacking leucine and tryptophan), 2% glucose, (2% bacto agar)

SD-LWH

0.67% yeast nitrogen base (triple drop-out; SD lacking leucine, tryptophan and histidine), 2% glucose, (2% bacto agar)
SD media might be supplemented with 5-10 mM 3-AT

Growth conditions were as follows: E.coli for standard molecular biology was grown at 37 °C overnight. Yeast AH109 was grown at 30 °C for 2-3d. Seedlings were grown on 1/2 MS with or without 1% sucrose at 22 °C and continuous light for 5-7d.

2.14 Bioinformatics

Protein domain searches were conducted using the PFAM database. Bioinformatic analysis was mainly performed using geneious software. Alignments were generated with geneious software using a ClustalW algorithm with BLOSUM62 matrix. Sequencing results were analyzed in geneious software using the map to reference tool with geneious mapper and highest sensitivity.

3 Results

3.1 The endocytic route of SUB:EGFP

To investigate the endocytic pathway followed by SUB I made use of a previously well-characterized line carrying the *sub-1* null allele and a transgene encoding a SUB:EGFP translational fusion driven by its endogenous promoter (pSUB::SUB:EGFP). The line exhibits a wild-type phenotype demonstrating the presence of a functional reporter (Vaddepalli *et al.*, 2011; Vaddepalli *et al.*, 2014). I studied the subcellular distribution of the pSUB::SUB:EGFP reporter signal in epidermal cells of the root meristem using confocal laser scanning microscopy. These cells serve as an ideal model as *SUB* promotes the early patterning of root hairs, cells that are generated by the epidermis (Dolan *et al.*, 1993).

In the absence of any obvious exogenous stimulation of SUB signaling I observed SUB:EGFP signal at the PM and in cytoplasmic foci (Figure 12 A). Moreover, I noticed that the SUB:EGFP signal labelled structures resembling vesicles as well as the vacuole. These observations raise the possibility that SUB:EGFP undergoes internalization from the PM and is shuttled to the vacuole for degradation.

To assess the early process of SUB:EGFP endocytosis I imaged cells upon a 5-minutes treatment with the endocytic tracer dye FM4-64 (Figure 12 A,D). Using a previously described criterion for colocalization (Ito *et al.*, 2012) the internal SUB:EGFP and FM4-64 signals were considered colocalized when the distance between the centers of the two types of signals was below the limit of resolution of the objective, in this case 0.24 μm . I observed that 70 percent (n = 344) of all cytoplasmic SUB:EGFP foci were also marked by FM4-64 supporting endocytosis of SUB:EGFP. To further investigate internalization of SUB:EGFP I treated five days-old seedlings with Wortmannin. Wortmannin is a

Results

phosphatidylinositol-3-kinase inhibitor that among others interferes with vesicle formation from the PM (Tse *et al.*, 2004; Wang *et al.*, 2009; Ito *et al.*, 2012; Cui *et al.*, 2016). I analyzed the number of internal SUB:EGFP-labelled puncta in cells upon treatment with 33 μ M Wortmannin for 60 minutes. I found a substantial reduction in the number of such puncta in drug-treated cells when compared to mock-treated cells (Figure 13 A). Moreover, I noted a significant increase in SUB:EGFP signal intensity at the PM in Wortmannin-treated cells.

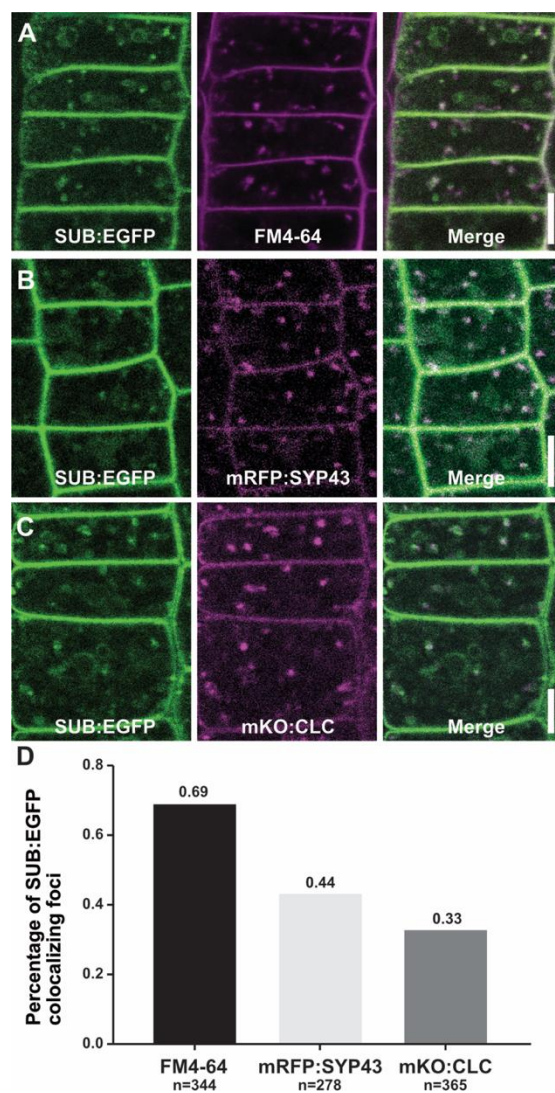


Figure 12 Subcellular localization of SUB:EGFP.

Fluorescence micrographs show optical sections of epidermal cells of root meristems of five to six days-old seedlings. (A) Partial colocalization of SUB:EGFP and FM4-64 foci upon treating cells

Results

with FM4-64 for five minutes. **(B)** Partial colocalization of SUB:EGFP and mRFP:SYP43 puncta. **(C)** Partial colocalization of SUB:EGFP and mKO:CLC signals. **(D)** Quantitative colocalization analysis of SUB:EGFP-positive foci and reporter signals shown in A, B and C. *n*, total number of analyzed SUB:EGFP foci. Scale bars: 5 μ m.

To explore if endosomal trafficking of SUB:EGFP involves the TGN/EE I investigated colocalization of SUB:EGFP with the TGN marker mRFP:SYP43 (Ebine *et al.*, 2011; Ito *et al.*, 2012; Uemura *et al.*, 2012) (Figure 12 B,D). I observed a frequency of 44 percent colocalization ($n = 278$) between internal SUB:EGFP and mRFP:SYP43 puncta. To further assess colocalization of SUB:EGFP with the TGN I made use of a previously characterized translational fusion between CLC2 and monomeric Kushiba Orange under the control of the cauliflower mosaic virus 35S promoter (mKO:CLC) (Fujimoto *et al.*, 2010). CLC2 fused to fluorescent tags also localizes to the TGN in live cell imaging experiments (Ito *et al.*, 2012). I observed a frequency of 33 percent colocalization ($n = 365$) between internal SUB:EGFP and mKO:CLC puncta (Figure 12 C,D). To corroborate the presence of SUB:EGFP at the TGN/EE I exposed *sub-1 pSUB::SUB:EGFP* seedlings to the fungal toxin Brefeldin A (BFA). Treatment with BFA results in the formation of so-called BFA compartments or bodies that contain secretory and endocytic vesicles (Robinson *et al.*, 2008; Paez Valencia *et al.*, 2016). I observed prominent SUB:EGFP signal in BFA compartments in root epidermal cells of seedlings treated with DMSO for 30 minutes followed by a DMSO/BFA (50 μ M) treatment for 60 minutes, confirming previous data (Figure 13 B) (Kwak and Schiefelbein, 2008; Yadav *et al.*, 2008; Vaddepalli *et al.*, 2011; Wang *et al.*, 2016a).

To explore the relative contribution of signal at the TGN/EE originating from the secretion of newly translated SUB:EGFP versus endocytic SUB:EGFP-derived signal I performed additional investigations. Treatment of cells with the phosphotyrosine analog tyrphostin A23 (TyrA23) leads to acidification of the cytoplasm and a block of membrane internalization (Dejonghe *et al.*, 2016).

Results

Pretreating seedlings with 75 μM TyrA23 for 30 minutes prior to co-incubation in 75 μM TyrA23/50 μM BFA for 60 minutes resulted in near complete absence of SUB:EGFP signal in BFA compartments (Figure 13 B). In another set of experiments I first treated seedlings with the protein synthesis inhibitor cycloheximide (50 μM) for 60 minutes followed by co-incubation with 50 μM BFA for 30 minutes. In those seedlings SUB:EGFP still prominently localized to BFA bodies (Figure 13 C) as noted earlier (Wang *et al.*, 2016a). Taken together, the results indicate that a large fraction of SUB:EGFP in BFA bodies originated from the PM.

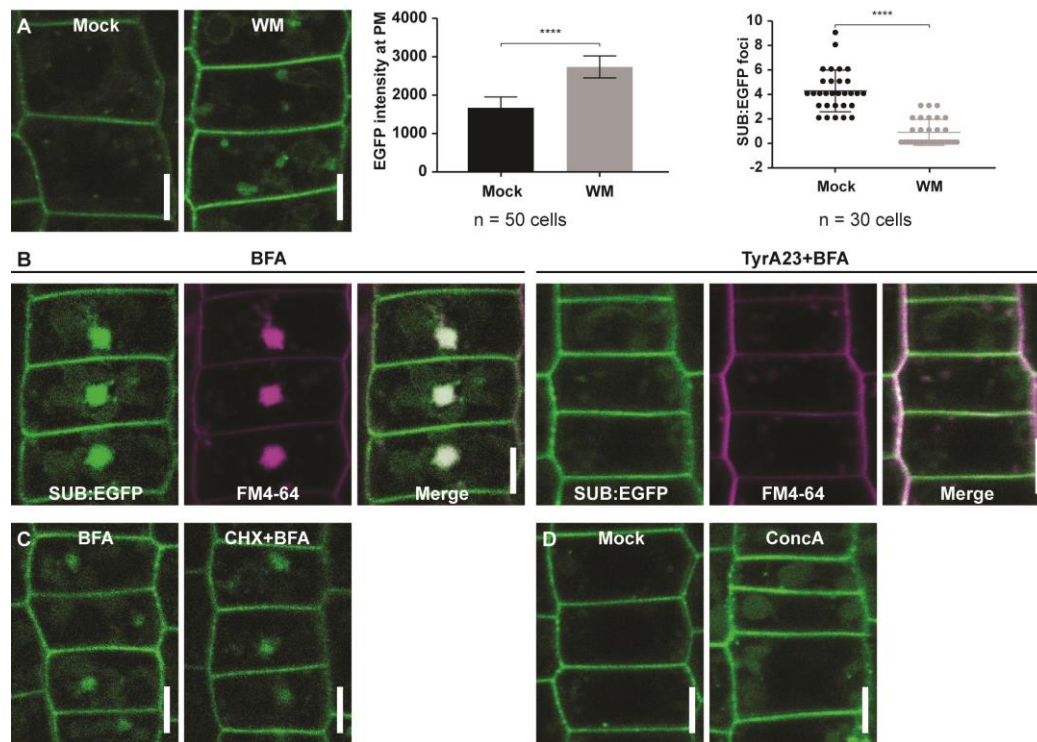


Figure 13 Subcellular localization of SUB:EGFP upon drug treatments.

Fluorescence micrographs show optical sections of epidermal cells of root meristems of five to six days-old seedlings. **(A)** Subcellular localization of SUB:EGFP signal in the presence of Wortmannin and DMSO (mock control) (left). Graphs represent quantification of the EGFP intensity at plasma membrane (middle panel, $n = 50$ cells across six roots) and the number of SUB:EGFP-positive endosomes per cell (right panel, $n = 30$ cells across six roots) after incubation. Asterisks represent statistical significances ($P < 0.0001$) as judged by Student's t test. **(B)** SUB:EGFP signal is detected in BFA bodies upon BFA treatment. TyrA23 efficiently inhibited

Results

BFA-induced intracellular accumulation of SUB:EGFP. (C) SUB:EGFP signal is detected in BFA compartments in the presence of CHX. (D) SUB:EGFP signal is observed in lytic vacuoles after ConcA treatment. Abbreviations: ROI, region of interest. Scale bars: 5 μ m.

I next investigated if internalized SUB:EGFP is sorted into MVBs. Apart from affecting vesicle formation at the PM Wortmannin also interferes with the maturation of LEs and causes formation of enlarged MVB/LEs (Tse *et al.*, 2004; Wang *et al.*, 2009; Cui *et al.*, 2016). Treating seedlings for 60 minutes with 33 μ M wortmannin results in the formation of large globular structures labelled by SUB:EGFP signal (Figure 13 A). Such structures are typical for enlarged MVBs (Jia *et al.*, 2013). In accordance with these results SUB:EGFP was detected at MVBs in immunogold electron microscopy experiments (Vaddepalli *et al.*, 2014).

Concanamycin A (ConcA) inhibits vacuolar ATPase activity at the TGN/EE and in the tonoplast thereby interfering with the trafficking of newly synthesized materials to the PM, the transport of cargo from the TGN/EE to the vacuole, and the vacuolar degradation of cargo (Dettmer *et al.*, 2006; Robinson *et al.*, 2008; Viotti *et al.*, 2010; Scheuring *et al.*, 2011). Upon treatment with 2 μ M ConcA for 1 hour seedlings showed large roundish structures labelled by a diffuse SUB:EGFP signal (Figure 13 D) indicating that SUB:EGFP was not degraded efficiently and thus accumulated in the vacuole.

Taken together the results are consistent with the notion that the endocytic route of SUB:EGFP involves the TGN/EE, the MVB/LEs, and the vacuole where it becomes degraded. A noticeable portion of SUB:EGFP puncta colocalizes with the TGN/EE, supporting passage of SUB:EGFP through the TGN/EE. However, I cannot exclude that a fraction of SUB:EGFP also traffics via an TGN/EE-independent route, as does for example the AtPep1-PEPR1 signaling complex (Ortiz-Morea *et al.*, 2016).

3.2 SUB:EGFP is ubiquitinated *in vivo*

Ubiquitination plays an important role in endocytosis and endosomal sorting of PM proteins (MacGurn *et al.*, 2012; Paez Valencia *et al.*, 2016; Isono and Kalinowska, 2017), such as the brassinosteroid receptor BRI1 (Martins *et al.*, 2015) or the auxin efflux facilitator PINFORMED 2 (PIN2) (Leitner *et al.*, 2012).

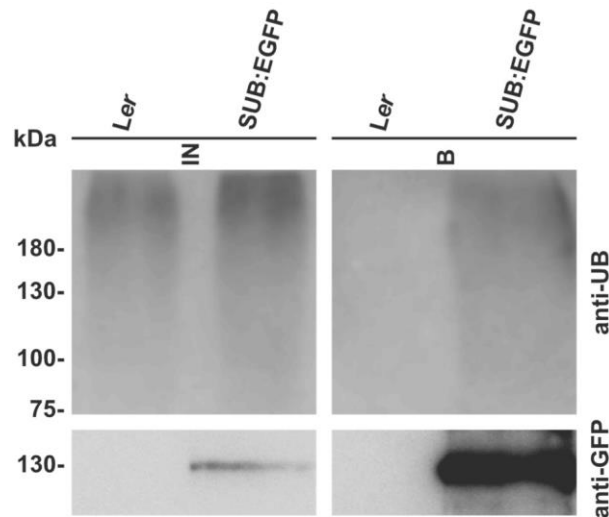


Figure 14 *In vivo* ubiquitination of SUB.

Western blot analysis of immunoprecipitates obtained from wild type (*Ler*) and *sub-1* pUBQ::gSUB:EGFP lines are shown. Immunoprecipitation was performed using an anti-GFP antibody. Immunoblots were probed with the P4D1 anti-Ub antibody (top panel) and an anti-GFP antibody (bottom panel). Abbreviations: B: bound fraction; IN, input.

To test if SUB:EGFP is ubiquitinated *in vivo* I made use of our *sub-1* pSUB::SUB:EGFP reporter line as well as a previously described line carrying the SUB:EGFP translation fusion driven by the UBIQUITIN10 (UBQ) promoter (pUBQ::SUB:EGFP) (Vaddepalli *et al.*, 2017). I immunoprecipitated SUB:EGFP from seven days-old, plate-grown seedlings using an anti-GFP antibody. Immunoprecipitates were subsequently probed with the commonly used P4D1 anti-ubiquitin antibody recognizing mono- and polyubiquitinated proteins. P4D1-dependent signal could not be reproducibly detected when testing immunoprecipitates from lines expressing the pSUB::SUB:EGFP reporter due to low abundance of SUB:EGFP in the immunoprecipitate. By contrast, I clearly

observed a high-molecular weight smear in immunoprecipitates obtained from *pUBQ::SUB:EGFP* lines (Figure 14). This smear is typical for ubiquitinated proteins. I did not detect signals in immunoprecipitates obtained from wild-type seedlings. The results indicate that a fraction of SUB proteins becomes ubiquitinated.

3.3 SUB:EGFP internalization involves clathrin-mediated endocytosis

So far, the obtained results indicate that SUB:EGFP is continuously internalized and eventually targeted to the vacuole for degradation. Next I wanted to assess if SUB:EGFP relates to a clathrin-dependent process.

3.3.1 SUB interacts with Clathrin *in vivo*

I first tested if SUB:EGFP and endogenous CHC occur in the same complex *in vivo*. To this end I immunoprecipitated SUB:EGFP from seven days-old, plate-grown *pUBQ::SUB:EGFP sub-1* seedlings using an anti-GFP antibody. Immunoprecipitates were subsequently probed using an anti-CHC antibody. I could detect a CHC-signal in immunoprecipitates derived from SUB:EGFP plants but not from wild-type (Figure 15) indicating that SUB:EGFP and CHC are present in the same protein complex *in vivo*.

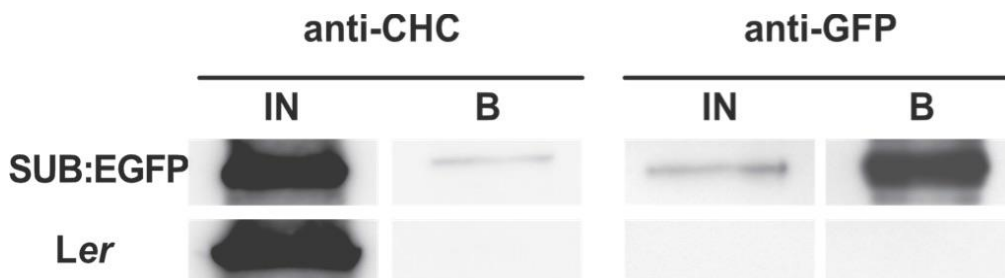


Figure 15 Co-immunoprecipitation of CHC with SUB:EGFP.

Results

Total extracts of seven day-old SUB:EGFP-expressing seedlings (upper panel) or wild-type seedlings (lower panel) were immunoprecipitated using GFP-Trap MA beads. Immunoblots were probed with anti-CHC (left panel) or anti-GFP antibodies (right panel). Abbreviations: B: bound fraction; IN, input.

3.3.2 CME is required for SUB internalization

In plants, CME is the major internalization route of plant PM proteins (Dhonukshe *et al.*, 2007). Next I assessed the contribution of clathrin to the internalization and subcellular distribution of SUB:EGFP. To this end, I investigated the effects of a transient but robust impairment of clathrin activity on the internalization and subcellular distribution of SUB:EGFP. Ectopic expression of the C-terminal part of CHC1 (HUB1) results in a dominant-negative effect due to the HUB1 fragment binding to and out-titrating clathrin light chains (Liu *et al.*, 1995). To assess the effect of the presence of the HUB fragment on the subcellular distribution of SUB:EGFP I crossed a previously characterized 4-hydroxytamoxifen-inducible INTAM>>RFP-CHC1 (HUB) line (Robert *et al.*, 2010; Kitakura *et al.*, 2011) into a Col-0 wild-type line carrying the pUBQ::SUB:EGFP reporter. I then analyzed epidermal cells of the root meristem of HUB/pUBQ::SUB:EGFP plants, hemizygous for each transgene, upon induction.

I first determined the length of induction period that enabled us to detect by confocal microscopy a defect in endocytosis, as indicated by a reduction of internal FM4-64 foci following a 5 to 10 minutes exposure to the stain. Under our growth conditions a significant reduction of internal FM4-64 puncta was observed after three days of continuous growth on induction medium while near complete absence of internal FM4-64 foci was detected after four days (Figure 16 B,C). If SUB:EGFP participates in CME a block in HUB-sensitive endocytosis should result in fewer internal SUB:EGFP-labelled foci and higher SUB:EGFP signal at the PM when compared to the SUB:EGFP-derived signal of a control line. I found

Results

a significant reduction in cytoplasmic SUB:EGFP puncta in the HUB/pUBQ::SUB:EGFP line after three days of growth on induction medium in comparison to the control (Figure 16 B). Upon four days of induction I detected an increase in SUB:EGFP signal at the PM (Figure 16 C). Taken together, our results suggest that CME contributes to the internalization of SUB:EGFP.

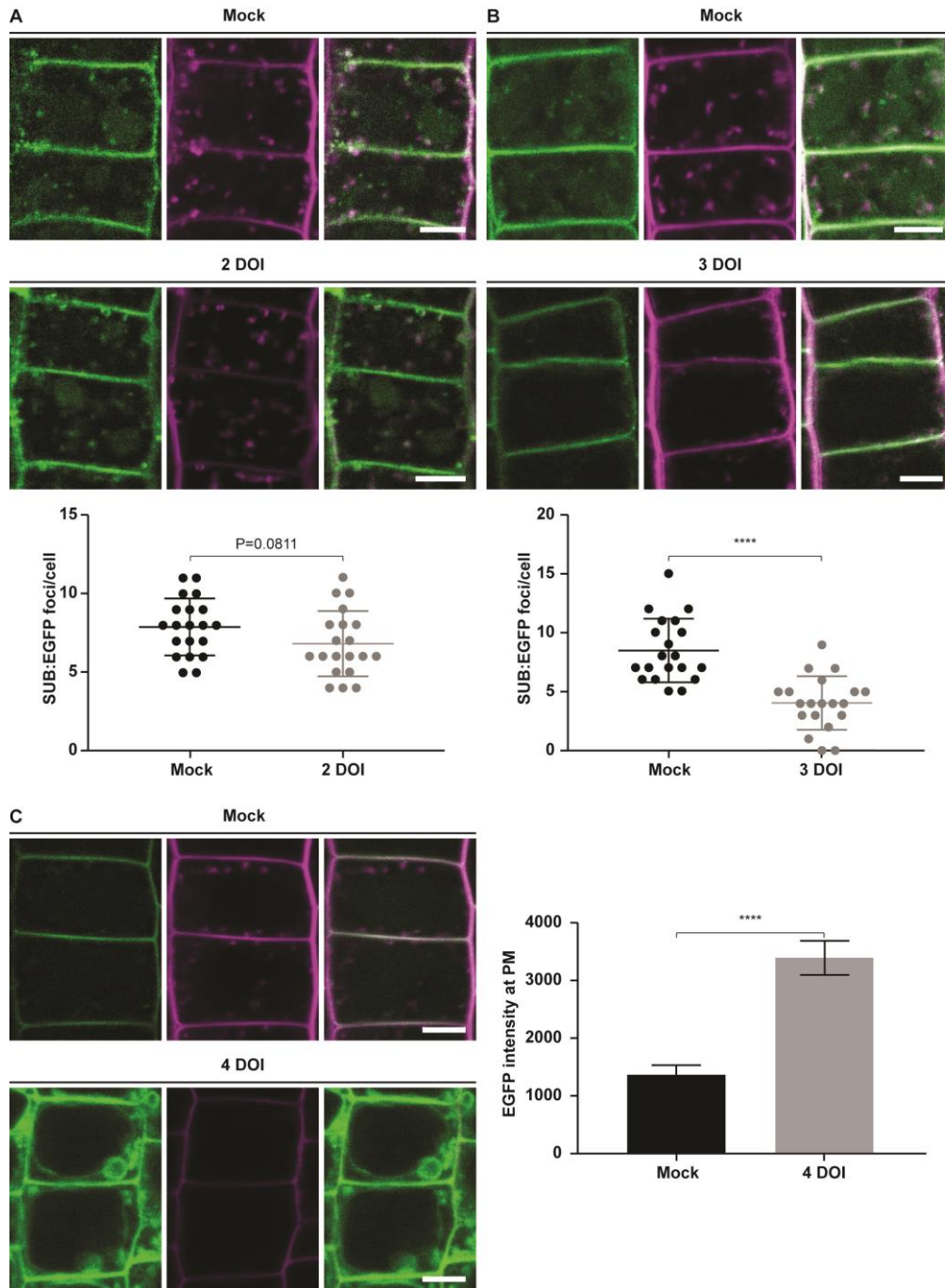


Figure 16 Requirement of clathrin function for SUB endocytosis.

Results

Fluorescence micrographs show optical sections of epidermal cells of root meristems. (A) to (C) Internalization of SUB:EGFP and uptake of endocytic tracer dye FM4-64 in epidermal meristems cells of three days-old INTAM>>RFP-CHC1 (HUB1)/pUBQ::SUB:EGFP seedlings that were placed on 2 μ M 4- hydroxytamoxifen-containing induction medium for two, three, or four days, respectively. Ethanol served as mock. Graphs represent quantification of the number of SUB:EGFP-positive spots per cell (A, B) and of the EGFP intensity at plasma membrane (C) after incubation. Abbreviation: DOI, days on induction medium. Scale bars: 5 μ m.

3.4 SUB genetically interacts with CLATHRIN HEAVY CHAIN

To further assess the role of clathrin in the SUB signaling mechanism I tested a possible genetic interaction between *SUB* and *CHC*. To this end I made use of several previously characterized T-DNA insertion lines carrying knock-out alleles of *CHC1* and *CHC2* (Kitakura *et al.*, 2011) (Figure 17). Plants lacking *CHC1* as well as *CHC2* function appear to be lethal (Kitakura *et al.*, 2011). However, mutations in individual *CHC* genes result in endocytosis defects and affect for example polar distribution of PIN proteins, internalization of ATRBOHD, stomatal movement, and resistance to powdery mildew (Kitakura *et al.*, 2011; Hao *et al.*, 2014; Wu *et al.*, 2015; Larson *et al.*, 2017).

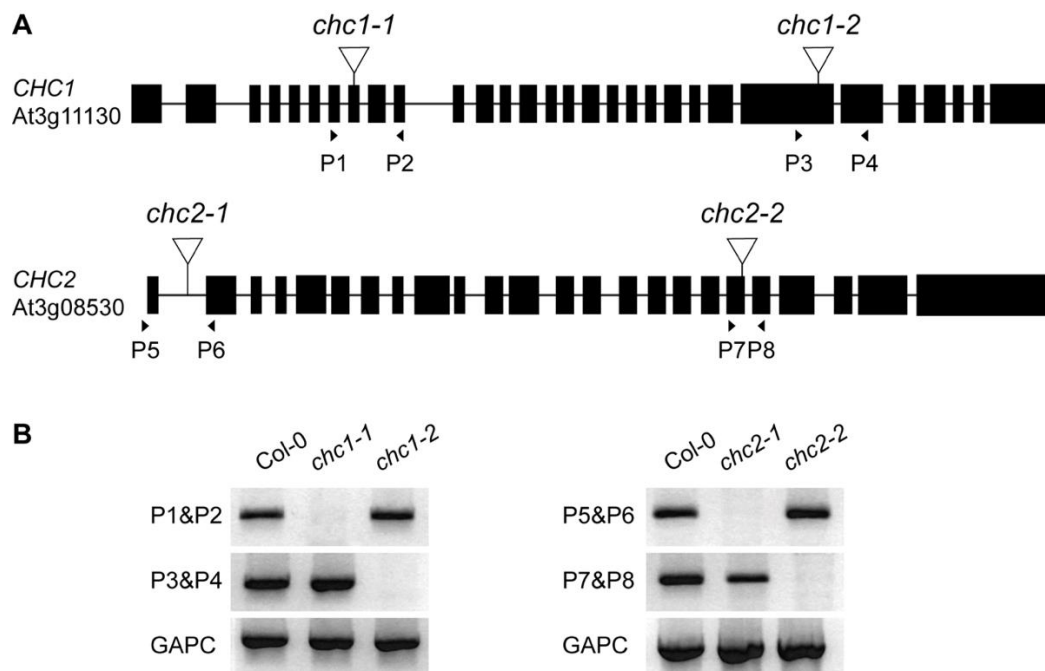


Figure 17 Characterization of *chc* mutant alleles.

Results

(A) Schematic representation of *CHC1* and *CHC2* genes structure. Black boxes and bars represent exons and introns respectively. The triangles indicate the T-DNA insertion site. (B) RT-PCR from RNA extracts of the *chc1* and *chc2* single mutants and wild-type Col-0. The positions of primers are shown in (A), GAPC primers were used as internal controls.

To test if clathrin is involved in *SUB*-controlled processes I first investigated if *chc1* and *chc2* mutants show a defect in root hair patterning. To this end I generated homozygous *chc* mutants carrying a translational fusion of bacterial β -glucuronidase (GUS) to EGFP (GUS:EGFP) under the control of the Arabidopsis *GLABRA2* (*GL2*) promoter (pGL2::GUS:EGFP). The *GL2* promoter drives expression specifically in non-root hair cells and is commonly used to monitor root hair patterning (Masucci *et al.*, 1996; Kwak *et al.*, 2005). Interestingly, I found that all *chc* alleles tested showed root hair patterning defects similar to *sub-9* with *chc2* alleles causing more prominent aberrations compared to *chc1* mutations (Figure 18, Figure 19). In addition, *chc1 sub-9* or *chc2 sub-9* double mutants did not show an obviously exacerbated phenotype indicating that *CHC1*, *CHC2* and *SUB* do not act in an additive fashion. Thus, the results indicate that *CHC1* and *CHC2* promote root hair pattern formation and that they function in the same genetic pathway as *SUB*.

Next, I assessed if *CHC1* and *CHC2* participate in *SUB*-dependent floral development. In the Col-0 background null alleles of *SUB* cause a weaker floral phenotype when compared to similar alleles in the *Ler* background (Vaddepalli *et al.*, 2011). Still, the *sub-9* allele causes mild silique twisting, mis-oriented cell division plants in the L2 layer of floral meristems, and ovule defects (Figure 19) (Tables 4 and 5) (Vaddepalli *et al.*, 2011). By contrast, I did not detect any obvious defects in floral meristems, flowers and ovules of plants homozygous for the tested *chc1* or *chc2* alleles (Figure 20, Figure 21) (Tables 4 and 5).

Results

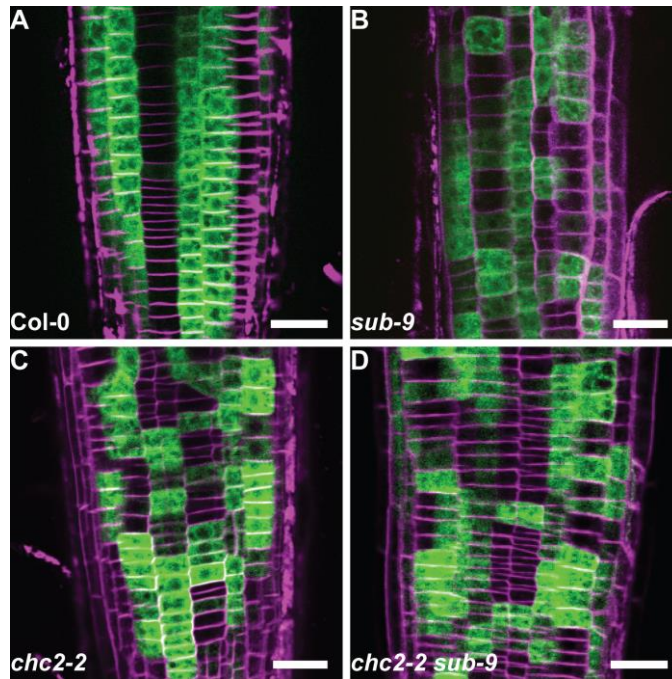


Figure 18 Expression pattern of the pGL2::GUS:EGFP reporter in *chc2-2* and *chc2-2 sub-9* mutants.

Fluorescence micrographs show optical sections of epidermal cells of root meristems of seven days-old seedlings. FM4-64 was used to label cell outlines. (A) Col-0. (B) *sub-9*. (C) *chc2-2*. (D) *chc2-2 sub-9*. Note the similarly altered pattern in (B) to (D). Scale bars: 25 μ m.

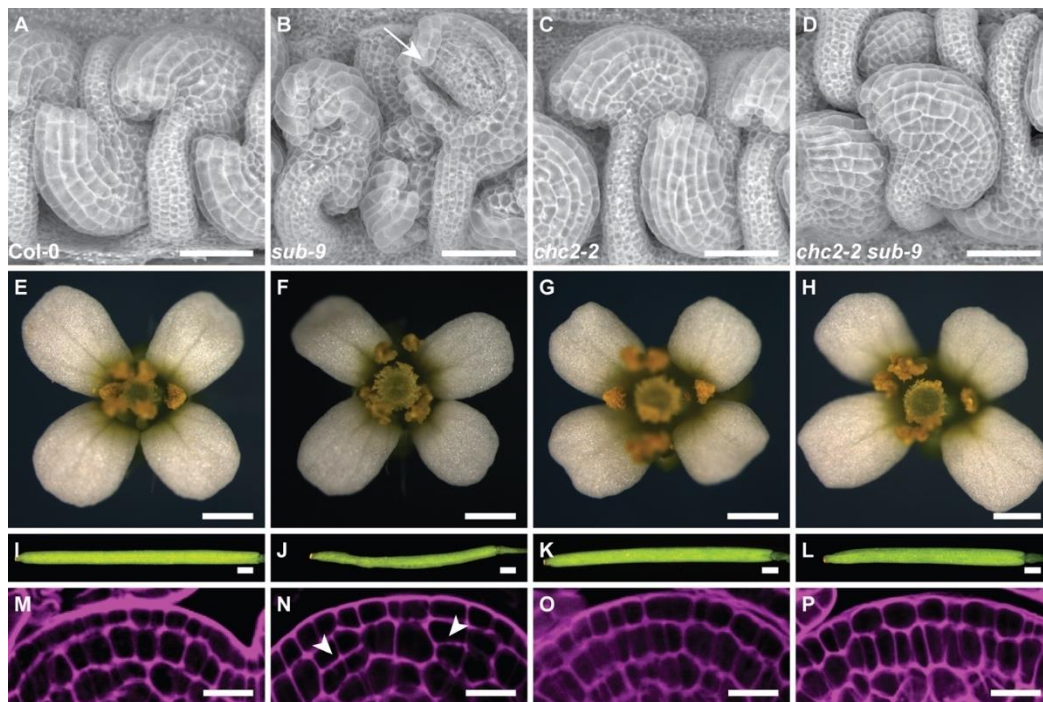


Figure 19 Phenotype comparison between Col-0, *sub-9*, *chc2-2* and *chc2-2 sub-9*.

Results

(A) to (D) Scanning electron micrographs of stage 4 ovules (stages according to (Schneitz *et al.*, 1995)). (B) Note the aberrant outer integument (arrow). (E) to (H) Morphology of mature stage 13 or 14 flowers (stages according to (Smyth *et al.*, 1990)). (I) to (L) Morphology of siliques. (M) to (P) Central region of stage 3 floral meristems stained with pseudo-Schiff propidium iodide (mPS-PI). (N) Arrowheads indicate aberrant cell division planes. (P) Note the defects of the *sub-9* phenotype were partially rescued in *chc sub-9* double mutants. Scale bars: (A) to (D) 50 μ m, (E) to (H) 0.5 mm, (I) to (L) 1 mm, (M) to (P) 10 μ m.

I then investigated the phenotype of *chc1 sub-9* and *chc2 sub-9* double mutants. Interestingly, the cell division defects in the L2 layer of the FM were reduced in *chc1 sub-9* and *chc2 sub-9* double mutants in comparison to *sub-9* single mutants (Figure 19, Figure 21) (Table 4). Suppression of the *sub-9* phenotype in *chc1 sub-9* or *chc2 sub-9* double mutants was also observed for silique twisting and ovule development (Figure 19, Figure 21) (Table 5). The results suggest that *SUB* is a negative genetic regulator of *CHC1* and *CHC2* function in floral meristem, ovule and silique development.

Table 4 Number of periclinal cell divisions in the L2 layer of stage 3 floral meristems.

Genotype	NPCD ^a	Percentage	NFM ^b
Col	12	17.6	68
<i>sub-9</i>	17	36.2	47
<i>chc1-1</i>	6	23.1	26
<i>chc1-2</i>	7	20.0	35
<i>chc2-1</i>	7	22	31
<i>chc2-2</i>	5	22.5	25
<i>chc1-1 sub-9</i>	6	20.0	30
<i>chc1-2 sub-9</i>	7	19.4	36
<i>chc2-1 sub-9</i>	7	25.9	27
<i>chc2-2 sub-9</i>	7	18.9	37

^aNumber of periclinal cell divisions observed

^bNumber of floral meristems observed

Results

Table 5 Comparison of integument defects between *sub-9*, *chc* and *chc sub-9* mutants.

Genotype	N total	N with defects	Percentage
Col	274	0	0
<i>sub-9</i>	291	82	28.2
<i>chc1-1</i>	130	0	0
<i>chc1-2</i>	121	0	0
<i>chc2-1</i>	126	0	0
<i>chc2-2</i>	230	0	0
<i>chc1-1 sub-9</i>	235	14	6
<i>chc1-2 sub-9</i>	185	11	6
<i>chc2-1 sub-9</i>	211	14	6.6
<i>chc2-2 sub-9</i>	237	13	5.5

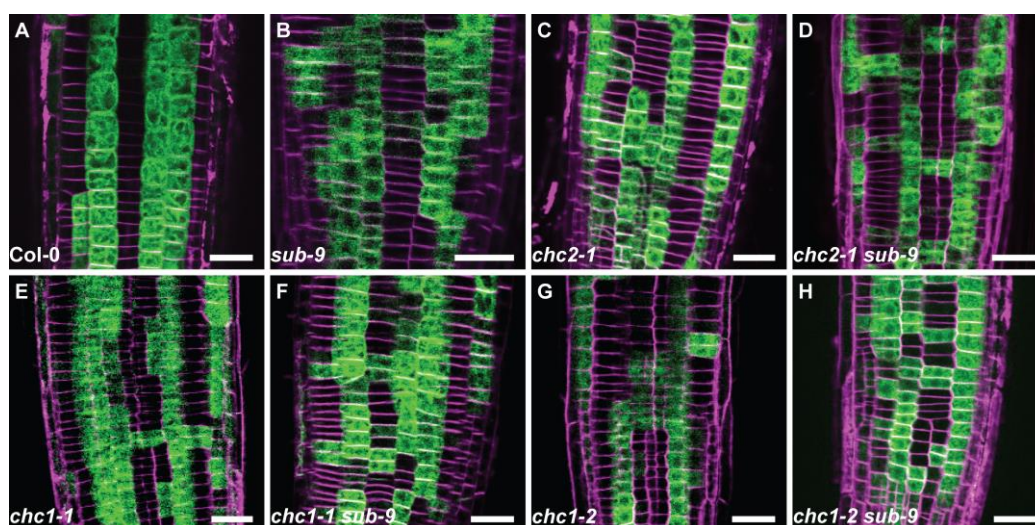


Figure 20 Expression pattern of pGL2::GUS:EGFP in wild-type, *chc2-1*, *chc2-1 sub-9*, *chc1-2*, and *chc1-2 sub-9* mutants.

Fluorescence micrographs show optical sections of epidermal cells of root meristems of seven days-old seedlings. FM4-64 was used to label cell outlines. Genotypes are indicated. Note the similarly aberrant root hair patterning in *sub-9* and different *chc* mutants. Scale bars: 25 μ m.

Results

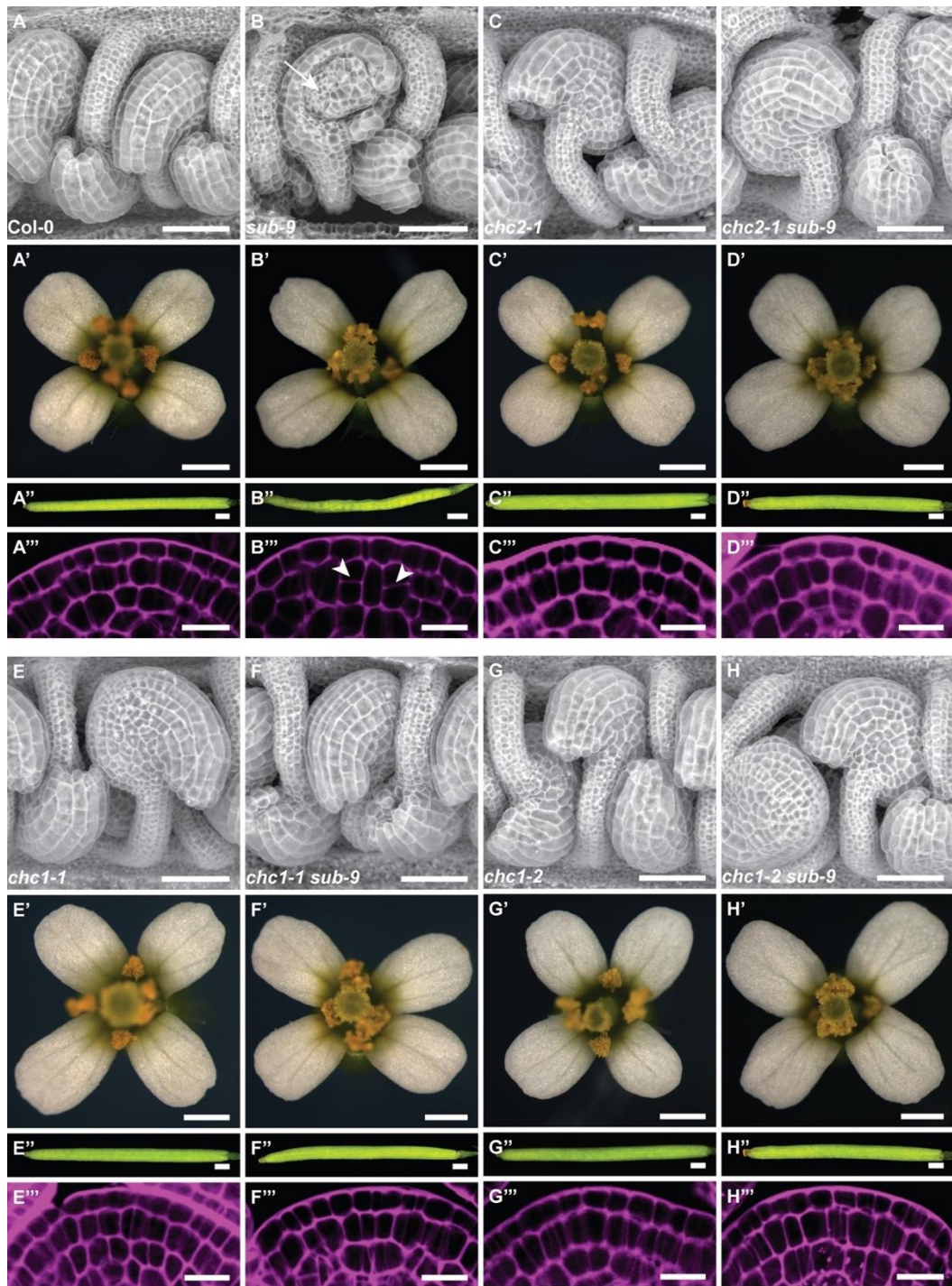


Figure 21 Comparison of the floral phenotypes between Col-0, *sub-9*, and various *chc* mutants.

(A) to (D) and (E) to (H). Scanning electron micrographs of stage 4 ovules (stages according to (Schneitz *et al.*, 1995)). (A') to (D') and (E') to (H') Morphology of mature stage 13 or 14 flowers (stages according to (Smyth *et al.*, 1990)). (A'') to (D'') and (E'') to (H'') Morphology of siliques. (A''') to (D''') and (E''') to (H''') Central region of stage 3 floral meristems stained with pseudo-Schiff propidium iodide (mPS-PI). Scale bars: (A) to (D) and (E) to (H) 50 μ m, (A') to (D') and (E') to (H')

Results

(E') to (H') 0.5 mm, (A'') to (D'') and (E'') to (H'') 1 mm, (A''') to (D''') and (E''') to (H''') 10 μ m. Genotypes are indicated.

3.5 Characterization of the Arabidopsis CHC1 and CHC2

Two *CHC* (*CHC1-2*) and three *CLC* (*CLC1-3*) genes were identified in *Arabidopsis thaliana* genome (Holstein, 2002; Chen *et al.*, 2011). In order to evaluate the importance of CHCs, I have performed *in silico* analyses regarding structural and functional properties and conservation within Arabidopsis. CHC proteins of *Arabidopsis thaliana* (AtCHC1: At3g11130, accession number Q0WNJ6, sequence length 1705 aa; AtCHC2: At3g08530, accession number Q0WLB5, sequence length 1703 aa) showed 97% sequence homology when compared to each other (Figure 22, FigureS1). The high degree of sequence identity between the two *CHC* gene products raises the potential of a functional redundancy. No double mutants nor plants that were homozygous for one mutation and heterozygous for the other were found. Thus, *CHC1* and *CHC2* genes are redundantly crucial for the viability of gametophytes and/or zygotes (Kitakura *et al.*, 2011). CHC proteins are highly conserved among plant species (Wang *et al.*, 2015b), with an amino acid identity of over 90%.

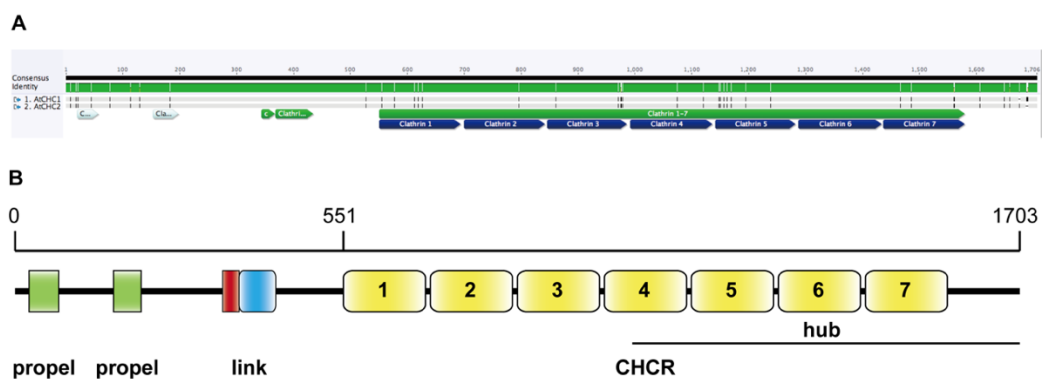


Figure 22 Structure properties of CHC2 and conservation between the Arabidopsis CHC1 and CHC2 proteins.

Results

(A) Alignment of CHC1 and CHC2 protein sequences of Arabidopsis. Green bars indicate identity or high similarity and lines show gaps. Alignment was performed in Geneious software using ClustalW algorithm with BLSM62 matrix. Detailed sequence information is shown in supplementary Figure 1. (B) Schematic depiction of functional domain structures of CHC2. CHC2-Hub is indicated at the corresponding region. Yellow rectangles indicate the seven CHCR motifs.

3.6 Mapping the interaction domain of CHC2 in a Y2H

The full-length *CHC2* cDNA contains a 5722-bp open reading frame encoding a peptide of 1703 amino acids with a molecular mass of 193.31 kD. Like other CHCs, CHC2 has multiple subdomains starting with an N-terminal domain and followed by linker, distal leg, knee, proximal leg, and trimerization domains (Ybe *et al.*, 1999). The N-terminal domain folds into a seven-bladed β -propeller structure. The other domains form a superhelix of short α -helices composed of the smaller structural module CHCRs (Smith and Pearse, 1999). Seven CHCRs are presented in both CHC1 and CHC2 (Figure 22).

Co-IP experiments indicate that SUB and CHC appear in the same complex (Figure 15). To further investigate a direct physical interaction between SUB and CHC2 targeted yeast-two-hybrid (Y2H) assay was performed. I observed that the intracellular domain of SUB (SUB-ICD, aa 364 to 769) can interact with a CHC2 fragment spanning residues 551 to 1703, encompassing the seven CHCR domains and the C-terminal end, in this system (Figure 23).

I further determined that the entire juxta-membrane domain (SUB-JM, residues 364 to 496) was required for the observed interaction with CHC2-2 in the Y2H assay. Furthermore, the SUB kinase domain (SUB-KD, residues 497 to 769) or a fragment of the first half of SUB-JM (SUB Juxta 1st half, residues 364 to 429) and the second half of SUB-JM plus the first half of SUB-KD (SUB Juxta 2nd half, residues 430 to 630) failed to interact with CHC2-2 (Figure 24).

Results

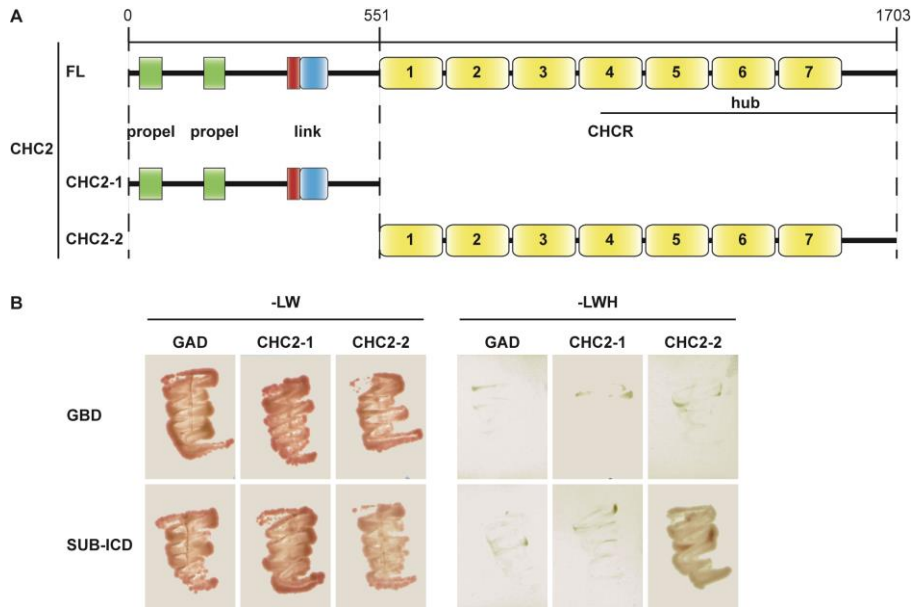


Figure 23 SUB-ICD interacts directly with CHC2.

(A) Schematic presentation of full-length CHC2 (FL) and truncated constructs CHC2-1 and CHC2-2 used for yeast-two-hybrid (Y2H). (B) Y2H assay involving the intracellular domain (ICD) of SUB fused to the GAL4 DNA-binding domain (GBD) and CHC2-1 or CHC2-2 fused to the GAL4 activating domain (GAD), respectively. Growth on -LW panel indicates successful transformation of both plasmids and on -LWH panel indicates presence or absence of interaction. Empty vectors, GAD and GBD, were used as negative controls.

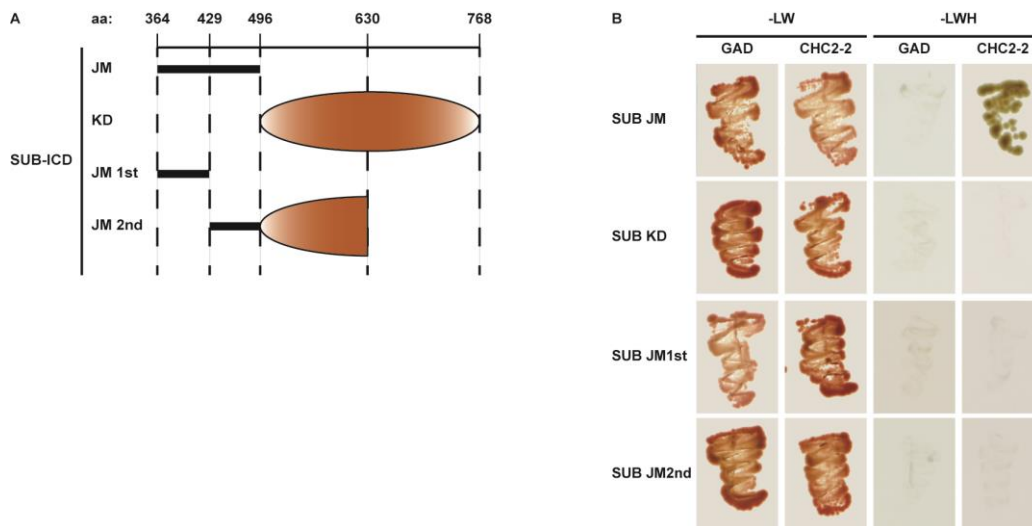


Figure 24 SUB-JM interact with CHC2-2.

(A) Schematic presentation of various truncated versions of SUB-ICD. (B) Y2H analysis of GAD-CHC2-2 with GBD-fusions of SUB-ICD variants.

3.7 SUB intracellular domain does not interact with the μ -adaptin of AP2 complex in a Y2H

CME requires a network of proteins including clathrin, adaptors and accessory proteins responsible for selection and recruitment of cargos (Traub, 2009; McMahon and Boucrot, 2011; Di Rubbo *et al.*, 2013). Internalization of RLKs from the PM by clathrin-mediated endocytosis involves binding of the intracellular domain of the RLK to the μ unit of the AP2 adaptor protein complex (Robinson and Pimpl, 2014; Paez Valencia *et al.*, 2016). Thus, I tested if SUB-ICD can interact with μ -adaptin of AP2 (AP2M) in yeast. Surprisingly, I could not detect a signal using SUB-ICD, SUB-JTM or SUB-KD as bait indicating that the intracellular domain of SUB does not interact with AP2M in a Y2H system (Figure 25).

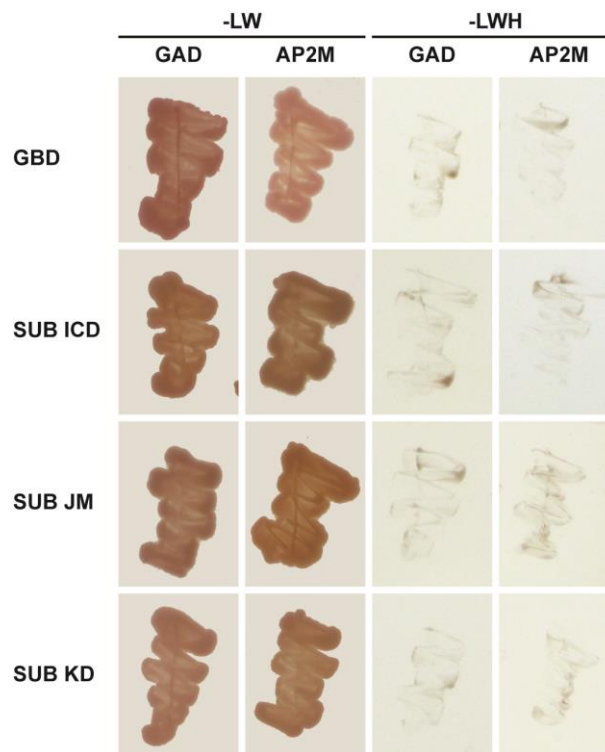


Figure 25 Y2H analysis of SUB-ICD deletion variants with AP2 μ subunit.

AD: activation domain of GAL4 TF; BD: DNA-binding domain of GAL4 TF; SD-LW: SD medium lacking Leu and Trp (transformation control); SD-LWH: SD medium lacking Leu, Trp, and His (interaction control).

3.8 *ap2* mutants do not rescue *sub-9* phenotype

In animals, the endocytic adaptor AP2 complex is formed by assembly of four distinct types of subunits, α -adaptin, β -adaptin, μ -adaptin and σ -adaptin (Boehm and Bonifacino, 2001). Arabidopsis clathrin chains associate with AP2 subunits and form punctate foci at the plasma membrane (Kim *et al.*, 2013; Yamaoka *et al.*, 2013; Fan *et al.*, 2013). Similar to clathrin mutants, plants impaired in AP2 subunits show alterations in general endocytosis and PIN internalization and/or polarity, as well as defects in the endocytosis of BRI1, which correlates with severe developmental defects (Di Rubbo *et al.*, 2013; Kim *et al.*, 2013; Yamaoka *et al.*, 2013; Fan *et al.*, 2013; Luschnig and Vert, 2014).

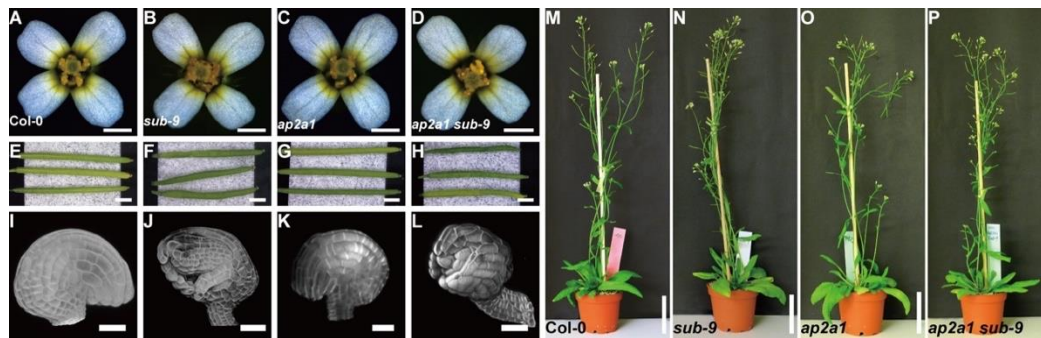


Figure 26 Phenotypal characterization of *ap2a1* and *ap2a1 sub-9*.

(A) to (D) Morphology of mature stage 13 or 14 flowers. (E) to (H) Morphology of siliques. (I) to (L) MorphoGraphX images of stage 4 ovules. (M) to (P) Whole plants of indicated genotypes. Scale bars: (A) to (D) 0.5 mm, (E) to (H) 2 mm, (I) to (L) 25 μ m and (M) to (P) 5 cm.

To further investigate whether the CME AP2 complex is involved in the SUB mediated floral organ development, homozygous *ap2* mutants and double mutant *ap2 sub-9* were used for genetic analysis. I obtained the AP2 knockout mutants *ap2* from NASC and screened for the homozygous lines via genotyping and sequencing (Bashline *et al.*, 2013; Kim *et al.*, 2013; Yamaoka *et al.*, 2013). Phenotypic analysis showed that flowers, siliques, ovules and overall phenotype were not disturbed in the *ap2a1* and *ap1/2b2* mutants compared with Col-0 wild

Results

type (Figure 26, 27) (Table 6). The *ap2m* and *ap2s* mutants exhibited morphologically abnormal flowers, shorter siliques, aberrant ovules and dwarf overall plant phenotype (Kim et al., 2013; Yamaoka et al., 2013; Fan et al., 2013) (Figure 28, 29) (Table 6).

Next, I analyzed the phenotype of the *ap2a1 sub-9*, *ap1/2b2 sub-9*, *ap2m sub-9* and *ap2s sub-9* double mutants. Since the *ap2m* and *ap2s* mutant anthers exhibited indehiscence and severely reduced fertility problem, the AP2M and AP2S heterozygous T-DNA mutants were used for crossing. The phenotype of *ap2a1 sub-9* and *ap1/2b2 sub-9* mutants is similar to *sub-9*, whereas *ap2m sub-9* and *ap2s sub-9* show similar defects as the *ap2m* and *ap2s* single mutants (Figure 26, 27, 28, 29) (Table 6).

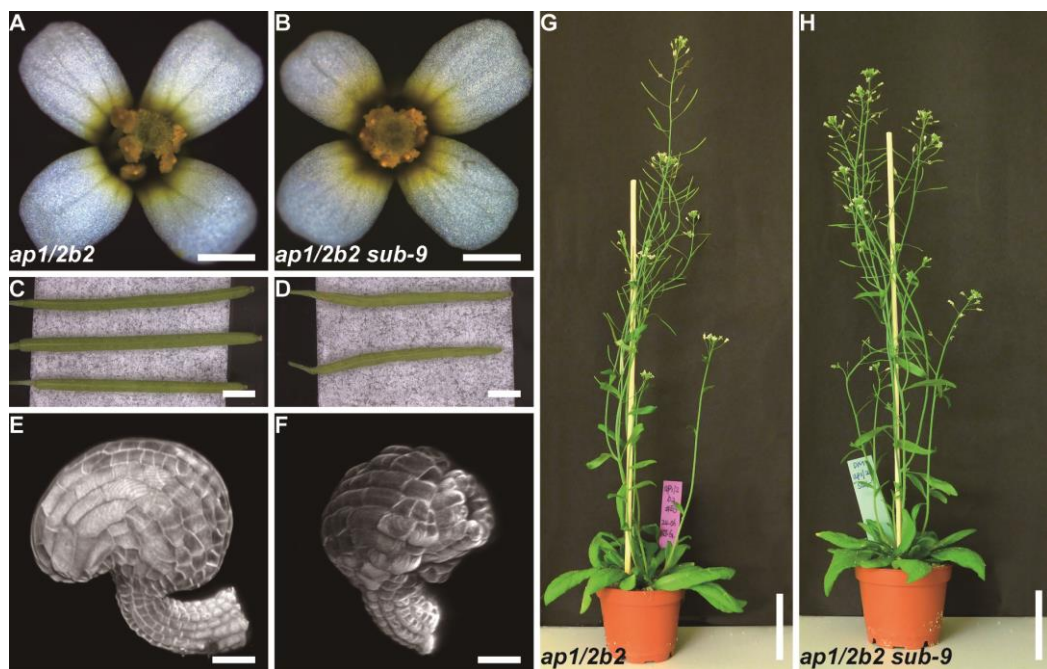


Figure 27 Phenotypic analysis of *ap1/2b2* and *ap1/2b2 sub-9*.

Floral shapes (A, B), silique (C,D), ovules (E,F) and overall plants (G,H) of *ap1/2b2* (A, C, E, G) and *ap1/2b2 sub-9* (B, D, F, H) were shown. Scale bars: (A) to (B) 0.5 mm, (C) to (D) 2 mm, (E) to (F) 25 μ m, (G) to (H) 5 cm.

Results

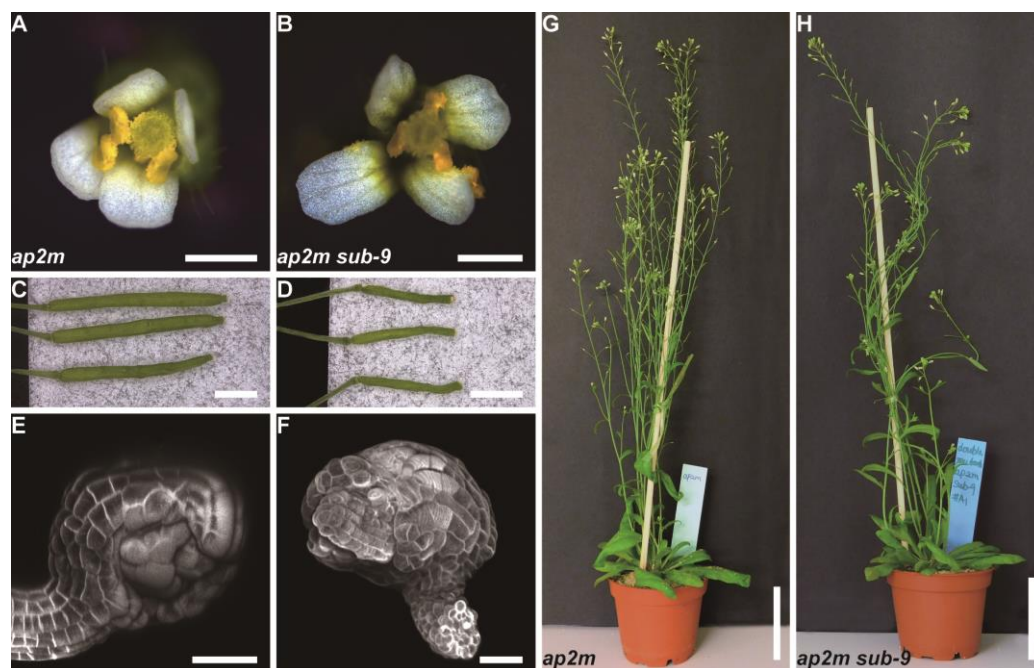


Figure 28 The *ap2m* and *ap2m sub-9* mutants show multiple morphological abnormalities.

Images of flowers (A) and (B), siliques (C) and (D), ovules (E) and (F), whole plants (G) and (H). Scale bars: (A) to (B) 0.5 mm, (C) to (D) 2 mm, (E) to (F) 25 μm, (G) to (H) 5 cm.

Table 6 Comparison of integument defects between *sub-9*, *ap2* and *ap2 sub-9* mutants.

Genotype	N total	N with defects	Percentage
Col	52	0	0
<i>sub-9</i>	48	15	31.2
<i>ap2a1</i>	59	0	0
<i>ap1/2b2</i>	60	0	0
<i>ap2m</i>	43	39	90.6
<i>ap2s</i>	33	29	87.8
<i>ap2a1 sub-9</i>	42	13	30.9
<i>ap1/2b2 sub-9</i>	51	17	33.3
<i>ap2m sub-9</i>	34	34	100
<i>ap2s sub-9</i>	30	29	96.7

Results

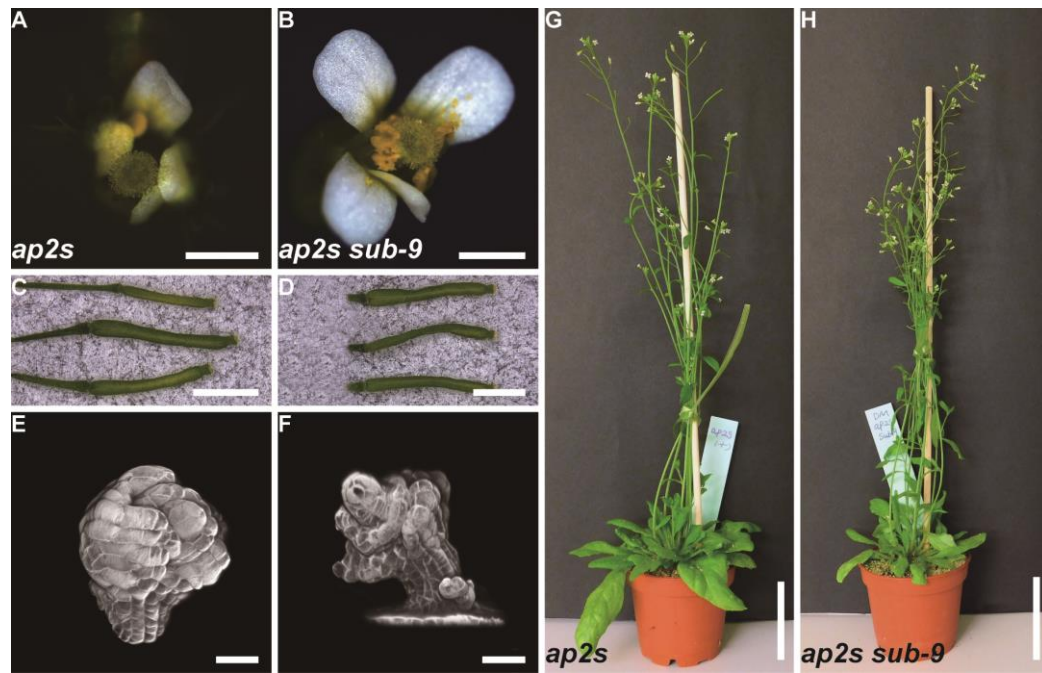


Figure 29 Phenotypic analysis of *ap2s* and *ap2s sub-9*.

(A) and (B) The *ap2s* and double mutant *ap2s sub-9* showed abnormal flowers. (C) and (D) Morphology of siliques. (E) and (F) Morphology of ovules. Scale bars: (A) to (B) 0.5 mm, (C) to (D) 2 mm, (E) to (F) 25 μ m, (G) to (H) 5 cm.

4 Discussion

Well-coordinated cell-to-cell communication plays a crucial role in organogenesis. The relevance of cell surface-localized RLKs for this intercellular communication network is becoming more evident, but the knowledge about their trafficking mechanisms and the respective relationship with signaling is poorly characterized. The atypical RLK SUB is required for tissue morphogenesis such as proper floral organ shaping, integument outgrowth, leaf development and root hair cell specification (Chevalier *et al.*, 2005; Kwak *et al.*, 2005; Vaddepalli *et al.*, 2011; Lin *et al.*, 2012). In this work, I approached the endocytic mechanism of SUB to get a better understanding of the role of SUB signaling in morphogenesis.

4.1 The endocytic route of SUB

An impressive body of published work has elucidated many of the intricacies of receptor-mediated endocytosis of plant RLKs. Much is known about the internalization and endocytic trafficking of plant RLKs with functional kinase domains. The atypical RLK SUB carries an inconspicuous kinase domain, however, enzymatic kinase activity could not be demonstrated in *in vitro* biochemical experiments and is not required for its function *in vivo* (Chevalier *et al.*, 2005; Vaddepalli *et al.*, 2011; Kwak *et al.*, 2014). Using SUB as a model I explored the endocytic route of an atypical RLK. I investigated this process by examining the subcellular distribution of a functional SUB:EGFP reporter in epidermal cells of the root meristem. No ligand for SUB has been described to date rendering an experimental strategy currently impossible. However, some RLKs undergo endocytosis independently of exogenous application of ligand, including BRI1 (Ruscinova *et al.*, 2004; Geldner *et al.*, 2007; Jaillais *et al.*, 2008), SOMATIC EMBRYOGENESIS RECEPTOR-LIKE KINASE 1 (SERK1) (Shah *et al.*, 2001; Shah *et al.*, 2002), BRI1-ASSOCIATED RECEPTOR KINASE 1

Discussion

(BAK1)/SERK3 (Rusinova *et al.*, 2004), and Arabidopsis CRINKLY4 (ACR4) (Gifford *et al.*, 2005). My data are compatible with the notion that PM-localized SUB becomes internalized and traffics from the TGN/EEs to MVB/LEs and eventually the vacuole where it is destined for degradation. SUB:EGFP was observed to enter this endocytic route in the apparent absence of activation of SUB signaling by artificial stimulation or application of exogenous ligand. A similar observation was for example made for ACR4 (Gifford *et al.*, 2005). One interpretation of this finding could be that endogenous SUB ligand is always present in sufficient levels to promote SUB endocytosis. In another possible scenario, the rate of SUB internalization may be independent from ligand availability as was shown for BRI1 (Rusinova *et al.*, 2004; Geldner *et al.*, 2007). In any case, my data indicate that the endocytic route of the atypical RLK SUB for the most part seems to adhere to the established pattern of plant receptor-mediated endocytosis (Figure 30).

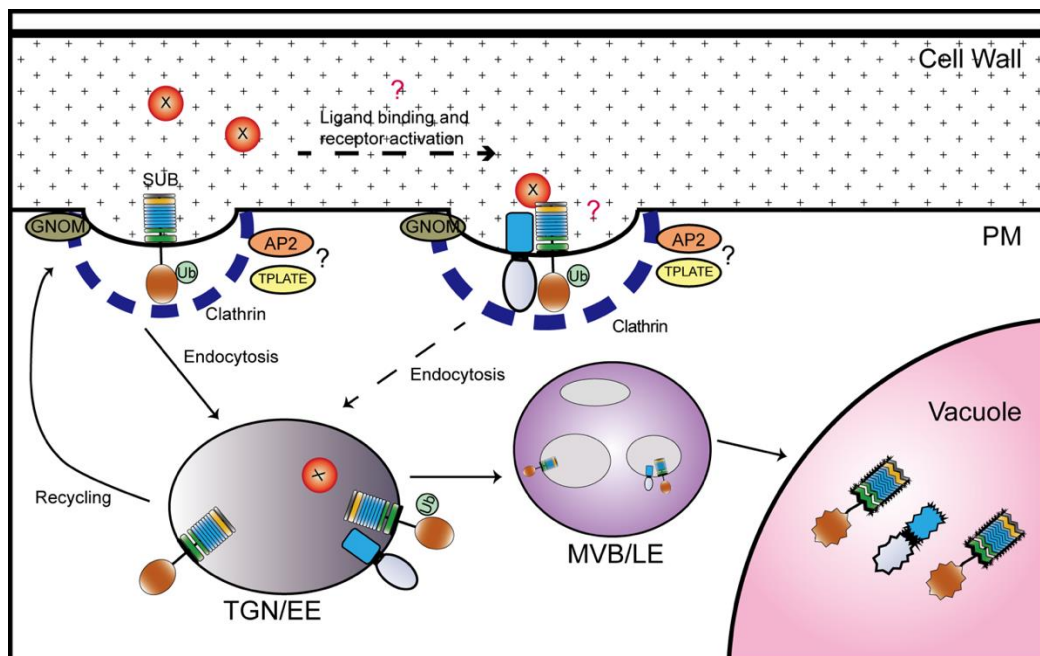


Figure 30 Schematic model of the SUB trafficking to and from the cell surface.

Independent of ligand SUB traffics from the PM to the vacuole via TGN/EEs and MVBs. TGN/EE, trans-Golgi network/early endosomes; MVB, multivesicular body; Ub, ubiquitination. Red

question marks, ligand X and unknown factors may be involved in the activation of SUB internalization; Black question marks, the two early adaptor protein AP2 and TPLATE need to be further clarified.

4.2 SUB receptor is ubiquitinated *in vivo*

Apart from being a central signal for proteasome-mediated degradation ubiquitination is a major endocytosis determinant of PM proteins (Haglund and Dikic, 2012; Isono and Kalinowska, 2017). Several plant RLKs are known to be ubiquitinated, including FLS2 (Lu *et al.*, 2011), BRI1 (Martins *et al.*, 2015; Zhou *et al.*, 2018), and LYK5 (Liao *et al.*, 2017). The observed *in vivo* ubiquitination of SUB:EGFP is compatible with the notion of SUB being internalized and transported to the vacuole for degradation. However, it remains to be determined which E3 ubiquitin ligase promotes ubiquitination of SUB and how SUB endocytosis relates to the control of its signaling. Internalization can be linked with downstream responses, as was demonstrated for FLS2 or the *AtPep1*-PEPR complex (Mbengue *et al.*, 2016; Ortiz-Morea *et al.*, 2016), or contribute to signal downregulation, as it is the case for BRI1 (Irani *et al.*, 2012; Zhou *et al.*, 2018) or LYK5 (Liao *et al.*, 2017).

4.3 Signaling mediated by SUB involves CME

Several lines of evidence support the notion of SUB:EGFP undergoing CME. First, CHC *in vivo* co-immunoprecipitated with SUB:EGFP. Second, I observed a reduction in intra-cellular SUB:EGFP puncta accompanied with a stronger SUB:EGFP signal at the PM in the HUB-line upon induction. Third, the genetic analysis revealed a connection of SUB with a clathrin-dependent process. Plants with a defect in *CHC2* show significantly reduced endocytosis rate of FM4-64 and aberrant polar localization of the polar auxin transporter PINFORMED 1 (PIN1) (Kitakura *et al.*, 2011) as well as reduced internalization of, for example, PEP1 (Ortiz-Morea *et al.*, 2016), FLS2 (Mbengue *et al.*, 2016), and BRI1 (Wang

et al., 2015a). Accordingly, *chc2* mutants show multiple defects, including patterning defects in the embryo (Kitakura *et al.*, 2011), impaired mitogen-activated protein kinase (MAPK) activation (Ortiz-Morea *et al.*, 2016), and defective stomatal closure and callose deposition upon bacterial infection (Mbengue *et al.*, 2016). My genetic analysis revealed that *CHC2*, and to a lesser effect *CHC1*, also affects root hair patterning. Importantly, it provides evidence for a biologically relevant interaction between *SUB* and a *CHC*-dependent process.

4.4 *SUB* genetically interacts with clathrin-mediated pathways in a tissue-specific manner

Interestingly, the data suggest that the type of genetic interaction between *SUB* and *CHC* depends on the tissue context. In the root, *SUB* and *CHC* promote root hair patterning. Several hypotheses are conceivable that could explain the result. As my data support the notion of *SUB*:EGFP undergoing CME, one model states that CME of *SUB* is required for root hair patterning. Therefore, *SUB* internalization in single *chc* mutants would be reduced resulting in a hyperaccumulation of *SUB* at the PM. Two alternative further scenarios are compatible with this notion. In the first scenario hyperaccumulation of *SUB* at the PM interferes with root hair patterning. This view is supported by the observation that not just a reduction of *SUB* activity but also ectopic expression of *SUB* in *p35S::SUB* plants results in a weak defect in root hair patterning (Kwak and Schiefelbein, 2007), similar to what I observed for *chc2* mutants. In the second scenario, a reduction of *SUB* internalization leads to fewer *SUB*-labelled endosomes, which in turn impairs root hair patterning. This scenario implies that *SUB* signals while being present on endosomes. In another model, a reduction of *CHC* activity could influence clathrin-dependent secretion of newly translated and/or recycled *SUB* to the PM thereby reducing the level of active *SUB* at the PM below a certain threshold. Finally, given the pleiotropic phenotype of *chc*

Discussion

mutants the genetic data do not rule out a more indirect interaction between *SUB* and *CHC* (Figure 31). Further work remains to be done to discriminate between the different possibilities. However, I currently favor the notion that CME of SUB is critical for root hair patterning as a block of CME of SUB:EGFP in the HUB line results in a reduction of internalized SUB:EGFP vesicles and elevated levels of SUB:EGFP at the PM.

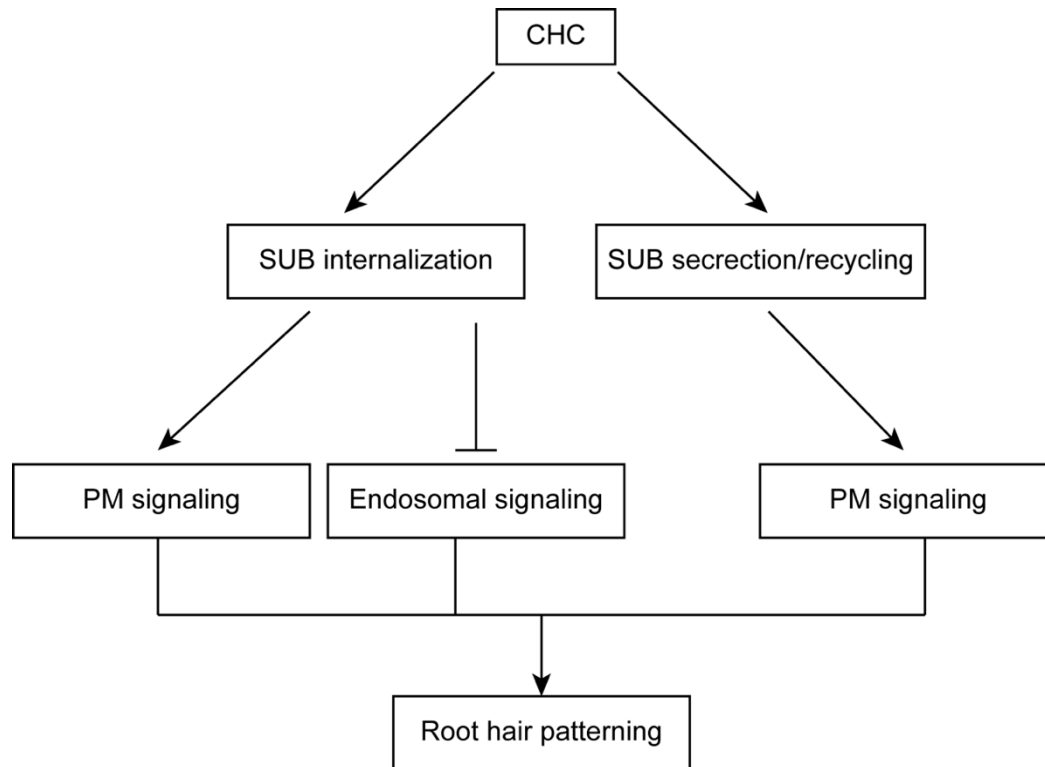


Figure 31 Hypothetical scheme of the molecular mechanisms underlying the *SUB* signaling pathway with respect to root hair patterning.

CME of SUB is possibly required for root hair patterning via PM platform and/or signaling endosomes. The effects of CHC activity could also regulate the active SUB at PM through secretion/ recycling pathway and mediate root hair patterning.

In contrast to the positive genetic role of *SUB* and *CHC* in root hair patterning the apparent wild-type appearance of floral organs of *sub chc* double mutants indicates that *SUB* is a negative regulator of a *CHC*-dependent process during floral development. The molecular mechanism remains to be investigated. CME could for instance promote the internalization of a PM-resident signaling molecule, thereby attenuating its activity. This endocytic process could be

counteracted upon by SUB. For example, in a *sub* mutant the activity of the hypothetical signaling factor at the PM is reduced through increased endocytosis. In a *sub chc* double mutant the principally higher level of internalization caused by the lack of SUB activity is offset by reduced CME due to impaired CHC function. Thus, the individual *sub* and *chc* effects cancel each other out in *sub chc* double mutants and the respective plants show flowers with apparent wild-type morphology. It will be an exciting challenge to unravel the molecular details of how SUB and clathrin interact to allow tissue morphogenesis in future studies.

4.5 How does AP2 relate to CME with respect to SUB signaling?

The AP2 that represents the core complex during the cargo recognition/selection of CME in animals has also been reported to mediate CME of several plasma membrane-localized proteins, such as the cellulose synthase CESA6, the auxin-efflux carrier PIN FORMED2 (PIN2), and BRI1 in plants (Bashline *et al.*, 2013; Di Rubbo *et al.*, 2013; Kim *et al.*, 2013). Thus, I was interested in the function of AP2 in CME with respect to SUB signaling. Interestingly, AP2M, which recognizes specific sorting motifs on cargo proteins, does not interact with SUB intracellular domain. On the contrary, CHC2 interacts with SUB in yeast. This may be due to the artefact as it is not expected to occur *in vivo*. Alternatively, some native proteins from yeast help the interaction. Consistent with the AP2M yeast data, genetics analysis revealed that *ap2 sub-9* double mutants do not show any rescue of *sub-9* mutant silique twisting, ovule phenotype as *chc sub-9* do. A simple explanation is possibly due to the newly identified TPLATE complex (TPC) redundancy. TPC that consists of eight core subunits has been found to accumulate at the PM, preceding the recruitment of future components for formation of CCVs (Gadeyne *et al.*, 2014; Zhang *et al.*, 2015). TPC is required for clathrin recruitment to the PM, even after AP2 depletion (Wang *et al.*, 2016b). However, to get a deeper insight whether CME in SUB

Discussion

signaling is AP2 dependent or not, it is still necessary to elucidate how they participate in the internalization of cargos with biological and pharmacological approaches. For instance, triple or quadruple mutant combinations of *ap2* and *sub-9* are needed for further phenotypic analysis. Besides, I identified three putative endocytic motifs at the JM and KD of SUB (Figure 32). It would be worthwhile to generate specific mutations into these endocytic binding motifs and to explore whether through this approach the *sub* mutant phenotype is rescued in transgenic Arabidopsis and the SUB trafficking could be changed.

```
410 FDGYGAGDRK YGYPMPQRAEESRRAMPPTSYYNKDVNTPQKPLQQPPRQFQSNDTASKRA
470 AHFPPGLNSSSSATVFTIASLQQYTNNFSEENIIGEGSIGNVYRAELRHGKFLAVKKLSN
530 TINRTQSDGEFLNLVSNVLKLRGHILELLGYCNEFGQRLLVYEYCPNGSLQDALHLDRK
590 LHKKLTWNVRIINALGASKALQFLHEVCQPPVVHQNFKSSKVLLDGKLSVRVADSGLA YM
650 LPPRPTSQMAG YAAPEVEYGSYTCQSDVFSLGVVMLELLTGRRPFDRTRPRGHQTLAQWA
710 IPRLHDIDALTRMVDP SLHGAYPMKSLSRFADIISRSLQMEPGFRPPISEIVQDLQHMI
```

Figure 32 SUB-JM and KD domain sequence with putative protein endocytic motifs.

YXXΦ functions as cargo sorting signals, X for any residue and Φ for a bulky hydrophobic amino acid.

5 Conclusion

Proper organ development relies on spatiotemporal regulation of cell proliferation, division plane determination and growth. Intercellular cell-to-cell communication is important for tissue morphogenesis.

RLKs are cell-surface receptors that perceive and pass intercellular information. In *Arabidopsis* the atypical LRR-RLK SUB was demonstrated to be of extremely importance in leaf and floral organ shape, ovule integument initiation and outgrowth, and root hair patterning (Chevalier *et al.*, 2005; Kwak *et al.*, 2005; Vaddepalli *et al.*, 2011; Lin *et al.*, 2012). CME and subcellular distribution of RLKs play an active role in their response and signaling. Nonetheless, the underlying trafficking mechanisms of the PM-localized receptors remain to be elucidated. Studying clathrin-dependent SUB signaling will contribute to our understanding of how atypical RLKs mediate signal transduction and how cells co-ordinate their behavior to allow appropriate three-dimensional organ architecture. In this thesis, I explored the endocytic trafficking of SUB, providing new information to understand the atypical RLK internalization.

I found that SUB undergoes internalization from PM to the vacuole for degradation in the absence of any exogenous stimulation. My data reveal that SUB endocytic route involves the TGN/EE, the MVB/LEs. The functional SUB:EGFP is also ubiquitinated *in vivo*. The ubiquitination of SUB is matched with the observation of SUB being internalized and degraded in the vacuole. Additionally, coimmunoprecipitation experiments revealed that clathrin and SUB interacted. With HUB-line induction, the decreased SUB endosomes and a stronger SUB signal at PM is observed. According to my genetic data, SUB behaves a positive role to *CHC* in root hair patterning. However, SUB is a negative regulator of the clathrin-dependent process with respect to floral organ development. All in all, the *Arabidopsis* receptor kinase SUB is internalized by

Conclusion

CME and affects clathrin-dependent in a tissue-dependent manner. Moreover, *ap2* mutants do not rescue *sub-9* phenotype and AP2M does not interact with SUB-ICD which hints SUB internalization is probably AP2 independent. Nevertheless, further analysis needs to be done to resolve this conflict.

Since SUB undergoes CME and can be ubiquitinated *in vivo*. It would be of great interest to find out the corresponding ligand which is essential for the advancement of our understanding of SUB signaling network in plants. An open question that remains to be elucidated is the ubiquitination mechanism of SUB and how it relates to the CME to control SUB signaling.

6 Supplement

AtCHC2 MAAANAPITMKEVLTLPISIGINQQFITFTNVTMESDKYICVRETSPQNSVVIIDMNMPMQ
 AtCHC1 MAAANAPIIMKEVLTLPVIGIQQFITFTNVTMESDKYICVRETAPQNSVVIIDMNMPMQ
 ***** : ***** : ***** : ***** : *****

AtCHC2 PLRRPITADSALMNPNSKILALKAQVPGTTQDHLQIFNIEAKAKLKSHPQEQVVFVKWI
 AtCHC1 PLRRPITADSALMNPNSRILALKAQVPGTTQDHLQIFNIEAKAKLKSHPQEQVAFVKWI
 ***** : ***** : ***** : ***** : *****

AtCHC2 TPKMLGLVTQNSVYHWSIEGDSEPVKMFDRATANLANNQIINYKCSNPKEKWLVLIGIAPGS
 AtCHC1 TPKMLGLVTQTSVYHWSIEGDSEPVKMFDRATANLANNQIINYKCSNPKEKWLVLIGIAPGS
 ***** : ***** : ***** : ***** : *****

AtCHC2 PERQQLVKGNMQLFSVDQQRSQLAHAASFAQFKVPGNENPSILISFASKSFNAGQITS
 AtCHC1 PERPQLVKGNMQLFSVDQQRSQLAHAASFAQFKVPGNENPSILISFASKSFNAGQITS
 *** ***** : ***** : ***** : ***** : *****

AtCHC2 KLHVIELGAQPGKPSFTKKQADLFFPPDFADDFPVAMQVSHKFNLIYVITKLGLLFVYDL
 AtCHC1 KLHVIELGAQPGKPSFTKKQADLFFPPDFADDFPVAMQVSHKFNLIYVITKLGLLFVYDL
 ***** : ***** : ***** : ***** : *****

AtCHC2 ETASAIYRNRISDPDIFLTSEASSVGGFYAINRRGQVLLATVNEATIIPFISGQLNNLEL
 AtCHC1 ETASAIYRNRISDPDIFLTSEASSVGGFYAINRRGQVLLATVNEATIIPFISGQLNNLEL
 ***** : ***** : ***** : ***** : *****

AtCHC2 AVNLAKRGNLPGAENLVVQRFQELFAQTKYKAAELAAESPQGILRTPDTPVAKFQSVVPVQ
 AtCHC1 AVNLAKRGNLPGAENLVVQRFQELFAQTKYKAAELAAESPQGILRTPDTPVAKFQSVVPVQ
 ***** : ***** : ***** : ***** : *****

AtCHC2 AGQTPPLLQYFGTLLTRGKLSYSELSRLVVNQNKNLLENWLAEDKLECSEELGDLV
 AtCHC1 AGQTPPLLQYFGTLLTRGKLSYSELSRLVVNQNKNLLENWLAEDKLECSEELGDLV
 ***** : ***** : ***** : ***** : *****

AtCHC2 KTVDNDLALKIYIKARATPKVVAFAERREFDKILYISKQVGYTPDYFLQLTILRTDPQ
 AtCHC1 KTVDNDLALKIYIKARATPKVVAFAERREFDKILYISKQVGYTPDYMFLLQTLILRTDPQ
 ***** : ***** : ***** : ***** : *****

AtCHC2 GAVNFALMMSQMEGGSPVDYNTITDLFLQRNLIREATSFLLDVLPKNLPEHAFLOTKVLE
 AtCHC1 GAVNFALMMSQMEGGCPVDYNTITDLFLQRNLIREATAFLLDVLPKNLPEHAFLOTKVLE
 ***** : ***** : ***** : ***** : *****

AtCHC2 INLVTFPNVADAVLANGMFTHYDRPRIAQLCEKAGLYIQSLKHYSLELPIKRVIINTHAI
 AtCHC1 INLVTFPNVADAILANGMFSHYDRPRVAQLCEKAGLYIQSLKHYSLELPIKRVIINTHAI
 ***** : ***** : ***** : ***** : *****

AtCHC2 EPQALVEFFGTLSEWAMECMKDLLLVNLRGNLQIIVQACKEYCEQLGVDACIKLFEQFK
 AtCHC1 EPQALVEFFGTLSEWAMECMKDLLLVNLRGNLQIIVQACKEYCEQLGVDACIKLFEQFK
 ***** : ***** : ***** : ***** : *****

AtCHC2 SYEGLYFFLGSYLSMSSEDPFIHFYIEAAAKTGOIKEVERVTRESNFYDAEKTKNFLMEA
 AtCHC1 SYEGLYFFLGSYLSMSSEDPFIHFYIEAAAKTGOIKEVERVTRESNFYDAEKTKNFLMEA
 ***** : ***** : ***** : ***** : *****

AtCHC2 KLPDARPLINVCDRFSFVVDLTHYLYTNMMLRYIEGYVQKVNPGNAPLVVQQLLDDECP
 AtCHC1 KLPDARPLINVCDRFGFVVDLTHYLYTNMMLRYIEGYVQKVNPGNAPLVVQQLLDDECP
 ***** : ***** : ***** : ***** : *****

AtCHC2 DFIKGLILSVRSLLPVEPLVEEKEKRNRLRLLTQFLEHLVSEGSQDVHVHNALGKIIIDS
 AtCHC1 DFIKGLILSVRSLLPVEPLVAEKEKRNRLRLLTQFLEHLVSEGSQDVHVHNALGKIIIDS
 ***** : ***** : ***** : ***** : *****

AtCHC2 NNNPEHFLTTPNYDYSKVGKYCEKRDPTLAVVAYRRGQCDEELINVTNKNSLFLQARY
 AtCHC1 NNNPEHFLTTPNYDYSKVGKYCEKRDPTLAVVAYRRGQCDEELINVTNKNSLFLQARY
 ***** : ***** : ***** : ***** : *****

AtCHC2 VVERMDGDLWDKVLDENNDYRRQLIDQVSTALPESKSPQVSAAVKAFMTADLPHELIE
 AtCHC1 VVERMDGDLWEKVLTEENEYRRQLIDQVSTALPESKSPQVSAAVKAFMTADLPHELIE
 ***** : ***** : ***** : ***** : *****

1

Supplement

```

AtCHC2      LLEKIVLQNSAFSGNFNLQNLILLITAIKADPSRVMDYINRLDNFDGPAVGEVAVEAQLYE
AtCHC1      LLEKIVLQNSAFSGNFNLQNLILLITAIKADPSRVMDYINRLDNFDGPAVGEVAVDAQLYE
*****:*****

AtCHC2      EAFAIFFKFNLNVAQVNVLLDNVRSIERAVEFAFRVEEDSVWSQVAKAQLREGLVSDAIE
AtCHC1      EAFAIFFKFNLNVAQVNVLLDNVRSIERAVEFAFRVEEDAVWSQVAKAQLREGLVSDAIE
*****:*****

AtCHC2      SFIRADDATHFLEVIRVSEDTDVYDDLKYLMLMVRQVKPKVDSELIYAYAKIDRLGEI
AtCHC1      SFIRADDTTQFLEVIRASEDTNVYDDLVRVYLLMVRQVKPKVDSELIYAYAKIERLGEI
*****:*:*****.***:*****:*****:*****:*****

AtCHC2      EEFILMPNVANLQHVGDRLYDEALYEAAKIIYAFISNWGLAVTLVKLQFQGAVDAARK
AtCHC1      EEFILMPNVANLQHVGDRLYDEALYEAAKIIYAFISNWKAVTLVKLQFQGAVDAARK
*****:*****

AtCHC2      ANSAKTWKEVCFACVDAEEFRLAQICGLNIIIQVDDLEEVSEYQNRGCFNELISLMESG
AtCHC1      ANSAKTWKEVCFACVDAEEFRLAQICGLNIIIQVDDLEEVSEYQNRGCFNELISLMESG
*****:*****

AtCHC2      LGLERAHMGIFTELGVLRYRYEKLMEHIKLFSTRLNIPKLIRACDEQQHWQELTYLYI
AtCHC1      LGLERAHMGIFTELGVLRYRYEKLMEHIKLFSTRLNIPKLIRACDEQQHWQELTYLYI
*****:*****

AtCHC2      QYDFDQNAATTVMNHSPEAWEHMQFKDIVAKVANVELYKAVHFYQLQEHPIINDLLNVL
AtCHC1      QYDFDQNAATTVMNHSPEAWEHMQFKDIVAKVANVELYKAVHFYQLQEHPIINDLLNVL
*****:*****

AtCHC2      ALRLDHTRVVDIMRKAGHLRLIKPYMIAVQSNNSAVNEALNEIYVEEEDYDRLRESIDL
AtCHC1      ALRLDHTRVVDIMRKAGHLRLIKPYMIAVQSNNSAVNEALNEIYVEEEDYDRLRESIDL
*****:*****

AtCHC2      HDSFDQIGLAQKIEKHELVEMRVAAYIYKAGRWKQSIALSKKDNMYKDCMETASQSGE
AtCHC1      HDSFDQIGLAQKIEKHELVEMRVAAYIYKAGRWKQSIALSKKDNMYKDCMETASQSGD
*****:*****

AtCHC2      HELAEQLLVYFIEQGKKECFATCLFVYDLIRPDVALELAWINNMDFAPPYLLQFIREY
AtCHC1      HDLAEQLLVYFIEQGKKECFATCLFVYDLIRPDVALELAWINNMDFAPPYLLQFIREY
*.:*****:*****

AtCHC2      SGKVDELIKDKLEAQKEVKAKEQEEKDVISQQNMYAQLPLALPAPPMPGMGGGGYGP
AtCHC1      SGKVDELIKDKLEAQKEVKAKEQEEKDVMSQQNMYAQLPLALPAPPMPGMGG--GGYGP
*****:*****:*****:*****

AtCHC2      PQMGMPG---MPPMPYGMPPMGY
AtCHC1      PQMGMPGMSGMPMPYGMPPMGY
*****

```

Figure S1: Clathrin heavy chain proteins in *Arabidopsis thaliana*. Protein sequence alignment of clathrin heavy chain (AtCHC2 and AtCHC1) performed with ClustalW. Identical residues are highlighted with asterisk. Numbering of amino acid residues begins at the first methionine.

Primer name	Sequence	Purpose
SUB_LP158	5'-TTGTTTGAGTGGACAGGGAC-3'	Genotyping <i>sub-9</i>
SUB_RP158	5'-GATGTTGTTGTGGTTGCAGTG-3'	SAIL_1158_D09
SAIL_LB2	5'- GCTTCCTATTATATCTTCCCAAATTA CCAATACA-3'	Genotyping SAIL lines
CHC2-LP321	5'-TGTTCTGCAAGTTCATGTTCG-3'	Genotyping <i>chc2</i>
CHC2_RP321	5'-AGGTGGATGACCTGGAAGAAG-3'	SALK_042321

Supplement

SALK_LBb1.3	5'-ATTTTGCCGATTTCGGAAC-3'	Genotyping SALK lines
CHC2_LP826	5'- AAAAGTCATGACACTTCTTCCATTC- 3'	Genotyping <i>chc2</i> SALK_028826
CHC2_RP826	5'-AATTCGAGGAAACCGTTATGG-3'	
CHC1_LP213	5'-TGGTGAAAGGAAATATGCAGC-3'	Genotyping <i>chc1</i>
CHC1_RP213	5'-TATATTGAAACGGAGGAAGCG-3'	SALK_112213
CHC1_LP252	5'-TAATAAGGCGCAAGTGACCAG-3'	Genotyping <i>chc1</i>
CHC1_RP252	5'-TTTATCCGAGCTGATGACACC-3'	SALK_103252
CHC1_213_F (P1)	5'- TTATGTCATCACCAAGCTTGGCCTG C-3'	CHC1-1 primers for RT-PCR
CHC1_213_R (P2)	5'- CGTATCAGGTGTCCGTAGAATGCCC -3'	
CHC1_252_F (P3)	5'- GTGACCGTTTGTACGATGAAGCTCT G-3'	CHC1-2 primers for RT-PCR
CHC1_252_R (P4)	5'- CTGGCGTACAGTACTCCTAACTCGG- 3'	
CHC2_826_F (P5)	5'- ATTGGCGGTCAGGACTTCTCAGCCG -3'	CHC2-1 primers for RT-PCR
CHC2_826_R (P6)	5'- GTCTGCAGTAATAGGCCTCCTAAGA GGC-3'	
CHC2_321_F (P7)	5'- GTTGGGTGTA CTCTATGCTAGATAT CG-3'	CHC2-2 primers for RT-PCR
CHC2_321_R (P8)	5'- AACACGAGTATGGTCTAACCGCAAC -3'	
GAPC_F	5'-CACTTGAAGGGTGGTGCCAAG-3'	GAPC primers for RT-PCR
GAPC_R	5'-CCTGTTGTCGCCAACGAAGTC-3'	
AP2A1_LP252	5'-ATTTCTTCGATTGAAGGTGCC-3'	Genotyping
AP2A1_RP252	5'-CATATGGCCAAAATCCACATC-3'	<i>ap2a1</i> SALK_045252
AP1/2B2_LP980	5'-CTCGAAGTACCAGACAGGCTG-3'	Genotyping
AP1/2B2_RP980	5'-ATGTATTTGACGACAGGCCTG-3'	<i>ap1/2b2</i> SALK_150980

Supplement

AP2M_LP693	5'-GCACAAAGAAAAGTCAGTGGC-3'	Genotyping <i>ap2m</i> SALK_083693
AP2M_RP693	5'-GCAATGCTAATGTTGCTTGTG-3'	
AP2S_LPC03	5'-CAAATCTTTTCTAGCTCCAAGC-3'	Genotyping <i>ap2s</i> SAIL_240_C03
AP2S_RPC03	5'-AGACAAAGCAAAATCCCAGTG-3'	
pUBQ(KpnI)_F	5'- ATATGGTACCAGTCTAGCTCAACAG AGC-3'	Replacing pSUB in pCambia2300
pUBQ(AscI)_R	5'- ATTGGCGCGCCCTGTTAATCAGAAA ACT-3'	
cDNA-CHC2_F	5'-CCAGTCTTTCTCTCGTCTCGGTTC- 3'	Amplifying CHC2 CDS including 112 bp upstream of 5' UTR and 40 bp downstream of 3' UTR
cDNA-CHC2_R	5'- CTTTTCCAAATGCGGATATTAAGC- 3'	
CHC2-F_ClaI	5'- GCATCGATGCATGGCGGCTGCCAAC GCCCCATC-3'	Cloning CHC2 CDS into Y2H pGADT7
CHC2-R_SalI	5'- AATGTCGACTTAGTAGCCGCCATC GGTGGC-3'	
CHC2 CDS part1_F_Sfi I	5'- ATGGCCATGGAGGCCATGGCGGCTG CCAACGCCCCC-3'	Cloning CHC2 part1 into Y2H pGADT7
CHC2 CDS part1_R_SmaI	5'- TCCCCGGGAGACATCATTAAATGCAA AAT-3'	
CHC2 CDS part2_F_Sfi I	5'- ATGGCCATGGAGGCCCAAATGGAA GGAGGTTCTCC-3'	Cloning CHC2 part2 into Y2H pGADT7
CHC2 CDS part2_R_SmaI	5'- TCCCCGGGGTAGCCGCCATCGGTG GCA-3'	
SUB juxta_F	5'- GACATATGAGATGTTGCAGAAGTAA AATATATAACC-3'	Cloning SUB juxta into Y2H pGBKT7
SUB juxta_R	5'- GAGGATCCATTTGTGTATTGCTGAA GTGAAGC-3'	

Supplement

Juxta half_R	5'- GAGGATCCTTCAGCCCGCTGTGGCA T-3'	Cloning SUB juxta 1 st half into Y2H pGBKT7
Juxta half_F	5'- GACATATGGAGAGCCGGAGAGCAA TGCC-3'	Cloning SUB juxta 2 nd half plus SUB kinase 1 st half into Y2H pGBKT7
Kinase half_R	5'- GAGGATCCCTTGGAAGACTTGAAAT TCTGG-3'	
SUB_kinase_F	5'- GAGGATCCAATTTCTCAGAAGAGAA TATAATCGG-3'	Cloning SUB kinase into Y2H pGBKT7
SUB_kinase_R	5'- GAGGATCCGATCATATGTTGAAGAT CTTGGACT-3'	
pGL2_F	5'-CTCTACTTGAGAGATATATCTG-3'	Amplifying pGL2 from Col-0 gDNA
pGL2_R	5'-TTTTCTTCTTAATATTCG-3'	
pGL2_F1	5'- AACAGGTCTCAACCTCTCTACTTGA GAGATATATCTG-3'	Cloning pGL2 into Greengate vector
pGL2_R1	5'- AACAGGTCTCTTGTTTTTTCTTCTTA ATATTCGAT-3'	
pGL2_F2	5'- AACAGGTCTCAGAGGCCACCCCTA TGTGTTTTATG-3'	Removing internal BsaI site forward
pGL2_R2	5'- AACAGGTCTCGCCTCTCTCCTCCGG AATTCGATCACG-3'	Removing internal BsaI site reverse
GUS_F	5'- AACAGGTCTCAGGCTCAACAATGAT GTTACGTCCTGTAGAAACCC-3'	Amplifying GUS CDS from pBI121
GUS_R	5'- AACAGGTCTCTCTGATTGTTTGCCTC CCTGCTGCGGTTTTTC-3'	
GL_F1	5'-CATTTTTATTTCTGTTTG-3'	Sequencing pGL2
GL_F2	5'-CTTGAATCAACTTAAGG-3'	
GL_F3	5'-CAACATACACATACATG-3'	
GL_R1	5'-CATATATATATATTTGATAAG-3'	

Table S1. Primers used in this study. Sequence and purpose are indicated.

7 References

- Alonso JM, Stepanova AN, Leisse TJ, Kim CJ, Chen H, Shinn P, Stevenson DK, Zimmerman J, Barajas P, Cheuk R et al.** 2003. Genome-wide insertional mutagenesis of *Arabidopsis thaliana*. *Science* **301**, 653–657.
- Arrighi J-F, Barre A, Amor BB, Bersoult A, Soriano LC, Mirabella R, de Carvalho-Niebel F, Journet E-P, Ghérardi M, Huguet T, Geurts R, Dénarié J, Rougé P, Gough C.** 2006. The *Medicago truncatula* Lysine motif-receptor-like kinase gene family includes NFP and new nodule-expressed genes. *Plant Physiology* **142**, 265–279.
- Bakker J, Spits M, Neefjes J, Berlin I.** 2017. The EGFR odyssey – from activation to destruction in space and time. *Journal of Cell Science* **130**, 4087–4096.
- Balasubramanian S, Schneitz K.** 2000. *NOZZLE* regulates proximal-distal pattern formation, cell proliferation and early sporogenesis during ovule development in *Arabidopsis thaliana*. *Development* **127**, 4227–4238.
- Baral A, Irani NG, Fujimoto M, Nakano A, Mayor S, Mathew MK.** 2015. Salt-induced remodeling of spatially restricted clathrin-independent endocytic pathways in *Arabidopsis* root. *The Plant Cell* **27**, 1297–1315.
- Barberon M, Dubeaux G, Kolb C, Isono E, Zelazny E, Vert G.** 2014. Polarization of IRON-REGULATED TRANSPORTER 1 (IRT1) to the plant-soil interface plays crucial role in metal homeostasis. *Proceedings of the National Academy of Sciences* **111**, 8293–8298.
- Barbier de Reuille P, Routier-Kierzkowska A-L, Kierzkowski D, Bassel GW, Schüpbach T, Tauriello G, Bajpai N, Strauss S, Weber A et al.** 2015. MorphoGraphX: a platform for quantifying morphogenesis in 4D. *eLife* **4**, 1–20.

References

- Barth M, Holstein SEH.** 2004. Identification and functional characterization of Arabidopsis AP180, a binding partner of plant α C-adaptin. *Journal of Cell Science* **117**, 2051–2062.
- Bashline L, Li S, Anderson CT, Lei L, Gu Y.** 2013. The endocytosis of cellulose synthase in Arabidopsis is dependent on μ 2, a clathrin-mediated endocytosis adaptin. *Plant Physiology* **163**, 150–160.
- Bauer Z, Gómez-Gómez L, Boller T, Felix G.** 2001. Sensitivity of different ecotypes and mutants of Arabidopsis thaliana toward the bacterial elicitor flagellin correlates with the presence of receptor-binding sites. *Journal of Biological Chemistry* **276**, 45669–45676.
- Beck M, Zhou J, Faulkner C, MacLean D, Robatzek S.** 2012. Spatio-temporal cellular dynamics of the Arabidopsis flagellin receptor reveal activation status-dependent endosomal sorting. *The Plant Cell* **24**, 4205–4219.
- Boehm M, Bonifacino JS.** 2001. Adaptins: the final recount. *Molecular biology of the cell* **12**, 2907–20.
- Boudeau J, Miranda-Saavedra D, Barton GJ, Alessi DR.** 2006. Emerging roles of pseudokinases. *Trends in Cell Biology* **16**, 443–452.
- Buendia L, Girardin A, Wang T, Cottret L, Lefebvre B.** 2018. LysM receptor-like kinase and LysM receptor-like protein families: an update on phylogeny and functional characterization. *Frontiers in Plant Science* **9**, 1–25.
- Buist G, Steen A, Kok J, Kuipers OP.** 2008. LysM, a widely distributed protein motif for binding to (peptido)glycans. *Molecular Microbiology* **68**, 838–847.
- Busch W, Miotk A, Ariel FD, Zhao Z, Forner J, Daum G, Suzaki T, Schuster C, Schultheiss SJ, Leibfried A, Haubeiß S, Ha N, Chan RL, Lohmann JU.** 2010. Transcriptional control of a plant stem cell niche. *Developmental Cell* **18**, 841–853.
- Butenko MA, Vie AK, Brembu T, Aalen RB, Bones AM.** 2009. Plant peptides in signalling: looking for new partners. *Trends in Plant Science* **14**, 255–263.

References

- Cao X, Li K, Suh S-G, Guo T, Becraft PW.** 2005. Molecular analysis of the CRINKLY4 gene family in *Arabidopsis thaliana*. *Planta* **220**, 645–657.
- Castells E, Casacuberta JM.** 2007. Signalling through kinase-defective domains: the prevalence of atypical receptor-like kinases in plants. *Journal of Experimental Botany* **58**, 3503–3511.
- Chen X, Irani NG, Friml J.** 2011. Clathrin-mediated endocytosis: the gateway into plant cells. *Current Opinion in Plant Biology* **14**, 674–682.
- Chevalier D, Batoux M, Fulton L, Pfister K, Yadav RK, Schellenberg M, Schneitz K.** 2005. STRUBBELIG defines a receptor kinase-mediated signaling pathway regulating organ development in *Arabidopsis*. *Proceedings of the National Academy of Sciences* **102**, 9074–9079.
- Chinchilla D, Zipfel C, Robatzek S, Kemmerling B, Nürnberger T, Jones JDG, Felix G, Boller T.** 2007. A flagellin-induced complex of the receptor FLS2 and BAK1 initiates plant defence. *Nature* **448**, 497–500.
- Clark SE.** 1997. Organ formation at the vegetative shoot meristem. *The Plant Cell* **9**, 1067–1076.
- Clough SJ, Bent AF.** 1998. Floral dip: a simplified method for *Agrobacterium*-mediated transformation of *Arabidopsis thaliana*. *Plant Journal* **16**, 735–743.
- Clouse SD, Langford M, McMorris TC.** 1996. A Brassinosteroid-insensitive mutant in *Arabidopsis thaliana* exhibits multiple defects in growth and development. *Plant Physiology* **111**, 671–678.
- Crawford KM, Zambryski PC.** 2000. Subcellular localization determines the availability of non-targeted proteins to plasmodesmatal transport. *Current Biology* **10**, 1032–1040.
- Critchley WR, Pellet-Many C, Ringham-Terry B, Harrison MA, Zachary IC, Ponnambalam S.** 2018. Receptor tyrosine kinase ubiquitination and de-ubiquitination in signal transduction and receptor trafficking. *Cells* **7**, 22.

References

- Cui Y, Shen J, Gao C, Zhuang X, Wang J, Jiang L.** 2016. Biogenesis of plant prevacuolar multivesicular bodies. *Molecular Plant* **9**, 774–786.
- Dejonghe W, Kuenen S, Mylle E, Vasileva M, Keech O, Viotti C, Swerts J, Fendrych M, Ortiz-Morea FA, Mishev K, Delang S *et al.*** 2016. Mitochondrial uncouplers inhibit clathrin-mediated endocytosis largely through cytoplasmic acidification. *Nature Communications* **7**.
- Dettmer J, Hong-Hermesdorf A, Stierhof Y-D, Schumacher K.** 2006. Vacuolar H⁺-ATPase activity is required for endocytic and secretory trafficking in Arabidopsis. *The Plant Cell* **18**, 715–730.
- Dhonukshe P, Aniento F, Hwang I, Robinson DG, Mravec J, Stierhof Y-D, Friml J.** 2007. Clathrin-mediated constitutive endocytosis of PIN auxin efflux carriers in Arabidopsis. *Current Biology* **17**, 520–527.
- Di Rubbo S, Irani NG, Kim SY, Xu Z-Y, Gadeyne A, Dejonghe W, Vanhoutte I, Persiau G, Eeckhout D, Simon S, Song K, Kleine-Vehn J, Friml J, De Jaeger G, Van Damme D, Hwang I, Russinova E.** 2013. The clathrin adaptor complex AP-2 mediates endocytosis of BRASSINOSTEROID INSENSITIVE1 in Arabidopsis. *The Plant Cell* **25**, 2986–2997.
- Di Rubbo S, Russinova E.** 2012. Receptor-mediated endocytosis in plants. In: Šamaj J, ed. *Endocytosis in Plants*. Springer-Verlag Berlin Heidelberg, 151–164.
- Dodsworth S.** 2009. A diverse and intricate signalling network regulates stem cell fate in the shoot apical meristem. *Developmental Biology* **336**, 1–9.
- Dolan L, Janmaat K, Willemsen V, Linstead P, Poethig S, Roberts K, Scheres B.** 1993. Cellular organisation of the Arabidopsis thaliana root. *Development* **119**, 71–84.
- Du Y, Tejos R, Beck M, Himschoot E, Li H, Robatzek S, Vanneste S, Friml J.** 2013. Salicylic acid interferes with clathrin-mediated endocytic protein trafficking. *Proceedings of the National Academy of Sciences* **110**, 7946–7951.

References

- Dwyer KG, Kandasamy MK, Mahosky DI, Acciai J, Kudish BI, Miller JE, Nasrallah ME, Nasrallah JB.** 1994. A Superfamily of S Locus-Related Sequences in Arabidopsis: Diverse Structures and Expression Patterns. *The Plant Cell* **6**, 1829–1843.
- Ebine K, Fujimoto M, Okatani Y, Nishiyama T, Goh T, Ito E, Dainobu T, Nishitani A, Uemura T, Sato MH, Thordal-Christensen H, Tsutsumi N, Nakano A, Ueda T.** 2011. A membrane trafficking pathway regulated by the plant-specific RAB GTPase ARA6. *Nature Cell Biology* **13**, 853–859.
- Elkin SR, Oswald NW, Reed DK, Mettlen M, MacMillan JB, Schmid SL.** 2016. Ikarugamycin: a natural product inhibitor of clathrin-mediated endocytosis. *Traffic* **17**, 1139–1149.
- Elliott RC, Betzner AS, Huttner E, Oakes MP, Tucker WQJ, Gerentes D, Perez P, Smyth DR.** 1996. AINTEGUMENTA, an APETALA2-like gene of Arabidopsis with pleiotropic roles in ovule development and floral organ growth. *The Plant Cell* **8**, 155–168.
- Fan L, Hao H, Xue Y, Zhang L, Song K, Ding Z, Botella MA, Wang H, Lin J.** 2013. Dynamic analysis of Arabidopsis AP2 σ subunit reveals a key role in clathrin-mediated endocytosis and plant development. *Development* **140**, 3826–3837.
- Fan L, Li R, Pan J, Ding Z, Lin J.** 2015. Endocytosis and its regulation in plants. *Trends in Plant Science* **20**, 388–397.
- Fotin A, Cheng Y, Sliz P, Grigorieff N, Harrison SC, Kirchhausen T, Walz T.** 2004. Molecular model for a complete clathrin lattice from electron cryomicroscopy. *Nature* **432**, 573–579.
- Fritig B, Heitz T, Legrand M.** 1998. Antimicrobial proteins in induced plant defense. *Current Opinion in Immunology* **10**, 16–22.
- Fujimoto M, Arimura S, Ueda T, Takanashi H, Hayashi Y, Nakano A, Tsutsumi N.** 2010. Arabidopsis dynamin-related proteins DRP2B and DRP1A

References

- participate together in clathrin-coated vesicle formation during endocytosis. *Proceedings of the National Academy of Sciences* **107**, 6094–6099.
- Fulton L, Batoux M, Vaddepalli P, Yadav RK, Busch W, Andersen SU, Jeong S, Lohmann JU, Schneitz K.** 2009. DETORQUEO, QUIRKY, and ZERZAUST represent novel components involved in organ development mediated by the receptor-like kinase STRUBBELIG in *Arabidopsis thaliana*. *PLoS Genetics* **5**.
- Fulton L, Vaddepalli P, Yadav RK, Batoux M, Schneitz K.** 2010. Inter-cell-layer signalling during *Arabidopsis* ovule development mediated by the receptor-like kinase STRUBBELIG. *Biochemical Society Transactions* **38**, 583–587.
- Gadeyne A, Sánchez-Rodríguez C, Vanneste S, Di Rubbo S, Zauber H, Vanneste K, Van Leene J, De Winne N, Eeckhout D, Persiau G, Van De Slijke E, Cannoot B, Vercruyse L, Mayers JR, Adamowski M, Kania U, Ehrlich M, Schweighofer A, Ketelaar T, Maere S, Bednarek SY, Friml J, Gevaert K, Witters E, Russinova E, Persson S, De Jaeger G, Van Damme D.** 2014. The TPLATE adaptor complex drives clathrin-mediated endocytosis in plants. *Cell* **156**, 691–704.
- Galindo-Trigo S, Gray JE, Smith LM.** 2016. Conserved roles of CrRLK1L receptor-like kinases in cell expansion and reproduction from Algae to Angiosperms. *Frontiers in Plant Science* **07**, 1–10.
- Gallagher KL, Benfey PN.** 2005. Not just another hole in the wall: Understanding intercellular protein trafficking. *Genes and Development* **19**, 189–195.
- Geldner N, Hyman DL, Wang X, Schumacher K, Chory J.** 2007. Endosomal signaling of plant steroid receptor kinase BRI1. *Genes and Development*, 1598–1602.
- Geldner N, Robatzek S.** 2008. Plant receptors go endosomal: a moving view on signal transduction. *Plant Physiology* **147**, 1565–1574.

References

- Gifford ML, Dean S, Ingram GC.** 2003. The Arabidopsis ACR4 gene plays a role in cell layer organisation during ovule integument and sepal margin development. *Development* **130**, 4249–4258.
- Gifford ML, Robertson FC, Soares DC, Ingram GC.** 2005. ARABIDOPSIS CRINKLY4 function, internalization, and turnover are dependent on the extracellular crinkly repeat domain. *The Plant Cell* **17**, 1154–1166.
- Gish LA, Clark SE.** 2011. The RLK/Pelle family of kinases. *Plant Journal* **66**, 117–127.
- Gómez-Gómez L, Boller T.** 2000. FLS2: an LRR receptor-like kinase involved in the perception of the bacterial elicitor flagellin in Arabidopsis. *Molecular Cell* **5**, 1003–1011.
- Gómez-Gómez L, Boller T.** 2002. Flagellin perception: a paradigm for innate immunity. *Trends in Plant Science* **7**, 251–256.
- Gonzalez-Gutierrez G, Miranda-Laferte E, Neely A, Hidalgo P.** 2007. The Src homology 3 domain of the β -subunit of voltage-gated calcium channels promotes endocytosis via dynamin interaction. *Journal of Biological Chemistry* **282**, 2156–2162.
- Groß-Hardt R, Lenhard M, Laux T.** 2002. WUSCHEL signaling functions in interregional communication during Arabidopsis ovule development. *Genes & Development* **16**, 1129–1138.
- Gruszka D.** 2013. The Brassinosteroid signaling pathway-new key players and interconnections with other signaling networks crucial for plant development and stress tolerance. *International Journal of Molecular Sciences* **14**, 8740–8774.
- Haglund K, Dikic I.** 2012. The role of ubiquitylation in receptor endocytosis and endosomal sorting. *Journal of Cell Science* **125**, 265–275.
- Hanks SK, Quinn AM.** 1991. Protein kinase catalytic domain sequence database: Identification of conserved features of primary structure and classification of family members. *Methods in Enzymology* **200**, 38–62.

References

- Hao H, Fan L, Chen T, Li R, Li X, He Q, Botella MA, Lin J.** 2014. Clathrin and membrane microdomains cooperatively regulate RbohD dynamics and activity in Arabidopsis. *The Plant Cell* **26**, 1729–1745.
- He Z-H, Cheeseman I, He D, Kohorn BD.** 1999. A cluster of five cell wall-associated receptor kinase genes, Wak1–5, are expressed in specific organs of Arabidopsis. *Plant Molecular Biology* **39**, 1189–1196.
- Hématy K, Höfte H.** 2008. Novel receptor kinases involved in growth regulation. *Current Opinion in Plant Biology* **11**, 321–328.
- Heucken N, Ivanov R.** 2018. The retromer, sorting nexins and the plant endomembrane protein trafficking. *Journal of Cell Science* **131**, jcs203695.
- Holstein SEH.** 2002. Clathrin and plant endocytosis. *Traffic* **3**, 614–620.
- Huffaker A, Pearce G, Ryan CA.** 2006. An endogenous peptide signal in Arabidopsis activates components of the innate immune response. *Proceedings of the National Academy of Sciences* **103**, 10098–10103.
- Huse M, Kuriyan J.** 2002. The Conformational Plasticity of Protein Kinases. *Cell* **109**, 275–282.
- Hüttner S, Veit C, Vavra U, Schoberer J, Dicker M, Maresch D, Altmann F, Strasser R.** 2014. A context-independent N-glycan signal targets the misfolded extracellular domain of Arabidopsis STRUBBELIG to endoplasmic-reticulum-associated degradation. *Biochemical Journal* **464**, 401–411.
- Irani NG, Di Rubbo S, Mylle E, Van den Begin J, Schneider-Pizoń J, Hniliková J, Šiša M, Buyst D, Vilarrasa-Blasi J, Szatmári A-M, Van Damme D, Mishev K, Codreanu M-C, Kohout L, Strnad M, Caño-delgado AI, Friml J, Madder A, Russinova E.** 2012. Fluorescent castasterone reveals BRI1 signaling from the plasma membrane. *Nature Chemical Biology* **8**, 583–589.
- Irani NG, Russinova E.** 2009. Receptor endocytosis and signaling in plants. *Current Opinion in Plant Biology* **12**, 653–659.

References

- Isono E, Kalinowska K.** 2017. ESCRT-dependent degradation of ubiquitylated plasma membrane proteins in plants. *Current Opinion in Plant Biology* **40**, 49–55.
- Ito E, Fujimoto M, Ebine K, Uemura T, Ueda T, Nakano A.** 2012. Dynamic behavior of clathrin in *Arabidopsis thaliana* unveiled by live imaging. *The Plant Journal* **69**, 204–216.
- Jagodzik P, Tajdel-Zielinska M, Ciesla A, Marczak M, Ludwikow A.** 2018. Mitogen-Activated Protein Kinase Cascades in Plant Hormone Signaling. *Frontiers in Plant Science* **9**, 1–26.
- Jaillais Y, Fobis-Loisy I, Miège C, Gaude T.** 2008. Evidence for a sorting endosome in *Arabidopsis* root cells. *The Plant Journal* **53**, 237–247.
- Jefferson RA, Kavanagh TA, Bevan MW.** 1987. GUS fusions: β -glucuronidase as a sensitive and versatile gene fusion marker in higher plants. *EMBO Journal* **6**, 3901–3908.
- Jia T, Gao C, Cui Y, Wang J, Ding Y, Cai Y, Ueda T, Nakano A, Jiang L.** 2013. ARA7(Q69L) expression in transgenic *Arabidopsis* cells induces the formation of enlarged multivesicular bodies. *Journal of Experimental Botany* **64**, 2817–2829.
- Johnson LN, Noble MEM, Owen DJ.** 1996. Active and Inactive Protein Kinases: Structural Basis for Regulation. *Cell* **85**, 149–158.
- Kang B-H, Nielsen E, Preuss ML, Mastronarde D, Staehelin LA.** 2011. Electron tomography of RabA4b- and PI-4K β 1-labeled trans Golgi network compartments in *Arabidopsis*. *Traffic* **12**, 313–329.
- Kelly BT, Graham SC, Liska N, Dannhauser PN, Höning S, Ungewickell EJ, Owen DJ.** 2014. AP2 controls clathrin polymerization with a membrane-activated switch. *Science* **345**, 459–463.
- Kim I, Hempel FD, Sha K, Pfluger J, Zambryski PC.** 2002. Identification of a developmental transition in plasmodesmatal function during embryogenesis in *Arabidopsis thaliana*. *Development* **129**, 1261–1272.

References

- Kim SY, Xu Z-Y, Song K, Kim DH, Kang H, Reichardt I, Sohn EJ, Friml J, Juergens G, Hwang I.** 2013. Adaptor protein complex 2-mediated endocytosis is crucial for male reproductive organ development in Arabidopsis. *The Plant Cell* **25**, 2970–2985.
- Kim I, Zambryski PC.** 2005. Cell-to-cell communication via plasmodesmata during Arabidopsis embryogenesis. *Current Opinion in Plant Biology* **8**, 593–599.
- Kinoshita T, Caño-Delgado A, Seto H, Hiranuma S, Fujioka S, Yoshida S, Chory J.** 2005. Binding of brassinosteroids to the extracellular domain of plant receptor kinase BRI1. *Nature* **433**, 167–171.
- Kitakura S, Vanneste S, Robert S, Löffke C, Teichmann T, Tanaka H, Friml J.** 2011. Clathrin mediates endocytosis and polar distribution of PIN auxin transporters in Arabidopsis. *The Plant Cell* **23**, 1920–1931.
- Kohorn BD, Kohorn SL.** 2012. The cell wall-associated kinases, WAKs, as pectin receptors. *Frontiers in Plant Science* **3**, 1–5.
- Koncz C, Schell J.** 1986. The promoter of TL-DNA gene 5 controls the tissue-specific expression of chimaeric genes carried by a novel type of Agrobacterium binary vector. *Molecular & General Genetics* **204**, 383–396.
- Konopka CA, Backues SK, Bednarek SY.** 2008. Dynamics of Arabidopsis dynamin-related protein 1C and a clathrin light chain at the plasma membrane. *The Plant Cell* **20**, 1363–1380.
- Kroihner M, Miller MA, Steele RE.** 2001. Deceiving appearances: Signaling by ‘dead’ and ‘fractured’ receptor protein-tyrosine kinases. *BioEssays* **23**, 69–76.
- Krol E, Mentzel T, Chinchilla D, Boller T, Felix G, Kemmerling B, Postel S, Arents M, Jeworutzki E, Al-Rasheid KAS, Becker D, Hedrich R.** 2010. Perception of the Arabidopsis danger signal peptide 1 involves the pattern recognition receptor AtPEPR1 and its close homologue AtPEPR2. *Journal of Biological Chemistry* **285**, 13471–13479.

References

- Kunze G, Zipfel C, Robatzek S, Niehaus K, Boller T, Felix G.** 2004. The N terminus of bacterial elongation factor Tu elicits innate immunity in Arabidopsis plants. *The Plant Cell* **16**, 3496–3507.
- Kwak S-H, Schiefelbein J.** 2007. The role of the SCRAMBLED receptor-like kinase in patterning the Arabidopsis root epidermis. *Developmental Biology* **302**, 118–131.
- Kwak S-H, Schiefelbein J.** 2008. A feedback mechanism controlling SCRAMBLED receptor accumulation and cell-type pattern in Arabidopsis. *Current Biology* **18**, 1949–1954.
- Kwak S-H, Woo S, Lee MM, Schiefelbein J.** 2014. Distinct signaling mechanisms in multiple developmental pathways by the SCRAMBLED receptor of Arabidopsis. *Plant Physiology* **166**, 976–987.
- Kwak S-H, Shen R, Schiefelbein J.** 2005. Positional signaling mediated by a receptor-like kinase in Arabidopsis. *Science* **307**, 1111–1113.
- Lampropoulos A, Sutikovic Z, Wenzl C, Maegele I, Lohmann JU, Forner J.** 2013. GreenGate - a novel, versatile, and efficient cloning system for plant transgenesis. *PLoS ONE* **8**.
- Larson ER, Van Zelm E, Roux C, Marion-Poll A, Blatt MR.** 2017. Clathrin Heavy Chain subunits coordinate endo- and exocytic traffic and affect stomatal movement. *Plant Physiology* **175**, pp.00970.2017.
- Leitner J, Petrášek J, Tomanov K, Retzer K, Parezová M, Korbei B, Bachmair A, Zažímalová E, Luschign C.** 2012. Lysine63-linked ubiquitylation of PIN2 auxin carrier protein governs hormonally controlled adaptation of Arabidopsis root growth. *Proceedings of the National Academy of Sciences* **109**, 8322–8327.
- Li J, Chory J.** 1997. A putative leucine-rich repeat receptor kinase involved in brassinosteroid signal transduction. *Cell* **90**, 929–938.

References

- Li R, Liu P, Wan Y, Chen T, Wang Q, Mettbach U, Baluška F, Samaj J, Fang X, Lucas WJ, Lin J.** 2012. A Membrane Microdomain-Associated Protein, Arabidopsis Flot1, Is Involved in a Clathrin-Independent Endocytic Pathway and Is Required for Seedling Development. *The Plant Cell* **24**, 2105–2122.
- Li X, Pan SQ.** 2017. Agrobacterium delivers VirE2 protein into host cells via clathrin-mediated endocytosis. *Science Advances* **3**, e1601528.
- Liang X, Zhou J-M.** 2018. Receptor-like cytoplasmic kinases: central players in plant receptor kinase-mediated signaling. *Annual Review of Plant Biology* **69**, 267–299.
- Liao D, Cao Y, Sun X, Espinoza C, Nguyen CT, Liang Y, Stacey G.** 2017. Arabidopsis E3 ubiquitin ligase PLANT U-BOX13 (PUB13) regulates chitin receptor LYSIN MOTIF RECEPTOR KINASE5 (LYK5) protein abundance. *New Phytologist* **214**, 1646–1656.
- Lin L, Zhong S-H, Cui X-F, Li J, He Z-H.** 2012. Characterization of temperature-sensitive mutants reveals a role for receptor-like kinase SCRAMBLED/STRUBBELIG in coordinating cell proliferation and differentiation during Arabidopsis leaf development. *The Plant Journal* **72**, 707–720.
- Liu S-H, Wong ML, Craik CS, Brodsky FM.** 1995. Regulation of clathrin assembly and trimerization defined using recombinant triskelion hubs. *Cell* **83**, 257–267.
- Llompert B, Castells E, Río A, Roca R, Ferrando A, Stiefel V, Puigdomènech P, Casacuberta JM.** 2003. The direct activation of MIK, a Germinal Center Kinase (GCK)-like kinase, by MARK, a Maize atypical receptor kinase, suggests a new mechanism for signaling through kinase-dead receptors. *Journal of Biological Chemistry* **278**, 48105–48111.
- Long J, Barton MK.** 2000. Initiation of axillary and floral meristems in Arabidopsis. *Developmental Biology* **218**, 341–353.

References

- Lu P, Porat R, Nadeau JA, O'Neill SD.** 1996. Identification of a meristem L1 layer-specific gene in *Arabidopsis* that is expressed during embryonic pattern formation and defines a new class of homeobox genes. *The Plant Cell* **8**, 2155–2168.
- Lu D, Lin W, Gao X, Wu S, Cheng C, Avila J, Heese A, Devarenne TP, He P, Shan L.** 2011. Direct ubiquitination of pattern recognition receptor FLS2 attenuates plant innate immunity. *Science* **332**, 1439–1442.
- Lucas WJ, Bouché -Pillon S, Jackson DP, Nguyen L, Baker L, Ding B, Hake S.** 1995. Selective Trafficking of KNOTTED1 Homeodomain Protein and Its mRNA Through Plasmodesmata. *Science* **270**, 1980–1983.
- Lucas WJ, Lee J-Y.** 2004. Plasmodesmata as a supracellular control network in plants. *Nature Reviews Molecular Cell Biology* **5**, 712–726.
- Luschnig C, Vert G.** 2014. The dynamics of plant plasma membrane proteins: PINs and beyond. *Development* **141**, 2924–2938.
- Lyndon RF.** 1998. The shoot apical meristem: its growth and development. Cambridge University Press.
- MacGurn JA, Hsu P-C, Emr SD.** 2012. Ubiquitin and membrane protein turnover: from cradle to grave. *Annual Review of Biochemistry* **81**, 231–259.
- Martins S, Dohmann EMN, Cayrel A, Johnson A, Fischer W, Pojer F, Satiat-Jeunemaître B, Jaillais Y, Chory J, Geldner N, Vert G.** 2015. Internalization and vacuolar targeting of the brassinosteroid hormone receptor BRI1 are regulated by ubiquitination. *Nature Communications* **6**. 6151.
- Masucci JD, Rerie WG, Foreman DR, Zhang M, Galway ME, Marks MD, Schiefelbein JW.** 1996. The homeobox gene *GLABRA 2* is required for position-dependent cell differentiation in the root epidermis of *Arabidopsis thaliana*. *Development* **122**, 1253–1260.

References

- Matsubayashi Y, Ogawa M, Morita A, Sakagami Y.** 2002. An LRR receptor kinase involved in perception of a peptide plant hormone, phytoalexin. *Science* **296**, 1470–1472.
- Mbengue M, Bourdais G, Gervasi F, Beck M, Zhou J, Spallek T, Bartels S, Boller T, Ueda T, Kuhn H, Robatzek S.** 2016. Clathrin-dependent endocytosis is required for immunity mediated by pattern recognition receptor kinases. *Proceedings of the National Academy of Sciences* **113**, 11034–11039.
- McMahon HT, Boucrot E.** 2011. Molecular mechanism and physiological functions of clathrin-mediated endocytosis. *Nature Reviews Molecular Cell Biology* **12**, 517–533.
- Meyerowitz EM.** 1997. Genetic control of cell division patterns in developing plants. *Cell* **88**, 299–308.
- Morita MT, Shimada T.** 2014. The plant endomembrane system—a complex network supporting plant development and physiology. *Plant and Cell Physiology* **55**, 667–671.
- Morris ER, Walker JC.** 2003. Receptor-like protein kinases: the keys to response. *Current Opinion in Plant Biology* **6**, 339–342.
- Mulder L, Lefebvre B, Cullimore J, Imberty A.** 2006. LysM domains of *Medicago truncatula* NFP protein involved in Nod factor perception. Glycosylation state, molecular modeling and docking of chitoooligosaccharides and Nod factors. *Glycobiology* **16**, 801–809.
- Murashige T, Skoog F.** 1962. A revised medium for rapid growth and bioassays with tobacco tissue cultures. *Physiologia Plantarum* **15**, 473–497.
- Murphy AS, Bandyopadhyay A, Holstein SE, Peer WA.** 2005. Endocytotic cycling of PM proteins. *Annual Review of Plant Biology* **56**, 221–251.
- Musielak TJ, Schenkel L, Kolb M, Henschen A, Bayer M.** 2015. A simple and versatile cell wall staining protocol to study plant reproduction. *Plant Reproduction* **28**, 161–169.

References

- Nasrallah JB, Yu S-M, Nasrallah ME.** 1988. Self-incompatibility genes of *Brassica oleracea*: expression, isolation, and structure. *Proceedings of the National Academy of Sciences* **85**, 5551–5555.
- Oparka KJ.** 2004. Getting the message across: how do plant cells exchange macromolecular complexes? *Trends in Plant Science* **9**, 33–41.
- Ortiz-Morea FA, Savatin D V, Dejonghe W, Kumar R, Luo Y, Adamowski M, Van den Begin J, Dressano K, Pereira de Oliveira G, Zhao X, Lu Q, Madder A, Friml J, Schere de Moura D, Russinova E.** 2016. Danger-associated peptide signaling in *Arabidopsis* requires clathrin. *Proceedings of the National Academy of Sciences* **113**, 11028–11033.
- Otero S, Helariutta Y, Benitez-Alfonso Y.** 2016. Symplastic communication in organ formation and tissue patterning. *Current Opinion in Plant Biology* **29**, 21–28.
- Paez Valencia J, Goodman K, Otegui MS.** 2016. Endocytosis and endosomal trafficking in plants. *Annual Review of Plant Biology* **67**, 309–335.
- Park M, Song K, Reichardt I, Kim H, Mayer U, Stierhof Y-D, Hwang I, Jürgens G.** 2013. *Arabidopsis* μ -adaptin subunit AP1M of adaptor protein complex 1 mediates late secretory and vacuolar traffic and is required for growth. *Proceedings of the National Academy of Sciences* **110**, 10318–10323.
- Pastuglia M, Roby D, Dumas C, Cock JM.** 1997. Rapid induction by wounding and bacterial infection of an S gene family receptor-like kinase gene in *Brassica oleracea*. *The Plant Cell* **9**, 49–60.
- Pastuglia M, Swarup R, Rocher A, Saindrenan P, Roby D, Dumas C, Cock JM.** 2002. Comparison of the expression patterns of two small gene families of S gene family receptor kinase genes during the defence response in *Brassica oleracea* and *Arabidopsis thaliana*. *Gene* **282**, 215–225.

References

- Pizarro L, Norambuena L.** 2014. Regulation of protein trafficking: Posttranslational mechanisms and the unexplored transcriptional control. *Plant Science* **225**, 24–33.
- Reynolds GD, Wang C, Pan J, Bednarek SY.** 2018. Inroads into internalization: five years of endocytic exploration. *Plant Physiology* **176**, 208–218.
- Robatzek S, Chinchilla D, Boller T.** 2006. Ligand-induced endocytosis of the pattern recognition receptor FLS2 in Arabidopsis. *Genes & Development* **20**, 537–542.
- Robert S, Kleine-Vehn J, Barbez E, Sauer M, Paciorek T, Baster P, Vanneste S, Zhang J, Simon S, Covanova M *et al.*** 2010. ABP1 mediates auxin inhibition of clathrin-dependent endocytosis in arabidopsis. *Cell* **143**, 111–121.
- Robinson DG, Jiang L, Schumacher K.** 2008. The endosomal system of plants: charting new and familiar territories. *Plant Physiology* **147**, 1482–1492.
- Robinson DG, Pimpl P.** 2014. Clathrin and post-Golgi trafficking: a very complicated issue. *Trends in Plant Science* **19**, 134–139.
- Russinova E, Borst J-W, Kwaaitaal M, Caño-Delgado A, Yin Y, Chory J, de Vries SC.** 2004. Heterodimerization and endocytosis of Arabidopsis brassinosteroid receptors BRI1 and AtSERK3 (BAK1). *The Plant Cell* **16**, 3216–3229.
- Sager RE, Lee J-Y.** 2018. Plasmodesmata at a glance. *Journal of Cell Science* **131**, jcs209346.
- Salomon S and, Robatzek S.** 2006. Induced endocytosis of the receptor kinase FLS2. *Plant Signaling & Behavior* **1**, 293–295.
- Sambrook J, Fritsch EF, Maniatis T.** 1989. *Molecular cloning: a laboratory manual*. Cold Spring Harbor Laboratory Press 2nd Edition.
- Sampoli Benitez BA, Komives EA.** 2000. Disulfide bond plasticity in epidermal growth factor. *Proteins* **40**, 168–174.

References

- Samuels AL, Giddings TH, Staehelin LA.** 1995. Cytokinesis in tobacco BY-2 and root tip cells: a new model of cell plate formation in higher plants. *The Journal of Cell Biology* **130**, 1345–1357.
- Sánchez-Rodríguez C, Shi Y, Kesten C, Zhang D, Sancho-Andrés G, Ivakov A, Lampugnani ER, Sklodowshi K, Fujimoto M, Nakano A, Bacic A, Wallace IS, Ueda T, Van Damme D, Zhou Y, Persson S.** 2018. The cellulose synthases are cargo of the TPLATE adaptor complex. *Molecular Plant* **11**, 346–349.
- Satina S, Blakeslee AF, Avery AG.** 1940. Demonstration of the three germ layers in the shoot apex of *Datura* by means of induced polyploidy in periclinal chimeras. *American Journal of Botany* **27**, 895–905.
- Scheele U, Holstein SE.** 2002. Functional evidence for the identification of an *Arabidopsis* clathrin light chain polypeptide. *FEBS Letters* **514**, 355–360.
- Scheuring D, Viotti C, Krüger F, Künzl F, Sturm S, Bubeck J, Hillmer S, Frigerio L, Robinson DG, Pimpl P, Schumacher K.** 2011. Multivesicular bodies mature from the *trans*-Golgi network/early endosome in *Arabidopsis*. *The Plant Cell* **23**, 3463–3481.
- Schindelin J, Arganda-Carreras I, Frise E, Kaynig V, Longair M, Pietzsch T, Preibisch S, Rueden C, Saalfeld S, Schmid B, Tinevez J-Y, White DJ, Hartenstein V, Eliceiri K, Tomancak P, Cardona A.** 2012. Fiji: an open-source platform for biological-image analysis. *Nature Methods* **9**, 676–682.
- Schneitz K, Hülskamp M, Kopczak SD, Pruitt RE.** 1997. Dissection of sexual organ ontogenesis: a genetic analysis of ovule development in *Arabidopsis thaliana*. *Development* **124**, 1367–1376.
- Schneitz K, Hülskamp M, Pruitt RE.** 1995. Wild-type ovule development in *Arabidopsis thaliana*: a light microscope study of cleared whole-mount tissue. *The Plant Journal* **7**, 731–749.

References

- Schulze-Muth P, Irmeler S, Schröder G, Schröder J.** 1996. Novel type of receptor-like protein kinase from a higher plant (*Catharanthus roseus*). *The Journal of Biological Chemistry* **271**, 26684–26689.
- Sessions A, Weigel D, Yanofsky MF.** 1999. The *Arabidopsis thaliana* MERISTEM LAYER 1 promoter specifies epidermal expression in meristems and young primordia. *The Plant Journal* **20**, 259–263.
- Shah K, Russinova E, Gadella TWJ, Willemse J, De Vries SC.** 2002. The *Arabidopsis* kinase-associated protein phosphatase controls internalization of the somatic embryogenesis receptor kinase 1. *Genes & Development* **16**, 1707–1720.
- Shah K, Gadella TWJ, Van Erp H, Hecht V, De Vries SC.** 2001. Subcellular localization and oligomerization of the *Arabidopsis thaliana* somatic embryogenesis receptor kinase 1 protein. *Journal of Molecular Biology* **309**, 641–655.
- Shiu S-H, Bleecker AB.** 2001a. Receptor-like kinases from *Arabidopsis* form a monophyletic gene family related to animal receptor kinases. *Proceedings of the National Academy of Sciences* **98**, 10763–10768.
- Shiu S-H, Bleecker AB.** 2001b. Plant Receptor-Like Kinase Gene Family: Diversity, Function, and Signaling. *Science Signaling* **2001**, re22.
- Shiu S-H, Bleecker AB.** 2003. Expansion of the receptor-like kinase/pelle gene family and receptor-like proteins in *Arabidopsis*. *Plant Physiology* **132**, 530–543.
- Sieburth LE, Meyerowitz EM.** 1997. Molecular dissection of the AGAMOUS control region shows that cis elements for spatial regulation are located intragenically. *The Plant Cell* **9**, 355–365.
- Smith CJ, Pearse BMF.** 1999. Clathrin: anatomy of a coat protein. *Trends in Cell Biology* **9**, 335–338.
- Smyth DR, Bowman JL, Meyerowitz EM.** 1990. Early flower development in *Arabidopsis*. *The Plant Cell* **2**, 755.

References

- Stahelin LA, Moore I.** 1995. The plant Golgi apparatus: structure, functional organization and trafficking mechanisms. *Annual Review of Plant Physiology and Plant Molecular Biology* **46**, 261–288.
- Stierhof Y-D, El Kasmi F.** 2010. Strategies to improve the antigenicity, ultrastructure preservation and visibility of trafficking compartments in *Arabidopsis* tissue. *European Journal of Cell Biology* **89**, 285–297.
- Tang D, Christiansen KM, Innes RW.** 2005. Regulation of plant disease resistance, stress responses, cell death, and ethylene signaling in *Arabidopsis* by the EDR1 protein kinase. *Plant Physiology* **138**, 1018–1026.
- Tang J, Han Z, Sun Y, Zhang H, Gong X, Chai J.** 2015. Structural basis for recognition of an endogenous peptide by the plant receptor kinase PEPR1. *Cell Research* **25**, 110–120.
- Tang D, Wang G, Zhou J-M.** 2017. Receptor kinases in plant-pathogen interactions: more than pattern recognition. *The Plant Cell* **29**, 618–637.
- Taylor NG.** 2011. A role for *Arabidopsis* dynamin related proteins DRP2A/B in endocytosis; DRP2 function is essential for plant growth. *Plant Molecular Biology* **76**, 117–129.
- Teh O-K, Shimono Y, Shirakawa M, Fukao Y, Tamura K, Shimada T, Hara-Nishimura I.** 2013. The AP-1 μ adaptin is required for KNOLLE localization at the cell plate to mediate cytokinesis in *Arabidopsis*. *Plant and Cell Physiology* **54**, 838–847.
- Torii KU, Mitsukawa N, Oosumi T, Matsuura Y, Yokoyama R, Whitter RF, Komeda Y.** 1996. The *Arabidopsis* ERECTA Gene Encodes a Putative Receptor Protein Kinase with Extracellular Leucine-Rich Repeats. *The Plant Cell Online* **8**, 735–746.
- Torii KU, Clark S.** 2000. Receptor-Like Kinases in Plant Development. *Advances in Botanical Research* **32**, 225–267.

References

- Traub LM.** 2009. Tickets to ride: selecting cargo for clathrin-regulated internalization. *Nature Reviews Molecular Cell Biology* **10**, 583–596.
- Truernit E, Bauby H, Dubreucq B, Grandjean O, Runions J, Barthelemy J, Palauqui JC.** 2008. High-resolution whole-mount imaging of three-dimensional tissue organization and gene expression enables the study of phloem development and structure in *Arabidopsis*. *The Plant Cell* **20**, 1494-1503.
- Tse YC, Mo B, Hillmer S, Zhao M, Lo SW, Robinson DG, Jiang L.** 2004. Identification of multivesicular bodies as prevacuolar compartments in *Nicotiana tabacum* BY-2 cells. *The Plant Cell* **16**, 672–693.
- Uemura T, Kim H, Saito C, Ebine K, Ueda T, Schulze-Lefert P, Nakano A.** 2012. Qa-SNAREs localized to the trans-Golgi network regulate multiple transport pathways and extracellular disease resistance in plants. *Proceedings of the National Academy of Sciences* **109**, 1784–1789.
- Ursache R, Andersen TG, Marhavý P, Geldner N.** 2018. A protocol for combining fluorescent proteins with histological stains for diverse cell wall components. *Plant Journal* **93**, 399–412.
- Vaddepalli P, Fulton L, Batoux M, Yadav RK, Schneitz K.** 2011. Structure-function analysis of STRUBBELIG, an *Arabidopsis* atypical receptor-like kinase involved in tissue morphogenesis. *PLoS ONE* **6**.
- Vaddepalli P, Fulton L, Wieland J, Wassmer K, Schaeffer M, Ranf S, Schneitz K.** 2017. The cell wall-localized atypical β -1,3 glucanase ZERZAUST controls tissue morphogenesis in *Arabidopsis thaliana*. *Development* **144**, 2259–2269.
- Vaddepalli P, Herrmann A, Fulton L, Oelschner M, Hillmer S, Stratil TF, Fastner A, Hammes UZ, Ott T, Robinson DG, Schneitz K.** 2014. The C2-domain protein QUIRKY and the receptor-like kinase STRUBBELIG localize to plasmodesmata and mediate tissue morphogenesis in *Arabidopsis thaliana*. *Development* **141**, 4139–4148.

References

- Vaid N, Macovei A, Tuteja N.** 2013. Knights in action: Lectin receptor-like kinases in plant development and stress responses. *Molecular Plant* **6**, 1405–1418.
- Van Damme D, Gadeyne A, Vanstraelen M, Inzé D, Van Montagu MCE, De Jaeger G, Russinova E, Geelen D.** 2011. Adaptin-like protein TPLATE and clathrin recruitment during plant somatic cytokinesis occurs via two distinct pathways. *Proceedings of the National Academy of Sciences* **108**, 615–620.
- Viotti C, Bubeck J, Stierhof Y-D, Krebs M, Langhans M, van den Berg W, van Dongen W, Richter S, Geldner N, Takano J, Jürgens G, de Vries SC, Robinson DG, Schumacher K.** 2010. Endocytic and secretory traffic in *Arabidopsis* merge in the trans-Golgi network/early endosome, an independent and highly dynamic organelle. *The Plant Cell* **22**, 1344–1357.
- Wang J, Cai Y, Miao Y, Lam SK, Jiang L.** 2009. Wortmannin induces homotypic fusion of plant prevacuolar compartments. *Journal of Experimental Botany* **60**, 3075–3083.
- Wang J-G, Feng C, Liu H-H, Ge F-R, Li S, Li H-J, Zhang Y.** 2016a. HAPLESS13-mediated trafficking of STRUBBELIG is critical for ovule development in *Arabidopsis*. *PLOS Genetics* **12**, e1006269.
- Wang Z-Y, He J-X.** 2004. Brassinosteroid signal transduction - choices of signals and receptors. *Trends in Plant Science* **9**, 91–96.
- Wang C, Hu T, Yan X, Meng T, Wang Y, Wang Q, Zhang X, Gu Y, Sánchez-Rodríguez C, Gadeyne A, Lin J, Persson S, Van Damme D, Li C, Bednarek SY, Pan J.** 2016b. Differential regulation of clathrin and its adaptor proteins during membrane recruitment for endocytosis. *Plant Physiology* **171**, 215–229.
- Wang L, Li H, Lv X, Chen T, Li R, Xue Y, Jiang J, Jin B, Baluška F, Šamaj J, Wang X, Lin J.** 2015a. Spatiotemporal dynamics of the BRI1 receptor and its regulation by membrane microdomains in living *Arabidopsis* cells. *Molecular Plant* **8**, 1334–1349.

References

- Wang J-G, Li S, Zhao X-Y, Zhou L-Z, Huang G-Q, Feng C, Zhang Y.** 2013. HAPLESS13, the Arabidopsis 1 adaptin, is essential for protein sorting at the trans-Golgi Network/Early Endosome. *Plant Physiology* **162**, 1897–1910.
- Wang Z-Y, Seto H, Fujioka S, Yoshida S, Chory J.** 2001. BRI1 is a critical component of a plasma-membrane receptor for plant steroids. *Nature* **410**, 380–383.
- Wang X, Zafian P, Choudhary M, Lawton M.** 1996. The PR5K receptor protein kinase from Arabidopsis thaliana is structurally related to a family of plant defense proteins. *Proceedings of the National Academy of Sciences* **93**, 2598–2602.
- Wang C, Zhu M, Duan L, Yu H, Chang X, Li L, Kang H, Feng Y, Zhu H, Hong Z, Zhang Z.** 2015b. *Lotus japonicus* Clathrin Heavy Chain1 is associated with Rho-Like GTPase ROP6 and involved in nodule formation. *Plant Physiology* **167**, 1497–1510.
- Wu X.** 2003. Modes of intercellular transcription factor movement in the Arabidopsis apex. *Development* **130**, 3735–3745.
- Wu G, Liu S, Zhao Y, Wang W, Kong Z, Tang D.** 2015. ENHANCED DISEASE RESISTANCE4 associates with CLATHRIN HEAVY CHAIN2 and modulates plant immunity by regulating relocation of EDR1 in Arabidopsis. *The Plant Cell* **27**, 857–873.
- Yadav RK, Fulton L, Batoux M, Schneitz K.** 2008. The Arabidopsis receptor-like kinase STRUBBELIG mediates inter-cell-layer signaling during floral development. *Developmental Biology* **323**, 261–270.
- Yadav RK, Perales M, Gruel J, Girke T, Jönsson H, Venugopala Reddy G.** 2011. WUSCHEL protein movement mediates stem cell homeostasis in the Arabidopsis shoot apex. *Genes and Development* **25**, 2025–2030.
- Yamamoto M, Nishio T, Nasrallah JB.** 2018. Activation of self-incompatibility signaling in transgenic Arabidopsis thaliana is independent of AP2-based clathrin-mediated endocytosis. *Genes|Genomes|Genetics* **8**, g3.200231.2018.

References

- Yamaoka S, Shimono Y, Shirakawa M, Fukao Y, Kawase T, Hatsugai N, Tamura K, Shimada T, Hara-Nishimura I.** 2013. Identification and dynamics of Arabidopsis adaptor protein-2 complex and its involvement in floral organ development. *The Plant Cell* **25**, 2958–2969.
- Ybe JA, Brodsky FM, Hofmann K, Lin K, Liu S-H, Chen L, Earnest TN, Fletterick RJ, Hwang PK.** 1999. Clathrin self-assembly is mediated by a tandemly repeated superhelix. *Nature* **399**, 371–375.
- Yu Q, Zhang Y, Wang J, Yan X, Wang C, Xu J, Pan J.** 2016. Clathrin-mediated auxin efflux and maxima regulate hypocotyl hook formation and light-stimulated hook opening in Arabidopsis. *Molecular Plant* **9**, 101–112.
- Zhang Y, Persson S, Hirst J, Robinson MS, Van Damme D, Sánchez-Rodríguez C.** 2015. Change your Tplate, change your fate: plant CME and beyond. *Trends in Plant Science* **20**, 41–48.
- Zhou J, Liu D, Wang P, Ma X, Lin W, Chen S, Mishev K, Lu D, Kumar R, Vanhoutte I, Meng X, He P, Russinova E, Shan L.** 2018. Regulation of *Arabidopsis* brassinosteroid receptor BRI1 endocytosis and degradation by plant U-box PUB12/PUB13-mediated ubiquitination. *Proceedings of the National Academy of Sciences* **115**, E1906-E1915.
- Zipfel C, Kunze G, Chinchilla D, Caniard A, Jones JDG, Boller T, Felix G.** 2006. Perception of the bacterial PAMP EF-Tu by the receptor EFR restricts agrobacterium-mediated transformation. *Cell* **125**, 749–760.
- Zipfel C, Robatzek S, Navarro L, Oakeley EJ, Jones JDG, Felix G, Boller T.** 2004. Bacterial disease resistance in Arabidopsis through flagellin perception. *Nature* **428**, 764–767.

8 Acknowledgements

Foremost, I would like to thank Prof. Dr. Kay Schneitz for providing me the opportunity to work in his lab. I am particularly grateful to him for his excellent supervision, support, enthusiasm, motivation and immense knowledge throughout the course of this thesis. I am truly fortunate to have had the opportunity to work with him.

I gratefully acknowledge the funding received towards my PhD from the China Scholarship Council (CSC).

I would also like to thank Prof. Dr. Brigitte Poppenberger-Sieberer for appearing as the second examiner and Prof. Dr. Erwin Grill for accepting the chairmanship in my doctoral examination.

I feel grateful to Prof. Dr. Erika Isono and Marie-Kristin Nagel from Chair of Plant Physiology and Biochemistry, University of Konstanz for their constant help for the experiments of CCVs isolation and generously providing me with the *Arabidopsis* seeds for my thesis work.

I would like to thank Prof. Dr. Ramon Angel Torres Ruiz for the introduction of confocal microscopes and scientific suggestions.

I would like to thank Prasad for introducing me to the lab and his guidance during the early days of my thesis. He patiently taught me a lot about plant developmental biology and widen my knowledge in this field.

I would like to thank Ajeet for helping me in all the time of research of this thesis. Whenever I need help or discussion, he is always there.

I would like to thank past and present colleagues: Sebastian, Janys, Regina, Katrin, Athul, Rachele, Xia, Annermarie, and Barbara for the friendly atmosphere, scientific discussions and fun moments in lab.

Special thanks go to our administrative secretary Susanna for helping the department to run smoothly and for assisting me in many different ways.

Acknowledgements

I would like to thank my master student Zac. Your effort has been outstanding.

I would like to thank members of Lehrstuhl für Botanik and Lehrstuhl für Systembiologie der Pflanzen for their support.

I would like to thank the Center of Advanced Light Microscopy (CALM) for providing me the chance to make good images with several advanced confocal microscopes.

In particular I feel grateful to Jiangli. Your happy and optimistic character as well as your great support and patience during hard-working days gave me the confidence to continue and finish this thesis.

Last but not least, I am grateful to all my family members in China for their encouragement which enable me to complete my thesis work on time.

9 Curriculum Vitae

Persönliche Angaben

Nachname	Gao
Vorname	Jin
Geburtsdatum	11.04.1989
Geburtsort	Shandong, China
Staatsangehörigkeit	Chinesisch

Ausbildung und Beruf

seit 09/2014	Wissenschaftlicher Mitarbeiter, Professur für Entwicklungsbiologie der Pflanzen, TU München, Emil- Ramann-Str. 4, 85354 Freising. Studium
2011-2014	Master of Agriculture from Northwest A & F University, China
2006-2010	Bachelor of Agriculture from Shandong Agricultural University, China

Titel der Dissertation Endocytic trafficking of *Arabidopsis* receptor-like kinase STRUBBELIG

Betreuer Prof. Dr. Kay Schneitz

Publikationen

Gao J, Chaudhary A, Vaddepalli P, Nagel M-K, Isono E and Schneitz K. (2019). The Arabidopsis receptor kinase STRUBBELIG undergoes clathrin-dependent endocytosis. *Journal of Experimental Botany*, erz190, <https://doi.org/10.1093/jxb/erz190>.

Chaudhary A, **Gao J**, Schneitz K. 2018. The Genetic Control of Ovule Development. *Reference Module in Life Sciences*, 1-10.

Duan Y, Zhang M, **Gao J**, Li P, Goltsev V, Ma F. 2015. Thermotolerance of apple tree leaves probed by chlorophyll a fluorescence and modulated 820 nm reflection during seasonal shift. *Journal of Photochemistry and Photobiology B: Biology* 152, 347-356.

Gao J, Li P, Ma F, Goltsev V. 2014. Photosynthetic performance during leaf expansion in *Malus micromalus* probed by chlorophyll a fluorescence and modulated 820nm reflection. *Journal of Photochemistry and Photobiology B: Biology* 137, 144-150.